

**Aus der Klinik für Psychiatrie und Psychotherapie
Universitätsklinikum des Saarlandes, Homburg/Saar**

**Etiogenesis of Alzheimer`s disease
in transgenic mouse models**

**Dissertation zur Erlangung eines Doktors der Naturwissenschaften
der Medizinischen Fakultät
der UNIVERSITÄT DES SAARLANDES
2008**

**vorgelegt von: Henning Breyhan
geb. am. 11. Juni 1976 in Salzgitter**

TABLE OF CONTENTS

1	SUMMARY	7
2	INTRODUCTION	12
2.1	ALZHEIMER`S DISEASE	12
2.2	FAMILIAL AND SPORADIC TYPE OF ALZHEIMER`S DISEASE	13
2.3	NEUROPATHOLOGICAL HALLMARKS OF ALZHEIMER`S DISEASE IN HUMAN	15
2.3.1	AMYLOID BETA PLAQUE DEPOSITION	15
2.3.2	NEUROFIBRILLARY TANGLES	19
2.3.3	HIPPOCAMPAL SHRINKAGE, NEURON LOSS AND SYNAPTIC DEFICITS	20
2.3.4	INFLAMMATION OF THE BRAIN	24
2.3.5	CHOLESTEROL AND 24(S)-HYDROXYCHOLESTEROL IN PLASMA AS POTENTIAL BIOMARKERS OF ALZHEIMER`S DISEASE	27
2.4	MODELLING OF HUMAN ALZHEIMER`S DISEASE IN TRANSGENIC MICE	30
2.4.1	OVERVIEW ABOUT TRANSGENIC MOUSE MODELS OF ALZHEIMER`S DISEASE	30
2.4.2	THE APP/PS1KI MOUSE MODEL OF ALZHEIMER`S DISEASE	31
2.4.3	IN VIVO FORMATION OF PYROGLUAMATE A β IN TBA1 AND TBA2 MICE	33
3	MATERIALS AND METHODS	37
3.1	STATISTICAL ANALYSIS	37
3.2	IMMUNOHISTOCHEMISTRY AND HISTOLOGY	37
3.3	TRANSGENIC MICE	39
3.4	GENOTYPING	40
3.5	mRNA QUANTIFICATION FOR TBA1 AND TBA2 MICE	45
3.6	STAINING OF PARAFFIN-SECTIONS	46
3.7	HPLC-ASSAY FOR DETERMINATION QC-ACTIVITY IN PLASMA	47

3.8	QUANTIFICATION OF A β _{x-42} AND A β _{N3(pE)} BY ELISA	49
3.9	RNA PREPARATION AND REVERSE TRANSCRIPTION	49
3.10	QUANTITATIVE RT-PCR	49
3.11	WESTERN-BLOT	50
3.12	PHOTOMETRIC MEASUREMENT OF PROTEIN CONCENTRATION	51
3.13	AGAROSE GEL ELECTROPHORESIS	51
3.14	X-RAY EXAMINATION	51
3.15	BEHAVIOUR TESTS	52
3.16	STEREOLOGICAL QUANTIFICATION OF TOTAL NUMBERS OF NEURONS	55
3.17	HISTOLOGICAL STAININGS	56
3.18	PLASMA CHOLESTEROL MEASUREMENT USING GAS CHROMATOGRAPHY	57
4	RESULTS	58
4.1	DEFICITS IN WORKING MEMORY AND MOTOR PERFORMANCE DECLINE IN THE APP/PS1KI MOUSE MODEL FOR ALZHEIMER`S DISEASE ARE PARALLELED BY EXTENSIVE NEURON LOSS AND HIPPOCAMPAL SHRINKAGE	58
4.1.1	PHENOTYPICAL CHARACTERIZATION	58
4.1.2	APP/PS1KI MICE ARE STRONGLY IMPAIRED IN SENSORY- MOTOR TASKS	60
4.1.3	FORCED SWIMMING TEST	61
4.1.4	LOCOMOTOR AND EXPLORATORY BEHAVIOUR	63
4.1.5	AGE-DEPENDENT WORKING MEMORY IMPAIRMENT IN APP/PS1KI MICE	64
4.1.6	CA1 NEURON LOSS AND HIPPOCAMPAL ATROPHY	66
4.2	PATHOLOGY-DEPENDENT DEVELOPMENT OF INFLAMMATION IN AN APP/PS1KI MOUSE MODEL OF ALZHEIMER`S DISEASE	67
4.3	CHOLESTEROL METABOLISM IN APP/PS1KI MICE	73

4.4	24-(S)-HYDROXY-CHOLESTEROL AS A PREDICTIVE BIOMARKER IN ALZHEIMER`S DISEASE?	74
4.5	IN VIVO FORMATION OF PYROGLUTAMATE A β IN APP/PS1KI, TBA1 AND TBA2 MICE	76
4.5.1	DOMINANT AGGREGATION OF β -AMYLOID STARTING WITH PYROGLUTAMATE AT POSITION 3 IN THE APP/PS1KI MOUSE MODEL	76
4.5.2	TARGET GENE EXPRESSION IN HETEROZYGOUS AND HOMOZYGOUS TRANGENIC MICE WITH UBIQUITOUS OVEREXPRESSION OF GLUTAMINYL-CYCLASE (QC)	78
4.5.2.1	QC-ACTIVITY IN EDTA-PLASMA AND TISSUE HOMOGENATES	79
4.5.2.2	EVALUATION OF QC-TRANSCRIPT LEVELS USING REAL-TIME RT-PCR	80
4.5.2.3	QC-EXPRESSION IN THE KIDNEY	81
4.5.3	IN VIVO FORMATION OF PYROGLUAMATE A β IN TBA1 AND TBA2 MICE	82
5	DISCUSSION	89
5.1	DEFICITS IN WORKING MEMORY AND MOTOR PERFORMANCE DECLINE IN THE APP/PS1KI MOUSE MODEL FOR ALZHEIMER`S DISEASE ARE PARALLELED BY EXTENSIVE NEURON LOSS AND HIPPOCAMPAL SHRINKAGE	89
5.2	PATHOLOGY-DEPENDENT DEVELOPMENT OF INFLAMMATION IN AN APP/PS1KI MOUSE MODEL OF ALZHEIMER`S DISEASE	93
5.3	CHOLESTEROL AS A BIOMARKER IN ALZHEIMER`S DISEASE .	102
5.4	24(S)-HYDROXYCHOLESTEROL AS A BIOMARKER IN ALZHEIMER`S DISEASE	104
5.5	PYROGLUTAMATE AMYLOID BETA AS A POTENTIAL TRIGGER FOR SPORADIC ALZHEIMER`S DISEASE	106

5.5.1	DOMINANT AGGREGATION OF BETA-AMYLOID STARTING WITH PYROGLUTAMATE AT POSITION 3 IN THE APP/PS1KI MOUSE MODEL	106
5.5.2	OVEREXPRESSION OF mQC IN mQC-TRANSGENIC MICE ..	109
5.5.3	IN VIVO FORMATION AND NEUROTOXICITY OF PYRO-GLUTAMATE A β IN TBA1 AND TBA2 MICE	109
6	REFERENCES	111
7	PUBLICATIONS	133
8	DANKSAGUNG	136
9	CURRICULUM VITAE	137

TABLE OF ABBREVIATIONS

APP	amyloid precursor protein
AChE	acetylcholin esterase
AD	Alzheimer`s disease
ANOVA	one-way analysis of variance
ApoE	apolipoprotein E
A β	amyloid beta
BACE	beta-site amyloid precursor protein cleaving enzyme
BBB	blood brain barrier
CA	cornu ammunis
CNS	central nervous system
CSF	cerebrospinal fluid
DAB	3,3-diaminobenzidine
EC	entorhinal cortex
f	female
FAD	familial autosomal dominant
GSK3 β	glycogen synthase 3 β
HRP	horseradish-peroxidase
i.e.	id est
m	male
MAPK	mitogen-activated protein kinase
MRI	Magnetic Resonance Imaging
NFT	neurofibrillary tangles
NMDA	N-Methyl-D-Aspartat
NSAID	non-steroidal anti-inflammatory drug
PBS	phosphate-buffered saline
PCR	polymerase chain reaction
PHF	paired helical filaments
PS	presenilin
QC	glutaminyl cyclase
rpm	rounds per minute
RT	room temperature
RT-PCR	reverse transcription polymerase chain reaction
SDS	sodium dodecyl sulfate
TBA	truncated beta amyloid
w.w.	wet weight
WT	wildtype

1 SUMMARY

This thesis is about the following key issues:

1. Characterization of the APP/PS1KI mouse model of Alzheimer`s disease (AD) under aspects of changes in cholesterol metabolism, behavioural changes and neuropathological markers, e.g. neuron loss and neuroinflammation.
2. Characterization of transgenic mice transgenic for glutaminyl cyclase (mQC) A β _{N3Q-42} (TBA2) and A β _{N3E-42} (TBA1). Mice were analyzed under aspects of expression of transgene on mRNA and/or protein level. In mQC mice I assessed also activity data for glutaminyl cyclase in brain, plasma and peripheral organs. Furthermore, double-transgenic mice transgenic for A β _{N3E-42} and mQC to were bred to prove the *in vivo* potential of mQC to catalyze cyclization of A β _{N3E-42} to A β _{N3(pE)}. The question to answer was, if any of these models would meet the criteria as a model for sporadic AD. Moreover, the APP/PS1KI mice model was analyzed for aggregation of A β _{N3(pE)} at 2 and 6 months of age.

The results from this work allow to draw the following key assertions:

Ad 1.: A phenotypical analysis of the APP/PS1KI model using behavioral tests for working memory and motor performance, as well as an analysis of weight development and body shape was performed. At the age of 6 months, a dramatic, age-dependent change in all of these properties and characteristics was observed accompanied by a significant reduced ability to perform working memory and motor tasks. The APP/PS1KI mice were smaller and showed development of a thoracolumbar kyphosis, together with an incremental loss of body weight. While two month-old APP/PS1KI mice were inconspicuous in all of these tasks and properties, there is a massive age-related impairment in all tested behavioral paradigms. Abundant hippocampal CA1 neuron loss was detected by high precision design based sterology starting at 6 months of age in the APP/PS1KI mouse model, which coincides with the onset of motor and memory deficits.

Moreover, by use of realtime RT-PCR and immunohistochemical methods, I found broad evidence for neuroinflammation, micro- and astroglia activation in 6-month-old APP/PS1KI mice, while 2-month old mice appeared to be normal.

Regarding the analysis of cholesterol metabolism in APP/PS1KI mice, I determined a significant decline of plasma cholesterol in APP/PS1KI mice compared to control mice at 6 months of age, when AD-like pathology is already extensively present in these animals, while at two months of age no difference was observed. I also analyzed levels of 24(S)-hydroxycholesterol in plasma to test the reliability of this molecule as a plasma biomarker for progression of AD. However, I did not detect any correlation between the levels of 24(S)-hydroxycholesterol and the onset of pathology in APP/PS1KI mice.

Ad 2.: The mouse models TBA1 and TBA2 are based on neuron specific expression of $A\beta_{3E-42}$ and $A\beta_{3Q-42}$, which were fused to the pre-pro-sequence of murine thyrotropin-releasing hormone.

In mice heterozygous for $A\beta_{N3E-42}$ (TBA1) and mQC, I found evidence for the *in vivo* formation of $A\beta_{N3(pE)}$ driven by enzymatic catalysis of glutaminyl cyclase (QC) in three month old TBA1/QC mice compared to TBA1 and mQC single transgenic, as well as wildtype control mice.

In TBA2 mice, massive neurological impairments became apparent eight weeks after birth, which was likely due to Purkinje cell degeneration. Purkinje cells showed abundant staining for $A\beta$, including $A\beta_{3(pE)}$, and ubiquitin, and were decorated by micro- and astrogliosis. Extracellular $A\beta$ deposits appeared at the site of Purkinje cell degeneration. The results suggest that $A\beta_{3(pE)-42}$ due to its high stability and aggregation propensity triggers $A\beta$ accumulation. The correlation of substantial neuron loss and formation of $A\beta_{3(pE)}$, provides evidence that modified $A\beta$ species foster neurotoxicity. Therefore, reduction or clearance of those amyloidogenic peptides should be considered as novel treatment strategies.

ZUSAMMENFASSUNG

Die vorliegende Arbeit beschäftigt sich mit zwei thematischen Schwerpunkten:

1. Ein Teil der Promotionsschrift beschäftigt sich mit der Fortsetzung der Charakterisierung des APP/PS1KI Mausmodells. Neben einer Untersuchung des Cholesterollowerstoffs wurden diese Tiere insbesondere auch verhaltensbiologisch charakterisiert. Weiterhin wurde der bei diesen Tieren altersabhängig auftretende Neuronenverlust mithilfe stereologischer Methoden quantifiziert und die Entzündungspathologie im Gehirn dieser Tiere zu verschiedenen Altersstufen mittels immunhistochemischer Untersuchungen und real-time RT-PCR untersucht.
2. Der zweite Teil dieser Arbeit beschäftigt sich mit der Charakterisierung dreier neuer transgener Mauslinien, die jeweils heterozygot transgen für das Enzym Glutaminyl-Cyclase (mQC) oder für die Proteine A β _{N3E} (TBA1-Linie) bzw. A β _{N3Q} (TBA2) waren.

Die mQC-transgenen Tieren wurde hinsichtlich der Expression und Aktivität des Transgens charakterisiert.

Das Metalloenzym Glutaminyl Cyclase setzt A β _{N3E} bzw. A β _{N3Q} als Substrat *in vitro* zu Pyroglutamat A β _{N3(pE)} um. Ziel unserer Untersuchungen zum Pyroglutamat A β _{N3(pE)} war es, die Aggregationseigenschaften und die Neurotoxizität dieses speziellen A β -Peptides *in vivo* zu analysieren. Durch Kreuzung wurden Mäuse erzeugt, die sowohl heterozygot transgen für mQC als auch A β _{N3E} (TBA1-Linie) waren. In diesem doppelt transgenen Tiermodell sollte geklärt werden, ob die mQC die Umsetzung zum Pyroglutamat A β _{N3(pE)} auch *in vivo* katalysieren kann. In diesem sogenannten TBA1/QC- und im TBA2-Tiermodell wurde die *in vivo* Aggregation von A β _{N3(pE)} untersucht. Außerdem wurde auch das APP/PS1KI-Tiermodell im Hinblick auf die altersabhängige A β _{N3(pE)}- Bildung hin analysiert.

Bezogen auf die zuvor angeführte Fragestellung hat diese Arbeit zu folgenden Ergebnissen geführt:

Ad 1.: In dieser Arbeit wurde eine phänotypische Analyse des APP/PS1KI Tiermodells der Alzheimer Erkrankung durchgeführt, das im Alter von sechs Monaten viele der pathologischen Merkmale aufweist, wie sie auch für das humane Krankheitsbild beschrieben sind. Neben verhaltensbiologischen Untersuchungen des Arbeitsgedächtnis und der motorischen Leistungen dieser Tiere, wurden auch die altersabhängige Entwicklung des Körpergewichtes und der Körperform erfasst. Im Alter von sechs Monaten zeigten APP/PS1KI Mäuse signifikante Auffälligkeiten bezüglich aller untersuchten Parameter. Bei allen Tests zum Arbeitsgedächtnis und zu den motorischen Fähigkeiten zeigte sich ein stark herabgesetztes Leistungsvermögen sechs Monate alter APP/PS1KI Tiere im Vergleich zu PS1KI Kontrolltieren gleichen Alters. Im Alter von zwei Monaten wurden bei den APP/PS1KI Tiere hingegen noch keine diesbezüglichen Auffälligkeiten festgestellt. Insbesondere die Einschränkungen bei der Leistungsfähigkeit des Arbeitsgedächtnisses lassen sich dabei gut durch den mittels stereologischer Methoden festgestellten Neuronenverlust von 33% im CA1-Band des Hippocampus bei sechs Monate alten APP/PS1KI Tieren erklären.

Ebenso war im Gehirn sechs Monate alter APP/PS1KI Tieren eine ausgeprägte Entzündungspathologie feststellbar. Mittels immunhistochemischer Färbungen und real-time RT-PCR wurden eine Vielzahl gängiger Marker für Neuroinflammation sowie Micro- und Astrogliaaktivierung positiv getestet.

Bei der Analyse des Cholesterolmetabolismus stellte ich im Vergleich zu Kontrolltieren in sechs Monate alten APP/PS1KI Tieren eine signifikante Abnahme der Konzentration von Cholesterol im Plasma fest. Bei zwei Monaten war hier ebenfalls noch kein Unterschied feststellbar. Ebenso wurden die Konzentrationen von 24(S)-hydroxycholesterol altersabhängig in APP/PS1KI und Kontrolltieren bestimmt, um die Eignung dieses Moleküls als Plasma-Biomarker für den Verlauf der Alzheimer-Erkrankung zu untersuchen. In den untersuchten Tieren war jedoch kein Zusammenhang zwischen der Entwicklung der Plasmakonzentration von 24(S)-hydroxycholesterol und dem Fortschreiten der Alzheimer-Pathologie erkennbar.

Ad 2.: Die transgenen Mausmodellen TBA1 und TBA2 exprimieren neuronenspezifisch die N-terminal trunkierten A β -Varianten A β _{N3E} bzw. A β _{N3Q}. In drei Monate alten TBA/QC Mäusen, die heterozygot für das Enzym Gluaminyln

Cyclase (mQC) und $A\beta_{N3E}$ waren, gelang der *in vivo* Nachweis der Bildung von Pyroglutamat $A\beta_{N3(pE)}$ durch katalytische Umwandlung von $A\beta_{N3E}$ durch das Enzym Glutaminyl Cyclase.

In den TBA2 Mäusen, die im Vergleich zu den TBA1 Tieren etwa xfach höhere $A\beta_{N3(pE)}$ -Werte im Gehirn zeigen, zeigten sich bereits im Alter von acht Wochen schwere neurologische Beeinträchtigungen, die vermutlich auf die gezeigte Degeneration der Purkinje-Zellen im Kleinhirn zurückzuführen ist. Diese Zellen in den TBA2-Tieren zeigten eine deutliche immunhistochemische Färbung für $A\beta$, $A\beta_{N3(pE)}$ wie auch Ubiquitin und zeigten darüber hinaus Merkmale einer bestehenden Micro- und Astroglie. Soweit sich im Gewebe eine Degeneration der Purkinje-Zellen zeigte, fanden sich dort auch extrazelluläre Ablagerungen von $A\beta$. Auf Grundlage dieser Befunde könnte $A\beta_{N3(pE)}$ aufgrund seiner höheren Stabilität und seiner stärkeren Aggregationsneigung der Wegbereiter einer sich dann weiter entwickelnden Plauepathologie bei der Alzheimer Krankheit sein, indem es als Keimbildner die ersten extrazellulären amyloiden Aggregate bildet, an die sich anschließend weitere Formen von $A\beta$ anlagern können. Dass sich in den TBA2-Tieren neben der Akkumulation von $A\beta_{N3(pE)}$ auch Indizien für einen auftretenden Neuronenverlust zeigen, deutet auf das neurotoxische Potential dieser N-terminal modifizierten $A\beta$ -Variante hin. Eine Verminderung der QC-vermittelten Bildung von $A\beta_{N3(pE)}$ im menschlichen Gehirn weist daher möglicherweise den Weg zu neuen Therapieansätzen in der Alzheimererkrankung.

2 INTRODUCTION

2.1 ALZHEIMER`S DISEASE

Alzheimer`s disease nowadays is the most common neurodegenerative disease of the elderly. Referring to the affected patients, AD is characterized by proceeding memory deficits and ongoing loss of daily-life abilities. First signs of the early disease state are short-term memory loss and visual-spatial confusion, often accompanied by aphasia, disorientation or disinhibition. Many patients start to show changes in their behavior and therefore, for example, confront their social surrounding with formerly unknown violent outbursts or in contrast distinct passivity. Accordingly, close relatives are often the first ones that get aware of these early changes in the character and behaviour of a person that is on the way to develop early stage AD. With the disease taking its course, proceeding cognitive decline is met in addition by deterioration of musculature and a loss in mobility. Patients in the final stage are unable to perform even the most simple tasks like walking or eating without assistance, suffer from incontinence of the bladder and/or the bowel. Patients affected by late stage AD speak often very disorganized. Also, patients in this state of disease require permanent supervision. In Germany, this care is mostly achieved by close relatives of the demented persons. Therefore, besides the mentioned direct effects of AD on an affected person, AD also has a lot of impact on the social surrounding of the patient and often one family member signs out of its job to afford the time needed to take care. A further problematic social issue connected to AD is, that 80% of family members taking care of demented persons are themselves already in an advanced age between 50 and 75 years and therefore find themselves sometimes also not any more in best health condition.

In economic figures in 2006 in Germany 800.000 persons were living with a diagnosis of AD causing direct healthcare costs of 20 bn Euros. These numbers are estimated to rise until 2040 to between 1.5 and 2.0 million AD patients inflicting direct costs of about 50 bn Euros. prediction underlines the economic and social challenge ageing societies are going to face due to Alzheimer`s disease and related forms of dementia.

Despite the unquestioned economic potential of an effective cure targeting AD still none such has come to market or is known to appear in the horizon of the next few years. However a couple of standard therapy medications are already available to AD patients. Though, all of

these drugs do not target the underlying disease mechanism but deliver at least some symptomatic benefit, however without any slowdown in the total progress of the disease.

In terms of economical turnover, drugs from the group of acetylcholinesterase inhibitors (ChEIs) and NMDA receptor antagonist have greatly gained in importance.

In short, inhibitors of the enzyme acetylcholinesterase (AChE) aim to the detected decrease of the neurotransmitter acetylcholine due to reduced activity of cholinergic neurons in AD patients, which has been proposed to have some impact on the memory loss in AD. Acetylcholine is degraded by AChE. Therefore, inhibition of AChE stabilizes levels of acetylcholine in the brain and helps to delay some loss of memory symptoms in AD for a few months.

Another approach to overcome some of the symptoms of memory decline in AD with overall moderate efficacy is based on the finding that in AD excessive activation of N-methyl-D-aspartate (NMDA) receptors may finally lead to the degeneration of cholinergic cells. NMDA-receptor antagonists block the sustained activation of the receptor by glutamate that may occur under pathological conditions in AD. Thus, NMDA receptor function is attenuated. Epidemiological studies also suggested potential for NSAIDs, estrogen, HMG-CoA reductase inhibitors (statins) or tocopherol (vitamin E) to prevent AD. However, prospective, randomised studies have not convincingly been able to demonstrate clinical efficacy. (Hull *et al.* 2006) Besides these therapeutic approaches a wide variety of suggestions has been made how to reduce the risk of getting affected by AD including intake of red wine containing flavonoids with antioxidant activity, intake of omega-3-fatty acids, Ginkgo Biloba extracts, B-vitamins and others more. Also certain aspects of behaviour like intellectual activity are thought to have a beneficial overall influence. However, all these therapies and supplements lack, that they do not address the underlying disease pathomechanism.

2.2 FAMILIAL AND SPORADIC TYPE OF ALZHEIMER`S DISEASE

AD subdivides in so called familial or early onset AD and secondly sporadic AD, the latter representing the far more prominent part of people concerned. Spoken in numbers, 90 - 95% of AD cases appear in a sporadic manner with proceeding age as the major identified risk factor, while only 5 - 10% of the disease cases are genetically based (Tanzi 1999). Mutations typical for this familial early onset type of AD are associated with the genes encoding the β -

amyloid precursor protein (hAPP, chromosome 21), the presenilin 1 (PS1, chromosome 14), and the presenilin 2 (PS2) gene (on chromosome 1). These mutations foster abnormal processing of the amyloid precursor protein and therefore ameliorate overproduction of amyloid beta peptides A β ₁₋₄₀ and A β ₁₋₄₂. Additionally, the e4 allele of apolipoprotein E (ApoE) has also been shown to be associated with a increased risk for late-onset AD (St George-Hyslop 2000).

However, the causes of sporadic type of AD with age as the major identified risc factor still remain opaque, though extensive research efforts address this issue. Widely discussed is the influence of environmental agents (e.g., heavy metals), intrinsic factors (e.g., cytokines), and dietary factors (e.g., cholesterol) (Lahiri *et al.* 2007).

A)

Codon	Mutation	Phenotype
665	Gln Asp	Late onset AD - no segregation
670/671	Lys-Met Asn-Leu	FAD; increased A β production
673	Ala Thr	No disease phenotype
692	Ala Gly	FAD and cerebral hemorrhage; increased A β
693	Glu Gly	Late onset AD - no segregation
	Glu Gln	HCHWA-D
713	Ala Val	Schizophrenia - no segregation
	Ala Thr	AD - no segregation
716	Ile Val	FAD
717	Val Ile	FAD; increased long A β isoforms
	Val Phe	FAD
	Val Gly	FAD

B)

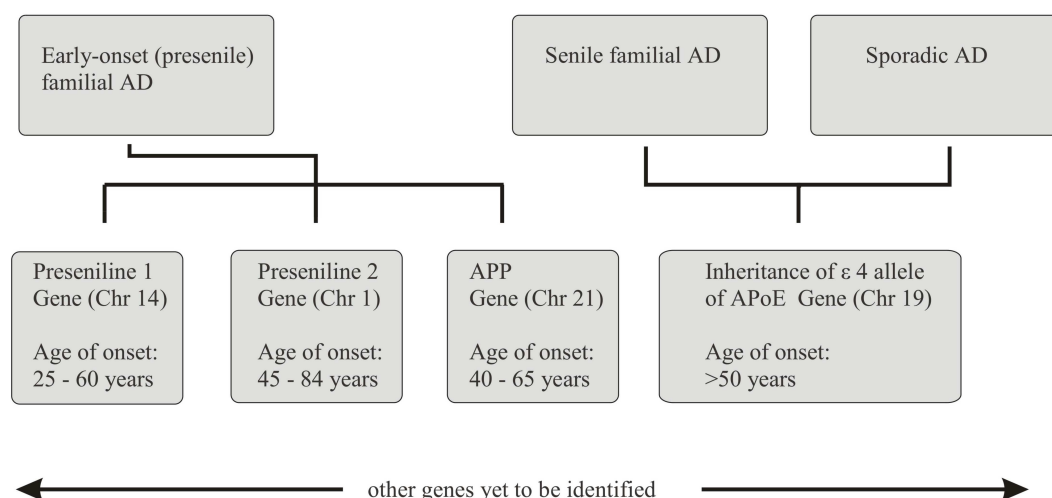


Fig. 1: (A) Missense mutations in the β APP gene (HCHWA-D: amyloidosis Dutch type; FAD: familial Alzheimer disease). Data taken from (St George-Hyslop 2000) (B) Genetic mutations implicated in familial or sporadic onset of Alzheimer's disease (according to (St George-Hyslop 2000)).

2.3 NEUROPATHOLOGICAL HALLMARKS OF ALZHEIMER'S DISEASE IN HUMAN

On a neuropathological level brains of AD patients suffer from a devastating extent of neuron loss accompanied by extensive formation of senile plaques consisting of amyloid beta ($A\beta$) and appearance of neurofibrillary tangles of hyper-phosphorylated tau-protein. Furthermore, vascular deficits and a pathology of inflammation are clearly associated with the AD affected brain.

2.3.1 AMYLOID BETA PLAQUE DEPOSITION

The formation of senile plaques consisting mainly of amyloid β peptides is one of the most typical and also prominent changes occurring in brains affected by AD, though it is also known, that people developing plaque pathology do not necessarily develop symptoms of AD. However, it is still a most widely accepted hypothesis, that production and aggregation of the amyloid β protein ($A\beta$) is a key event in the pathology of AD (Van Broeck *et al.* 2007). The role of extracellular $A\beta$ -plaques in the process of AD is widely established under the term “Amyloid- β hypothesis”, which assumes a dysfunction in the processing of amyloid precursor protein (APP) as the crucial trigger for AD onset (Hardy & Allsop 1991).

A revised version of the β -amyloid hypothesis was introduced by Wirths *et al.*, based on the finding that $A\beta$ accumulation takes place at first in the intraneuronally space while extracellular formation of plaques is a subsequent event (Masters *et al.* 1985; Wirths *et al.* 2004). Because extracellular plaque load was found not to be correlated with striking events of AD pathology like neuron loss, Wirths *et al.* focused on the development of AD symptoms depending on levels of intraneuronal $A\beta$. Evidence for this hypothesis was derived from the finding of deficits in behaviour, synaptic transmission or long-term potentiation well before first signs of plaque pathology in several transgenic mouse models of AD (Holcomb *et al.* 1998; Hsia *et al.* 1999; Moechars *et al.* 1999). The physiological potential of intracellular $A\beta$ was also supported by the finding, that this pool of $A\beta$ represents an early and integral component of the pathogenesis of the human muscle disorder IBM (Askanas *et al.* 1993; Mendell *et al.* 1991). Additionally, immunohistochemical analysis of postmortem DS and APP transgenic mouse brains by use of C-terminally specific antibodies directed against $A\beta_{1-42}$ gave evidence for an age-dependent increase of this neurotoxic $A\beta$ -species within neurons

(Busciglio *et al.* 2002; D'Andrea *et al.* 2001; Gouras *et al.* 2000; Tabira *et al.* 2002; Wirths *et al.* 2004). Meanwhile, the importance of intracellular A β has been underlined by a broad range of studies (Glabe 2001; Gouras *et al.* 2005). Most convincing, in an APP/PS1KI mouse model of AD a strong correlation between early accumulation of intraneuronal A β in CA1/2 region of the hippocampus already from 2 months of age on and an extensive neuron loss (~50%) in this area of the hippocampal pyramidal cell layer was reported (Casas *et al.* 2004).

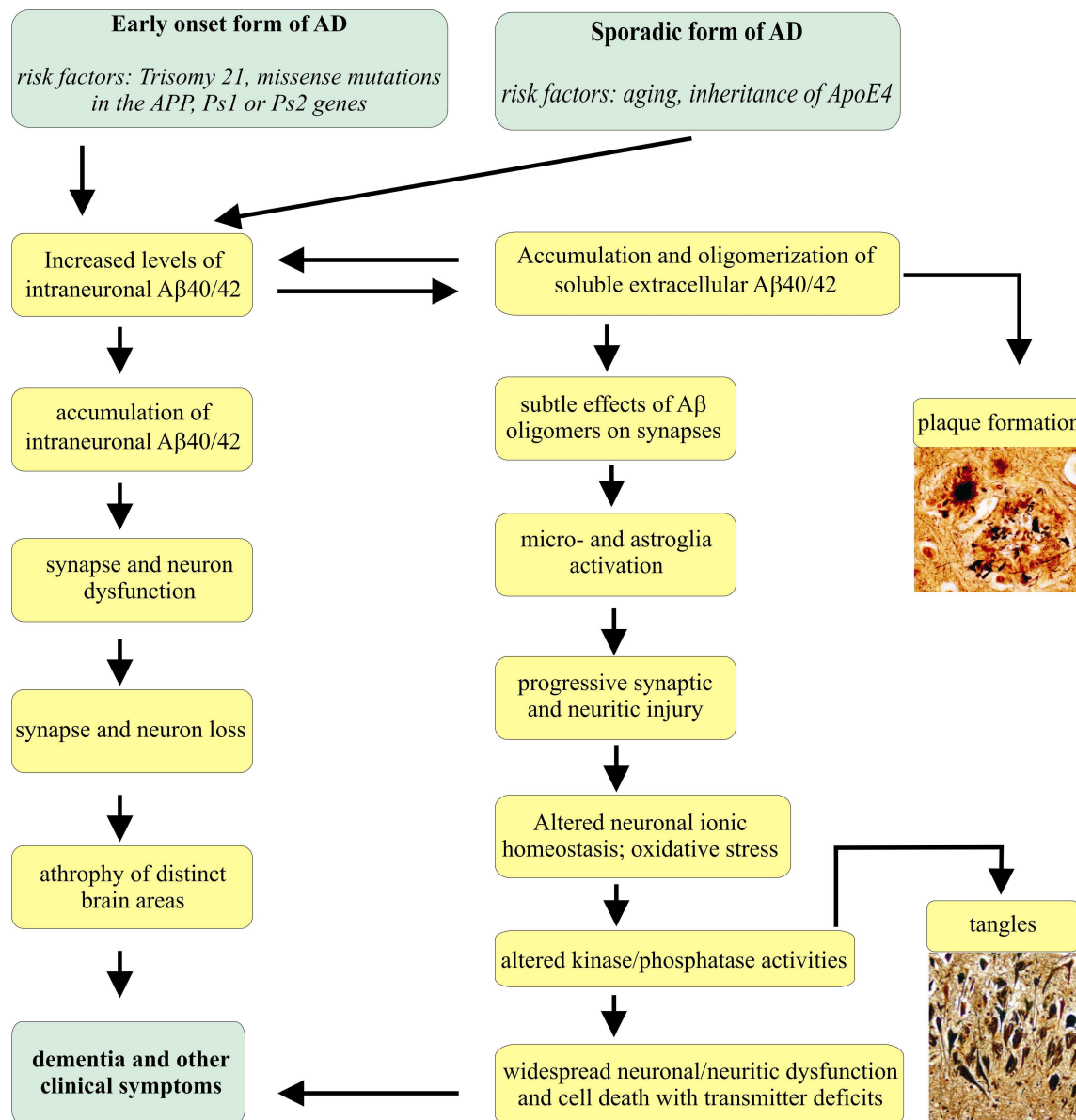


Fig. 2: Two versions of the Amyloid β hypothesis: Sequence of pathogenic events leading to AD pathology is shown in the classical understanding according to Hardy *et al.* (right part of figure) and in a revised version according to Wirths *et al.* (left part of figure) that focuses on the contribution of intraneuronal accumulation of A β 42 to the development of AD pathology. Both vicious cascades may interfere and contribute in parallel as well to the cognitive decline symptomatic for AD affected patients, as suggested by horizontal arrows.

A β is formed in the brain by enzymatic cleavage of the amyloid precursor protein (APP). APP is a protein with a single transmembrane domain (Gandy & Petanceska 2000). APP mRNA splicing undergoes in various ways leading to the generation of at least 8 distinct isoforms, namely APP677, APP695, APP696, APP714, APP733, APP751, APP752 and APP770. APP695 is the most common isoform in the brain (Golde *et al.* 1990; Sandbrink *et al.* 1997).

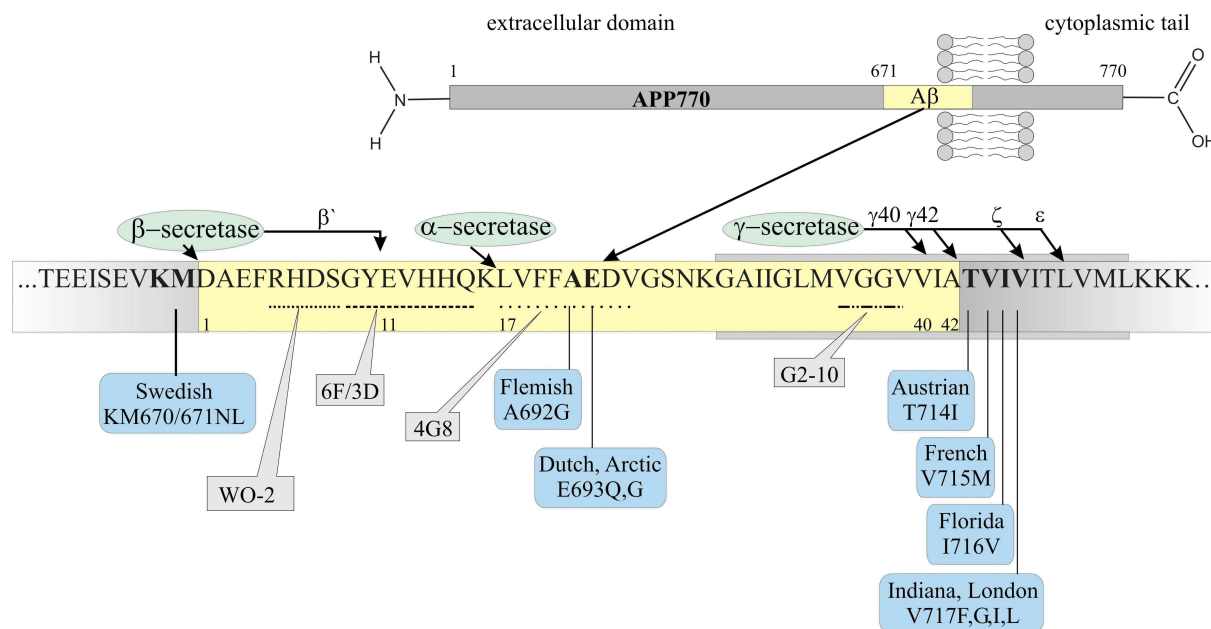


Fig. 3: Schematic representation of the APP protein, including the A β sequence, cleavage sites of α -, β -, and γ -secretase, important mutations in the APP protein related to familial AD and binding sites of important antibodies.

In AD, the focus is on two distinct pathways of APP processing. The first anticipated non-pathogenic and therefore referred to as non-amyloidogenic pathway is characterized by subsequent cleavage of APP by the enzyme α -secretase in the first step, which leads to release of α -APP, and further processing by γ -secretase to set free the N-terminally truncated A β fragment “p3” from the still membrane retained carboxy APP terminal “C83” (Carter & Lippa 2001). By α -secretase processing APP is being cut within the A β sequence at position 17 in the A β domain, therefore p3 can be referred as A β _{17-40/42}. In consequence, α -cut of APP prevents the formation of A β _{1-40/42} which are the most prominent A β -species in AD affected brains. The mechanism of α -secretase regulation remains unclear. However, three members of the ADAM family of proteases (**a** **d**isintegrin and **m**etalloprotease), namely ADAM 9, 10 and 17, have been supposed to represent the main candidates for α -secretases (Hiraoka *et al.* 2007).

A β _{1-40/42} are both formed via the so called amyloidogenic pathway, in that APP is first processed by the enzyme β -secretase to generate the amino terminal of A β and to set free the

so called β -APPs. Subsequently to action of β -secretase membrane retained C99 is being cut by the enzyme γ -secretase, which finally leads to generation of $A\beta_{1-40}$ and $A\beta_{1-42}$ (Van Broeck *et al.* 2007). β -Secretase has been reported to be a type I transmembrane glycosylated aspartyl protease, while γ -secretase has been identified to be a high-molecular-weight protein complex including the four proteins Aph-1, Pen-2, nicastrin and PS (Guntert *et al.* 2006; Van Broeck *et al.* 2007). Though the exact intracellular cleaving sites of γ -secretase and the nature of this enzyme are still not fully understood, it is well described that γ -secretase breakdown of APP metabolite leads in parallel to a short- and a long-tailed $A\beta$ metabolite as well, namely $A\beta_{1-40}$ and $A\beta_{1-42}$ (Carter & Lippa 2001).

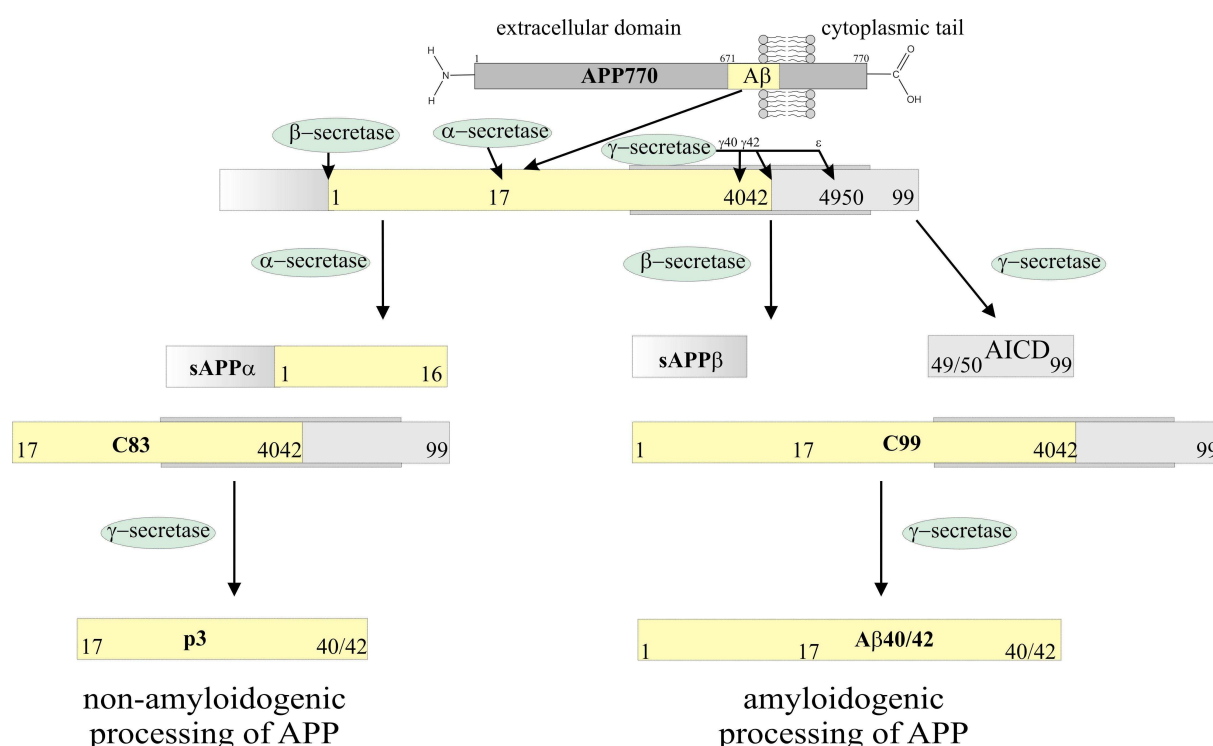


Fig. 4: Non-amyloidogenic and amyloidogenic pathway of APP processing by subsequent proteolytic cleavage by α -/ γ -secretase (non-amyloidogenic pathway) or β -/ γ -secretase (amyloidogenic pathway) leading to the generation of $A\beta_{1-40/42}$.

The cleavage sites of the enzymes involved in APP processing are all near or at those positions in APP, where AD related mutations of APP have been found. Furthermore, it has been shown, that all FAD-linked mutations in the genes of APP, PS1 and PS2 induce an increase in the generation of $A\beta$. Notably the mutations in PS1 and PS2 have been shown to enhance the production of $A\beta_{1-42}$ *in vitro* and *in vivo* (Takeda *et al.* 2004; Xia 2000). All this underlines the possible influence of familial autosomal AD mutations to direct APP processing to the amyloidogenic or non-amyloidogenic pathway (Hardy & Selkoe 2002).

While A β ₁₋₄₀ in human AD patients is the far most abundant A β species with an estimated 1000-fold excess compared to A β ₁₋₄₂, the latter one has been shown to be much more prone to aggregation and to obtain highly neurotoxic properties (Selkoe 2001).

2.3.2 NEUROFIBRILLARY TANGLES

Formation of neurofibrillary tangles (NFT) represents a second intracellular phenomenon associated to AD pathology in the human brain. NFTs appear as bundles of abnormal filaments called paired helical filaments (PHF), composed of highly phosphorylated forms of the ~55 kDa microtubule-associated protein tau. It is widely believed that the high degree of phosphorylation of PHF-tau is a critical event linked to microtubule disorganization and generation of neurofibrillary lesions typically occurring in AD pathology (Boutajangout *et al.* 2002). Though tau is encoded by a single gene, alternative splicing of corresponding RNA leads to multiple distinct isoforms of this protein. Six tau isoforms are known in the human brain (Wagner *et al.* 1996). Tau has been reported to bind to microtubules and to promote microtubule assembly *in vitro* (Goedert & Jakes 1990). Tau protein is assumed to be functional in the formation and maintenance of axons, due to the finding that antisense oligonucleotide mediated down-regulation of tau expression in primary cerebellar neurons impairs the generation of new axons in these cells (Wagner *et al.* 1996). The phosphorylation process of tau takes place at serine/threonine residues preceding a proline and has been shown to be mediated by a number of proline-directed kinases including e.g. members of the mitogen-activated protein kinase (MAPK) family, glycogen synthase 3 α (GSK3 α) or glycogen synthase 3 β (GSK3 β) or CDK5. At the cellular level, hyperphosphorylated tau is mostly found in the somatodendritic compartment of the neurons (Zheng *et al.* 2002).

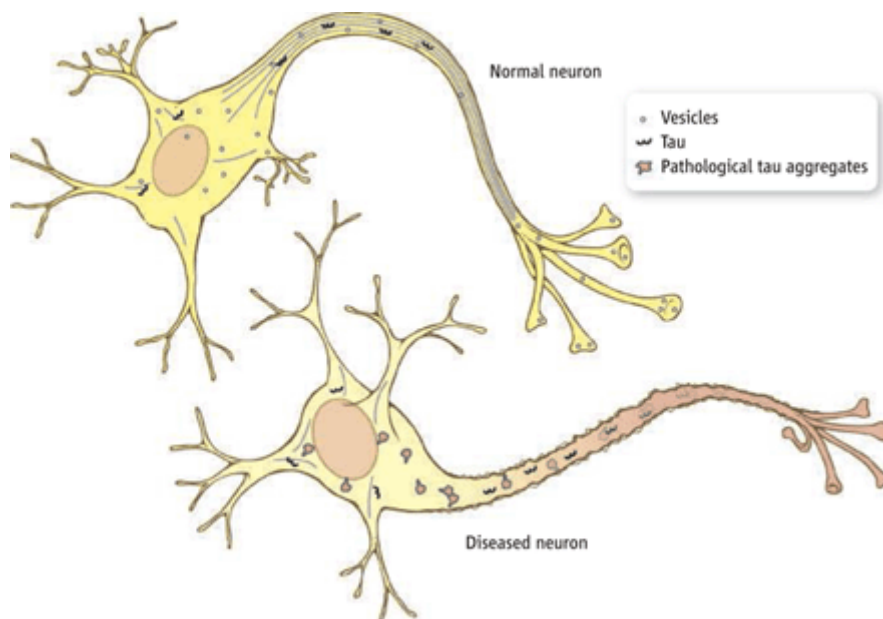


Fig. 5: Tau malfunction in AD: In a healthy neuron (top), tau stabilizes the microtubules (blue lines) that transport materials to the nerve terminals. In AD, tau is unable to bind to the microtubules and forms abnormal aggregates, the so called paired helical filaments (PHF-tau). This process fosters degeneration of microtubules and induces impaired neuronal functioning (graphics taken from Marx 2007).

The mechanism by that tau makes an impact on AD pathology is still a matter of discussion. Rapoport et al. reported about the ability of tau to induce β -amyloid induced neurotoxicity *in vitro*. Cultured hippocampal neurons expressing either mouse or human tau showed clear signs of neurodegeneration upon incubation with fibrillar A β , while no such effects were observed in tau-knockout mice under same treatment conditions (Rapoport *et al.* 2002). On the other hand, Zheng et al. demonstrated *in vitro*, that Amyloid β can induce tau hyperphosphorylation in rat primary septal cultures (Zheng *et al.* 2002). Additionally, hyperphosphorylated tau aggregates have been speculated to disrupt cellular transport, (Mandelkow *et al.* 2003) cellular geometry, and neuronal viability (Cummings *et al.* 1998).

2.3.3 HIPPOCAMPAL SHRINKAGE, NEURON LOSS AND SYNAPTIC DEFICITS

GENERAL REMARKS

In AD patients, the decline of synaptic density in the brain showed to be the most suitable marker correlating with the extent of cognitive loss during the disease process compared to e.g. plaque pathology, NFTs, neuron loss, and transmitter deficits (Coleman & Yao 2003). Two independent studies revealed a correlation coefficient of 0.7 between synapse density

and cognitive status of AD patients (Coleman & Yao 2003). In well accordance with the event of synapse loss, Reddy et al. analyzed levels of synaptic protein in brains of AD patients and reported about a loss of presynaptic (synaptotagmin, synaptophysin, and Rab 3A), synaptic membrane proteins (Gap 43 and synaptobrevin) and postsynaptic proteins (neurogranin and synaptopodin) in AD patients compared to healthy controls (Reddy *et al.* 2005). Synaptic decline appeared to be more severe in the frontal cortex compared to the parietal cortex of AD patients (Reddy *et al.* 2005).

Neuron loss in AD represents a further marker of cognitive decline. Shepherd et al. reported about a neuron loss in frontal superior cortex of 36% in early onset AD cases and of 22% in sporadic AD cases compared to healthy controls (Shepherd *et al.* 2007). Neuron counting in the entorhinal cortex (EC), that is believed to obtain a crucial role as a gateway connecting the neocortex and the hippocampal formation, showed a 32% neuron loss in EC in cases with a mild form of AD. The EC lies in a critical path in neural systems related to memory. It receives afferents from widespread association and limbic areas, projects to the dentate gyrus of the hippocampal formation, receives afferents from the hippocampus, and sends afferents back to association neocortex. The EC is a region highly vulnerable in AD and layers II and IV of the EC were shown to be among the first regions affected with tangles in Down syndrome and in normal aging. In layer II of the EC, which gives way to the perforant pathway, a decrease of even 60% and of 40% in layer IV of the EC was determined in a group of mild AD cases. In severe cases of AD, numbers of neurons in layer II decreased by ~90%, and the number of neurons in layer IV decreased by ~70% compared with controls, while in cognitive normal controls neuron numbers remained constant between 60 and 90 years of age (Gomez-Isla *et al.* 1996).

The hippocampal formation of the brain is the region that shows the most prominent atrophic changes in consequence of AD affection. In AD patients Bobinski et al. found a MRI-based decline of hippocampus volume of about 30% compared to healthy controls and a 40% volume loss of the hippocampal formation when applying histological methods in the same material (Bobinski *et al.* 2000). A broad range of MRI-based studies propose the event of hippocampal atrophy as a relatively specific marker of AD in its early stages (Bobinski *et al.* 2000; Jack *et al.* 2002; Silbert *et al.* 2003). Also a strong correlation between hippocampal atrophy and cognitive decline has been reported by several groups (Chetelat *et al.* 2003; Jack *et al.* 2002; Petersen *et al.* 2000). Though, other studies suggest MRI-assessment of entorhinal cortex volume as a more suitable marker for diagnosis of early stage AD compared to

hippocampal volume, allowing also better differentiation between mild cognitive impairment MCI and early stage of AD (Pennanen *et al.* 2004).

RELATED PROJECT

The APP/PS1KI mouse model for Alzheimer's disease (AD) exhibits robust brain and spinal cord axonal degeneration and hippocampal CA1 neuron loss starting at 6 months of age. It expresses human mutant APP751 with the Swedish and London mutations together with two FAD-linked knocked-in mutations (PS1M233T and PS1 L235P) in the murine PS1 gene. Aim of this study was a phenotypical analysis of this model using behavioral tests for working memory and motor performance, as well as an analysis of weight development and body shape. Furthermore, an exact quantification of the neuron loss occurring in APP/PS1KI mouse model was performed at 6 and 12 months of age by use of high precision design based stereology methods (Schmitz *et al.* 2004).

According to the prevailing amyloid β hypothesis A β amyloid plaques, mainly consisting of the 40- to 42-residue amyloid- β peptide (A β), take a central part in the typical Alzheimer's disease (AD) related pathological cascade. However, lately intraneuronal amyloid- β pathology has gained in importance (for review Wirths *et al.* 2004). A β peptides are derived from the larger amyloid precursor protein (APP) by consecutive proteolytical cleavages. Whereas the majority of all AD cases occurs sporadic, a small percentage of familial early-onset AD cases develops due to mutations in APP or in the Presenilin (PS1, PS2) genes, the latter proteins being an integral part of the β -secretase complex (reviewed in Bayer *et al.* 2001). Until recently, modeling axonal degeneration and neuronal loss remained elusive. APP23 transgenic mice yielded a small loss of pyramidal neurons of the hippocampal formation, (Calhoun *et al.* 1998) which does not reflect the dramatic reduction in AD patients (Gomez-Isla *et al.* 1996). Mild neuron loss has also been documented around amyloid plaques in PSAPP mice (Urbanc *et al.* 2002). This gap has recently been closed because significant neuron loss in the hippocampus has been described in two APP/PS1 mouse models with multiple mutations, (Schmitz *et al.* 2004) or using knock-in mutations (Casas *et al.* 2004). Schmitz *et al.* used human APP751 transgenic mice with the Swedish and London mutations (APP751SL), which had been crossed with the human mutant PS1 (M146L) transgenic line. In 17 month-old APP/PS1 M146L mice, there was a 35% reduction of CA1-3 neurons, an extent larger than could be explained only by amyloid plaque pathology (Schmitz *et al.* 2004). Casas *et al.* used the same APP751SL mice and crossed them with PS1 knock-in mice

harboring two human PS1 mutations (M233T/L235P) in the endogenous mouse PS1 gene. The latter transgenic model is named APP/PS1KI, displaying more than 50% CA1 neuron loss at 10 months of age, starting at approximately 6 months of age preceded by robust intraneuronal A β accumulation (Casas *et al.* 2004). Early pathological alterations before onset of plaque deposition that might be related to intraneuronal A β accumulation have also previously reported in other mouse models. These include deficits in synaptic transmission (Hsia *et al.* 1999) or changes in behavior and deficits in long-term potentiation (Moechars *et al.* 1999).

It is well established that APP undergoes fast axonal transport (Koo *et al.* 1990) and plays an important role in axonal and synaptic processes. Abnormal axons spatially distinct from the hallmark lesions of AD (plaques and tangles) are evident as focal axonal swellings that correspond to axonal cargoes and transport proteins (Stokin *et al.* 2005). Recently axonal deficits and degeneration have been described in AD (Dai *et al.* 2002) and in different APP transgenic mouse models overexpressing human APP in brain and spinal cord (Stokin *et al.* 2005; Wirths *et al.* 2006) including APP/PS1KI mice (Wirths *et al.* 2006). These axonal alterations manifest as varicosities and spheroids, which mostly contain abnormal accumulations of mitochondria, organelles and other axonally transported material like neurofilaments, synaptic proteins or APP. Stokin *et al.* have pointed out that inhibition of axonal transport leads to increased intraneuronal A β accumulation (Stokin *et al.* 2005). Interestingly, intraneuronal A β accumulation precedes axonal degeneration in APP/PS1 models (Wirths *et al.* 2006; Wirths *et al.* 2006). Aberrant intraneuronal A β accumulation resulted in impaired axonal integrity in the APP/PS1 mouse models.

It is well established that AD patients suffer from working memory deficits (Baddeley *et al.* 1991). However, motor performance deficits have also been described to occur in AD patients e.g. gait disturbances, disturbed activity level and balance, as well as general motor signs (Alexander *et al.* 1995; O'Keefe *et al.* 1996; Pettersson *et al.* 2002; Scarmeas *et al.* 2004). Since APP/PS1KI mice develop severe age-dependent axonal degeneration, (Wirths *et al.* 2006) as well as loss of hippocampal CA1/2 neurons starting at the age of 6 months (Casas *et al.* 2004), the aim of the present study was to investigate these mice with respect to impairment in motor performance and working memory, neuron loss and hippocampal shrinkage.

2.3.4 INFLAMMATION OF THE BRAIN

GENERAL REMARKS

The occurrence of neuroinflammation meanwhile is a well accepted constant feature of AD.

The process of plaque formation together with the formation of neurofibrillary tangles and neuronal degeneration is widely thought to play a key role for beginning inflammation in human AD cases (Arnaud *et al.* 2006). While the event of inflammation in the brain was formerly believed to be a peripheral phenomenon to the disease, meanwhile the hypothesis of neuroinflammation as one of the potential triggers for neurodegeneration and other pathological hallmarks of AD gains in acceptance (Arnaud *et al.* 2006; Streit *et al.* 2004).

Actually, the three main pathological hallmarks of AD like deposition of aggregated A β , intraneuronal neuritic tau pathology and the brain-specific inflammatory response are speculated to be linked by the fact that proinflammatory microglia, reactive astrocytes and their associated signalling cascades inflicting cytokines and chemokines are associated with the biology of the microtubule associated protein tau, A β speciation and aggregation (Lukiw & Bazan 2000; Moore & O'Banion 2002).

The importance of inflammation in the pathogenesis of AD was indirectly confirmed by epidemiological investigations that revealed a decreased incidence of AD in subjects using anti-inflammatory drugs, especially the non-steroidal anti-inflammatory drugs (NSAIDs) (Wyss-Coray 2006). However clinical trials designed to inhibit inflammation have failed in the treatment of AD patients suggesting that anti-inflammatory agents have more protective than therapeutic effect. Despite ongoing research, the extent to which neuroinflammation contributes to disease pathogenesis is still not fully understood. Moreover it is also not clear whether the inflammation in AD brains represent a protective reaction to neurodegeneration or it is rather a destructive process that contributes to further loss of brain function (Akiyama *et al.* 2000).

RELATED PROJECT

Though the occurrence of inflammatory events represents a phenomenon well described for Alzheimers disease (AD), the extent to which and the way how inflammatory processes interdigitate with the pathology of the disease are still a matter of intense surveillance.

The process of plaque formation together with the occurrence of neurofibrillary tangles and neuronal degeneration is widely thought to play a key role for beginning inflammation in human AD cases. In a classical understanding, tissue damage and chronic presence of highly inert abnormal material is a main cause of inflammation. In parallel it is often suggested that in AD plaques of A β , tangles and the event of neurodegeneration with the exposition of intracellular DNA and neurofilaments to the extracellular environment in the followup are the main trigger for the activation of several general inflammation pathways in human brains affected by AD. Human plaque pathology is characterized by diffuse A β deposits developing an amyloid core positive for staining with thioflavin-S or Congo-Red, with proceeding pathology that is accompanied by gradual accelerating cognitive dysfunction. While, in human, most cases of AD appear sporadically, about 10% of patients are being stroked by so-called early-onset AD, that is induced by range of different mutations in amyloid precursor protein (APP), presenilin 1 (PS1) or presenilin 2 (PS2).

Usually, transgenic mice capable of modelling the pathogenic processes associated with AD are produced by implementation of these familial autosomal dominant (FAD) mutations – based on the idea of the β -amyloid hypothesis assuming amyloid plaques to be the primary driver to propel the progress of AD (Chishti *et al.* 2001; Dudal *et al.* 2004; Ozmen *et al.* 2005; Richards *et al.* 2003). In numerous of these animal models of AD inflammation is a well described phenomenon. Most of them share several pathological characteristics of AD, e.g. extracellular amyloid peptide (A β) deposition in neuritic plaques often associated with activated microglia and surrounded by reactive astrocytes, and/or intracellular deposits of hyperphosphorylated Tau protein observable as the so called neurofibrillary tangles (NFT). However, though a lot of transgenic mouse models of AD available today manage to recapitulate AD pathology including behavioural deficits more or less extensively, still no current transgenic model is able to completely reflect all relevant features of this disease (Dodart *et al.* 1999; Eriksen & Janus 2007; Gordon *et al.* 2001).

Aim of this study is the analysis of the inflammation situation of the APP/PS1KI mouse model of AD introduced by Casas *et al.* (Casas *et al.* 2004).

This APP/PS1KI model is characterized through fast and aggressive formation of AD pathology and excels through an age-related neuron loss that is to be missed in most other transgenic animal models of AD. Neuron loss was detected to take place in the CA1/2 pyramidal cell layer of the hippocampus to an extent of 42% at 12 months of age with a macroscopically evident loss already at six months of age (see chapter 4.1.6). The histopathological onset of AD according to A β build-up starts in these mice with massive accumulation of intraneuronal A β already in the second month of life of these mice (Casas *et al.* 2004). Generally, plaque pathology in APP/PS1KI mice is preceded by the accumulation of oligomeric, fibrillar and various N-modified A β species in brain and spinal cord motor neurons in young mice (Wirths *et al.*, 2006). No behavioural phenotype was detected in these mice at 2 months of age compared to age matched PS1KI control mice according to motor or cognitive deficits. Additionally, no neuronal loss was present at 2 months of age. Based on the finding that APP/PS1KI mice appear to be normal at 2 months of age, I decided to analyze these young mice for signs of early inflammation.

At six months of age APP/PS1KI mice show strong impairments in their working and spatial memory performance and own a significant neuron loss in the CA1/2 pyramidal cell layer of the hippocampus (Casas *et al.* 2004). As a follow-up process to intracellular accumulation of A β six-month-old APP/PS1KI mice show abundant extracellular plaque pathology, dystrophic neurites and astrogliosis. Plaques of APP/PS1KI mice harbour a broad variety of N-truncated isoforms of A β (Casas *et al.* 2004).

Summing up, APP/PS1KI mice pattern typical pathological and behavioural hallmarks of AD model the human process of AD quite well. Therefore, they represent a suitable model for studying human-like AD-pathological processes.

Therefore, the APP/PS1KI mouse model is of interest to examine the development of inflammation in relation to the progress of the disease pathology. In difference to most other studies of inflammation in the ageing brain, I analyzed a broad range of inflammation markers from the field of cytokines and cytokine receptors, toll like receptors, transcription factors and acute phase proteins and looked as well for proteins involved in metal homeostasis and oxidative stress defense e.g. from the group of metallothioneins because of the presumed accelerating impact of free radicals on inflammatory processes. I analyzed the expression of

the genes of interest primarily by qPCR and validated some of the candidates found to be significantly changed in APP/PS1KI mice compared to control mice by Western Blot or immunohistochemical methods on the protein level. The scope of this study is to assign certain states of inflammation to certain states in the pathological processes inflicted with AD. Because the causality between AD and inflammation is still unclear, a closer look to the order of time by that changes in the expression of inflammation genes take place in comparison to the upcoming of typical AD pathological characteristics is of interest. Such information may help to answer the question, if inflammation of the brain is just a side effect of AD pathology or if inflammatory processes may contribute their deadly deed to the progress of cognitive decline in AD patients.

2.3.5 CHOLESTEROL AND 24(S)-HYDROXYCHOLESTEROL IN PLASMA AS POTENTIAL BIOMARKERS OF ALZHEIMER`S DISEASE

GENERAL REMARKS

Until today, for AD no biomarker is readily available to aid diagnosis or monitoring of this common neurodegenerative disorder (Hye *et al.* 2006). However, while diagnosis of AD is still made primarily on clinical grounds, early diagnosis of AD would be an indispensable tool to initiate symptomatic treatment of this disease e.g. with acetylcholine esterase inhibitors as one of the current standard therapies (Blennow 2005). In a large series of studies numerous potential biochemical biomarkers for AD have been investigated from various tissues including blood (Zhang *et al.* 2004) and cerebrospinal fluid (Hampel *et al.* 2004). Most of these studies report about decreased A β ₁₋₄₂ and increased tau and phosphor-tau in CSF of AD affected patients compared to non-demented persons (Blennow & Hampel 2003; Sunderland *et al.* 2005). However, broad appliance of CSF scans for early AD diagnosis is questioned by the circumstance, that the method of lumbar puncture, especially repeatedly, represents a relatively invasive procedure discomfitting to a lot of patients. Contrastingly, blood and plasma are easily accessible body fluids. Moreover, the fact that around 500 mL of CSF are absorbed into the blood every day renders obvious, that suitable AD biomarkers can be found also by specific plasma analysis (Hye *et al.* 2006).

Cholesterol represents an inevitable component of all cell mebranes and is important as a structural component and as a modulator of cell fluidity as well (Sjogren *et al.* 2006).

Cholesterol is synthesized in the liver. Another main source of cholesterol is its uptake by diet from animal products. Total cholesterol plasma levels increase steadily with age in men and women between ages 20 and 65 (Sjogren *et al.* 2006). Epidemiological, biochemical and genetic evidence links cholesterol to Alzheimer's disease, as it has been demonstrated that cholesterol modulates APP processing (Wirths *et al.* 2006).

Recently, Mielke *et al.* reported in a population-based 70-year-old birth cohort followed for 18 years that increasing levels of plasma total cholesterol at ages of 70, 75, and 79 are related to a reduced risk of dementia between ages 79 and 88 (Mielke *et al.* 2005). However, the association of high levels of plasma cholesterol with a decreased risk of AD is in contrast to other reports that suggest high total plasma cholesterol to be a risk factor for later dementia (Kuusisto *et al.* 1997).

Furthermore, also 24(S)-hydroxy-cholesterol has been discussed as a predictive biomarker for the incidence of Alzheimer disease. Therefore, I analyzed mice of the genotypes APP/PS1KI, APP, PS1KI and wildtype mice for age-dependent changes in levels of plasma cholesterol and 24(S)-hydroxycholesterol between the distinct genotypes.

24(S)-hydroxycholesterol has been suggested as a suitable biomarker for AD. 24(S)-hydroxycholesterol is a specific degradation product of brain cholesterol (Kolsch *et al.* 2001, Kolsch *et al.* 2003, Lutjohann *et al.* 2002). Brain cholesterol is assumed to represent a permanent pool of exclusively locally synthesized cholesterol that is protected from exchange with the periphery by its inability to cross the blood-brain-barrier (Bjorkhem & Meaney 2004). The main elimination reaction of cholesterol from the brain occurs by its conversion to 24(S)-hydroxycholesterol by enzymatic activity of CYP46, which is exclusively expressed in human brain, (Lutjohann *et al.* 2002, Dietschy & Turley 2001). It has been shown that 24(S)-hydroxycholesterol in contrast to cholesterol is capable of crossing the blood-brain-barrier and therefore can be detected in easily accessible body fluids like plasma or serum (Bjorkhem *et al.* 2001). In AD patients the levels of 24(S)-hydroxycholesterol have been shown to be significantly elevated in early stages of the disease, potentially due to disruptions in the blood-brain-barrier. The higher efflux of 24(S)-hydroxycholesterol has been hypothesized to be a result of neuron loss or an altered cholesterol metabolism in AD (Locatelli *et al.* 2002). Additionally, lower levels of cholesterol normalized 24(S)-hydroxycholesterol levels in plasma have been described in more advanced cases of AD, (Bretillon *et al.* 2000, Kolsch *et*

al. 2004). Therefore elevated 24(S)-hydroxycholesterol plasma levels have been discussed as an easily accessible biomarker for the diagnosis of AD in early stages of the disease. Although there are also reports about increased levels of 24(S)-hydroxycholesterol in CSF and plasma of AD patients, up to now there is no clear evidence for the suitability of plasma 24(S)-hydroxycholesterol as an early-onset marker for AD (Irizarry 2004, Schonknecht *et al.* 2002, Teunissen *et al.* 2003).

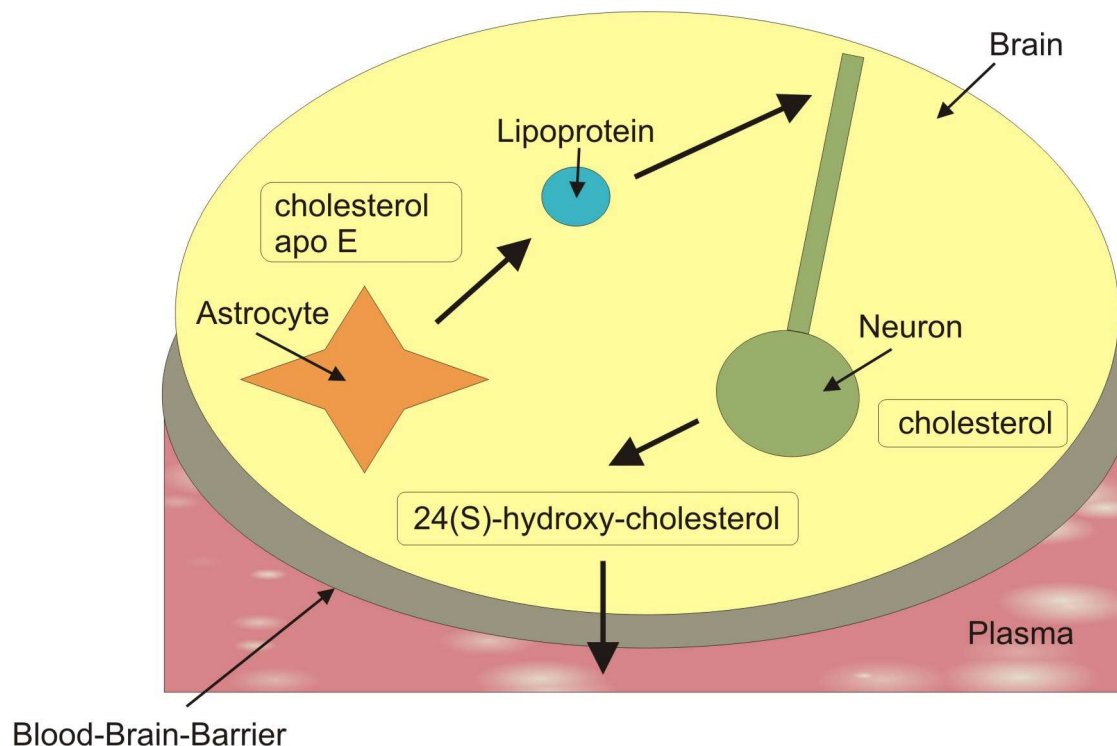


Fig. 6: Model of cholesterol homeostasis in the brain. Neurons synthesize cholesterol in cell bodies. However, additional cholesterol can be supplied to axons from glia-derived lipoproteins. Cholesterol and apo E are synthesized by glial cells (astrocytes) and associate to form lipoprotein particles. These lipoproteins can bind to neuronal surface receptors of the LDL receptor family. Excess cholesterol in the brain is converted to 24(S)-hydroxycholesterol in neurons, crosses the blood–brain barrier, enters the plasma and is delivered to the liver for excretion into bile.

RELATED PROJECT

To check for pathology-dependent changes of plasma cholesterol and 24(S)-hydroxycholesterol, levels of total cholesterol and 24(S)-hydroxycholesterol were determined in plasma of wildtype, APP^{SL}, PS1KI and APP/PS1KI transgenic mice. This latter mouse model has been shown to feature massive neuron loss in the hippocampus starting at an age of six months besides amyloid plaque formation starting already at two to three months of age.

This transgenic mouse model carries M233T/L235P knock-in mutations in presenilin-1 and overexpresses mutated human β -amyloid precursor protein. These mice recapitulate very well typical features of AD like dystrophic neuritis, synaptic dysfunction and behavioural deficits as well as neuronal loss.

Because the cause of the disease is very well described in this model of AD, it also volunteered to check the validity of 24(S)-hydroxycholesterol or total plasma cholesterol as a suitable biomarker for AD.

2.4 MODELLING OF HUMAN ALZHEIMER'S DISEASE IN TRANSGENIC MICE

2.4.1 OVERVIEW ABOUT TRANSGENIC MOUSE MODELS OF ALZHEIMER'S DISEASE

Transgenic mouse models of AD have greatly contributed to our understanding of this disease's pathogenesis. Transgenic mice models generally are designed on basis of mutant genes as they have been found in human early onset or familial cases of AD. They display to a higher or lower extent the neuropathological features that are seen as typical for human AD like aberrant $A\beta$ aggregation, formation of NFT's, neuron loss and synaptic deficits as well as a broadly established scenery of neuroinflammation in the brain. Transgenic mice models overexpressing human mutant APP typically show increased production of amyloid β and reveal a more or less severe pattern of diffuse or compact amyloid plaques in immunohistochemical stainings. These mice display also mostly synaptic transmission deficits, that are detectable well before the build-up of massive plaque pathology. Some of these APP based models also display features like neurodegeneration or cognitive deficits. The combination of APP transgens with an additional overexpression of PS1 further increases production of Amyloid β and significantly accelerates the development of an AD like phenotype and pathology respectively.

Other mice models contain a human mutant tau transgene as can be found in familial forms of frontotemporal dementia, for which extensive tangle formation is a dominant characteristics. Oddo et al. reported about a 3-fold transgenic mouse model, harbouring mutant transgenes for tau^{P301L}, APP^{K670N,M671L} and PS1^{M146V}. This model shows plaque pathology, tangles and also

displays synaptic transmission deficits. In the next chapter, the focus is on the so called APP/PS1KI mouse model of AD, which was first described by Casas et al. in the year of 2004 (Casas *et al.* 2004).

2.4.2 THE APP/PS1KI MOUSE MODEL OF ALZHEIMER`S DISEASE

GENERAL REMARKS

Casas et al. reported in 2004 about a new transgenic mouse model with altogether five mutant transgens, that are related to human early onset AD cases (Casas *et al.* 2004a). In detail, these mice carry the Swedish (K670N/M671L) and London (V717I) mutation in the APP gene controlled by the THY1-promotor, which drives gene expression specifically in neurons. In these mice, the APP₇₅₁ isoform is expressed. Additionally, these mice carry two knock-in mutations in the PS1 gene at codons M233T and L235P. Due to the choosen knock-in strategy, expression of these mutations takes place under control of the endogenous promotor. These mutations were specifically chosen because of their linkage to very early onset FAD at 29 (L235P) and 35 (M233T) years of age.

The predominant species of Amyloid β in these mice is $A\beta_{x-42}$. Calculated over total amyloid β plaque load, a relative share of $A\beta_{x-42}$ of 85% was determined at an age of already 4 months. This ratio showed a further age-dependent increase, while 4 months old APP^{SL} littermated revealed only a 30% share of $A\beta_{x-42}$. This indicates, that presence of FAD-linked PS1KI mutations in APP/PS1KI mice contribute significantly to the formation of $A\beta_{x-42}$. By immunohistochemical methods first plaque deposition using 4G8 antibody could be detected at 2.5 months of age in the subiculum area in APP/PS1KI mice compared to six months of age in APP^{SL} mice. APP/PS1KI mice display widespread and numerous round compact $A\beta$ deposits within the cortical, hippocampal, and thalamic areas. This is in contradiction to APP^{SL} mice, which show only very few deposits restricted to the areas of the subiculum and deeper cortical neuronal layers.

Detailed analysis of the hippocampal CA1-3 subfield and of the dentate gyrus showed, that APP/PS1KI mice show a significant reduction of the hippocampal pyramidal cell layer thickness, that was found to be particularly prominent in the CA1 region at 6 months of age in female mice to an extent of 33%. Assessment of neuron loss by high-precision design-

based stereology showed a neuron loss in CA1 hippocampal subfield of 42% in female APP/PS1KI mice of 12 month of age (see chapter 4.1.6).

It is to note, that by macroscopic analysis some CA1 neuron loss was present as early as 6 months of age in the brains of female APP/PS1KI mice but not in males, suggesting a gender effect in these mice (Casas *et al.* 2004).

This gender effect experienced a closer analysis in APP^{SL} mice, where in 3.5 month old mice well before onset of plaque pathology female mice showed significant higher levels of soluble A β and an elevated ratio of C99/APP as well compared to mal littermates (Schafer *et al.* 2007).

APP/PS1KI mice showed also prominent axonopathy, and actually A β is controversially discussed to work as a trigger for aberrant axonal transport in the pathophysiology of AD, finally ameliorating motor deficits as frequently observed in patients with AD. Immunohistochemical and ultrastructural analysis by electron microscopy in APP/PS1KI mice revealed characteristic axonal swellings, spheroids, axonal demyelination and ovoids, which are myelin remnants of degenerated nerve fibers, in an age dependent manner. Furthermore, abundant accumulation of intraneuronal N-modified A β , Thioflavine S-positive material and ubiquitin was found within the somatodendritic compartment of neurons. These pathological findings were confirmed in neurons of the brain and the spinal cord (Wirths *et al.* 2006).

RELATED PROJECT

A further striking feature of the APP/PS1KI mouse model besides the expression of A β_{x-42} is the progressive development of a complex pattern of N-truncated variants and dimers of Amyloid β that parallels well the composition of A β species observed in human AD brains. In detail, human A β isoforms 2/3-42, 4/5-42, 8/9/10/11-42, 12/13/14-42 and most notably pyroglutamate A β (A $\beta_{3(pE)}$) were determined by proteomic analysis of brain lysates of 10 months old APP^{SL}PS1KI mice in a two-dimensional western-blot (Casas *et al.* 2004). It is to emphasize, that the APP/PS1KI mouse model was the first to show accumulation of A $\beta_{3(pE)}$, which stands in the focus of the TBA1 and TBA2 mouse model because of its striking neurotoxic potential (see chapter).

The APP/PS1KI mouse model was the first transgenic AD mouse model, that was reported to combine a strongly increasing extracellular plaque pathology, consisting of a wide variety of N- and C-terminal truncated isoforms of A β , with a preceding accumulation of intracellular A β species especially in the CA1/2 region of the hippocampus. This was speculated to trigger neuron loss, that occurs as early as 6 months in this mouse model in the pyramidal cell layer of the hippocampus and is quantified to reach 33% in 6 months old APP/PS1KI mice.

Aim of this project was to analyze in a quantitative way the accumulation of N-terminal truncated or racemized A β peptides - especially A $\beta_{3(pE)}$ - in 2 and 6 month old APP/PS1KI mice by Sandwich-ELISA measurements and immunohistochemical stainings.

2.4.3 IN VIVO FORMATION OF PYROGLUTAMATE A β IN TBA1 AND TBA2 MICE

GENERAL REMARKS

One of the most coherent arguments pointing against the Amyloid- β hypothesis, is the finding of constant and abundant deposition of A β in the brains of elderly subject without any signs of cognitive decline. One suggested reason for this finding is speculated to be founded in differences of plaque composition in human AD brains and those of non AD-affected but plaque-bearing healthy controls (Piccini *et al.* 2005). Piccini et al. showed, that soluble A β aggregates as found in AD are characterized by a predominance of N-truncated variants of A β over the full-length protein A β_{1-42} . The authors noted, that A $\beta_{3(pE)}$ was the most prevailing N-truncated A β species in AD affected brains. Harigaya et al. reported already before, that A $\beta_{3(pE)}$ contributes to the total plaque load in AD patients up to an extent of 25% (Harigaya *et al.* 2000). Piccini et al. suggested, that the enrichment of A $\beta_{3(pE)}$ in plaques could be explained as consequence of a partial gain in resistance to extracellular aminopeptidase activity due to the cyclization of N-terminal glutamate of A β_{3-42} (Piccini *et al.* 2005).

Already before, it has been a well established fact, that amyloid plaques do not consist of only a few full length, unmodified A β proteins like A β_{1-40} and A β_{1-42} . Already in 1992, Mori et al. first described the presence of A $\beta_{3(pE)}$ using mass spectrometry of purified A β protein from AD brains, which explains the difficulties in sequencing the amino-terminus (Mori *et*

al. 1992). They reported that 10-15% of the total A β isolated by this method begins at position 3 with A $\beta_{3(pE)}$). Iwatsubo *et al.* analyzed the composition of diffuse plaques from cerebral and cerebellar cortex, neostriatum and hypothalamus of Down's syndrome, Alzheimer's disease and non-demented healthy control brains. First, they found by use of carboxy-terminal antibodies, that diffuse plaques show a positive staining for A β_{x-42} but were negative for A β_{x-40} . This finding strongly suggests, that A β_{x-42} variants are much more prone to aggregation than A β_{x-40} variants (Iwatsubo *et al.* 1996). Most interestingly, strong immunoreactivity was found in these diffuse plaques for N-terminal modified or truncated variants of A β_{x-42} . In detail, Iwatsubo *et al.* reported besides strong accumulation of A $\beta_{N1}(L-Asp)$, which represents the unmodified natural form of A β_{1-42} , also massive aggregation of A $\beta_{N1}(L-isoAsp)$, A $\beta_{N1}(D-Asp)$, and also for pyroglutamate Amyloid β (A $\beta_{3(pE)}$). Additionally, weak staining patterns were detected for pyroglutamate A $\beta_{N11-42(pE)}$ and for A $\beta_{N17}(Leu)$ (Iwatsubo *et al.* 1996). Lemere *et al.* reported in 29 year old Downs Syndrome patients immunoreactivity for A $\beta_{3(pE)}$ in a larger number of plaques than A β_{N1-42} , the former showing a stronger age-dependent increase than the latter (Lemere *et al.* 1996). A similar finding was reported by Saido *et al.*, who found A $\beta_{3(pE)}$ to represent the predominant species of A β in senile plaques of aged individuals (Saido *et al.* 1996). The authors speculated A $\beta_{3(pE)}$ aggregation to precede the aggregation of the full length protein A β_{N1-42} and suggested the increased aggregation predisposition of A $\beta_{3(pE)}$ to have its reason in the bigger hydrophobicity of this A β species due to the loss of one positive and two negative charges due to formation of the lactam functional group (Saido *et al.* 1996). The phenomenon of A $\beta_{3(pE)}$ aggregation preceding that of full length A β variants was also reconsidered by Lemere *et al.*, who found in Downs Syndrome patients of age 27 or older positive and stronger immunoreactivity for A $\beta_{3(pE)}$ at earlier and all ages as well than for A β_{N1-42} (Lemere *et al.* 1996). In general, N-terminal deletions enhance aggregation of β -amyloid peptides *in vitro* (Pike *et al.* 1995). Besides higher aggregation propensity (He & Barrow 1999; Schilling *et al.* 2006) and stability (Kuo *et al.* 1998b), A $\beta_{3(pE)}$ shows an increased toxicity compared to full-length A β (Russo *et al.* 2002). In the latter study, Russo *et al.* have shown, that A $\beta_{3(pE)-40/42}$ supplemented to the culture media affect cultured neuron and astrocyte survival to a significant higher extent compared to corresponding full-length peptides and, moreover, show resistance to degradation by astrocytes. However, other studies reported that the toxicity of A $\beta_{3(pE)-40/42}$ is similar to that of A β_{1-40} and A β_{1-40} (Tekirian *et al.* 1999), and that A $\beta_{3(pE)}$ is not the major variant in AD brain (Lemere *et al.* 1996).

RELATED PROJECT

Recently, Schilling *et al.* have demonstrated *in situ* that pyroglutamate-modified peptides display an up to 250-fold acceleration in the initial formation of A β aggregates (Schilling *et al.* 2006), and presented *in vitro* evidence that the cyclization of glutamate at position 3 of A β is driven enzymatically by glutaminyl cyclase (QC) (Schilling *et al.* 2004).

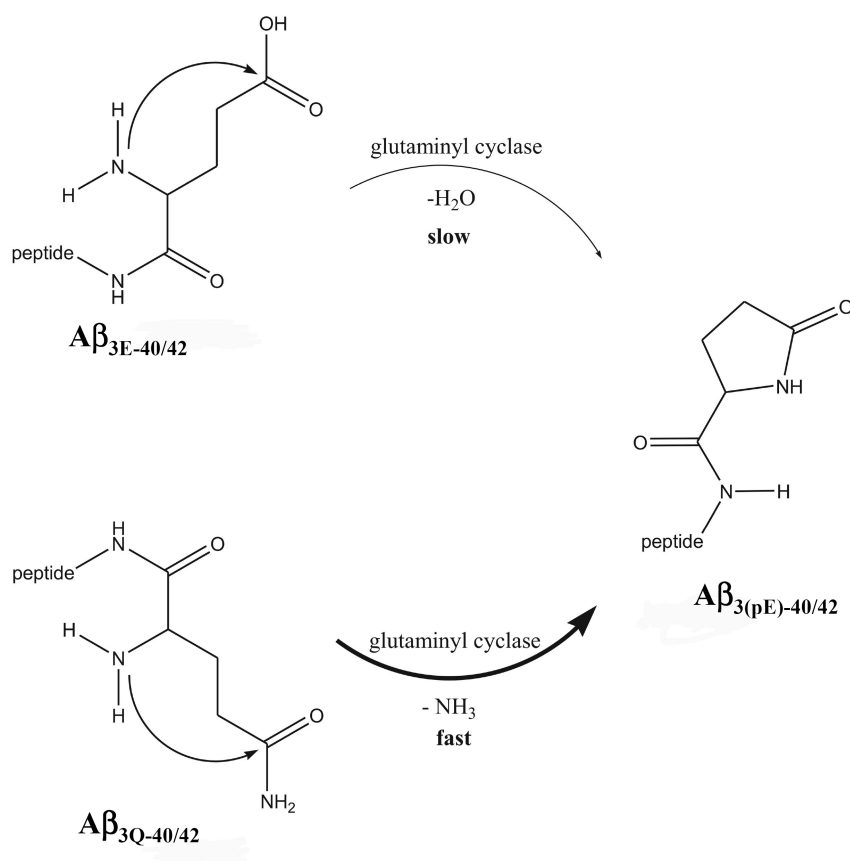


Fig. 7: Formation of A β starting at position 3 with pyroglutamate A β _{3(pE)} is catalyzed by glutaminyl cyclase (QC). N-terminal A β starting with glutamate (A β _{3E}) or glutamine (A β _{3Q}) at position 3 serve as substrates for QC activity to generate A β _{3(pE)} (Schilling 2007). A β _{3(pE)} is a dominant peptide in Alzheimer's disease brain (Saido *et al.* 1995), and aggregates 250 times faster than posttranslationally unmodified A β peptides *in vitro* (Schilling *et al.* 2006). The conversion of pyroglutamate from N-terminal glutamate is slow, in contrast to pyroglutamate formation from glutamine. Pharmacological inhibition of QC activity in cell culture (Schilling 2007) and in the tg2576 APP transgenic mouse model (Schilling 2007) leads to reduced A β _{3(pE)} levels.

While in human Alzheimer's disease as well as in Down's syndrome only a small proportion of A β peptides start at position 1 with aspartate (A β _{N1D}), the majority starts at position 3 with pyroglutamate (A β _{3(pE)}) (Kuo *et al.* 1997; Saido *et al.* 1995), and ends at position 42 (Piccini

et al. 2005). A β starting with N-terminal glutamine (A β_{3Q}) is a better substrate for cyclization by glutaminyl cyclase (QC) as A β starting with N-terminal glutamate (A β_{3E}) (Cynis *et al.* 2006; Schilling *et al.* 2004). To check the ability of QC to drive the formation of A $\beta_{3(pE)}$ *in vivo* I characterized in a first step a mQC transgenic mouse for overexpression of QC. In the next step, two mouse lines transgenic for substrates of QC to form A $\beta_{3(pE)}$ by QC catalysis were designed. These two transgenic mouse lines were expressing either A β_{N3E-42} (Thy1/ β -amyloid-1; TBA1) or A β_{N3Q-42} (Thy1/ β -amyloid-2; TBA2). TBA1 and TBA2 mice were checked for development of accumulation of Amyloid β and especially A $\beta_{3(pE)}$ and analyzed for hereby induced phenotypical changes. TBA1 and TBA2 mice showed mQC activity at endogenous levels. To verify the *in vivo* potential of mQC to catalyze the formation of A $\beta_{3(pE)}$, heterozygous mQC mice were crossed with heterozygous TBA1 mice and analyzed for increased accumulation of A $\beta_{3(pE)}$.

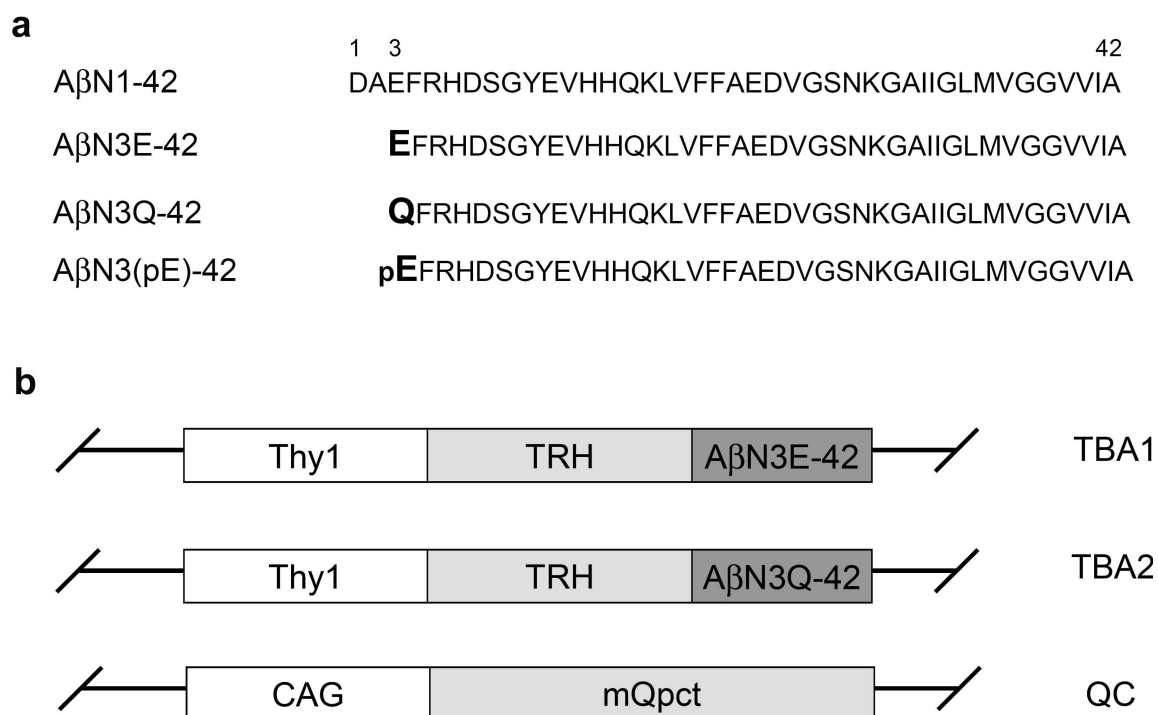


Fig. 8: Constructs to generate the transgenic mice and expression profile in brain at 2 months of age. (a). A β_{1-42} starts at position 1 with aspartate (D), A β_{3E-42} at position 3 with glutamate (E), and A β_{3Q-42} with glutamine (Q). Both N-truncated A β_{3E-42} and A β_{3Q-42} peptides can be converted by QC activity to generate A $\beta_{3(pE)-42}$ (Fig. 7). **(b)** Schematic drawing of the transgenic vectors. TBA1 and TBA2 transgenic mice express either A $\beta_{3(E)-42}$ or A $\beta_{3(Q)-42}$ under the control of the Thy1 promoter and are fused to the signal peptide of TRH. QC transgenic mice express the murine QC minigene (mQpct) under the control of the CAG promoter.

3 MATERIALS AND METHODS

3.1 STATISTICAL ANALYSIS

Differences between groups were tested with either one-way analysis of variance (ANOVA) followed by post-hoc Bonferroni's multiple comparison tests, paired t-test for pair-wise comparisons or unpaired t-tests as indicated in the figure legends. All data were given as means \pm s.e.m. Significance levels were given as follows: *** $P < 0.001$; ** $P < 0.01$; * $P < 0.05$. All calculations were performed using GraphPad Prism version 4.03 for Windows (GraphPad Software, San Diego, CA, USA).

3.2 IMMUNOHISTOCHEMISTRY AND HISTOLOGY

Mice were anaesthetized and transcardially perfused with ice-cold phosphate-buffered saline (PBS) followed by 4% paraformaldehyde. Brain samples were carefully dissected and post-fixed in 4% phosphate-buffered formalin at 4 °C. Immunohistochemistry was performed on 4 μ m paraffin sections. The following antibodies were used: 4G8 (A β 17-24, Signet), GFAP (Chemicon), Iba1 (Waco), ubiquitin (DAKO), AT8 (Innogenetics), PS199 (Biosource), activated caspase-3 (Chemicon), calbindin (Swant) and against A β with pyroglutamate at position 3 (a generous gift of Dr. Takaomi Saido). Biotinylated secondary anti-rabbit and anti-mouse antibodies (1:200) were purchased from DAKO. Staining was visualized using the ABC method, with a Vectastain kit (Vector Laboratories) and diaminobenzidine as chromogen. Counterstaining was carried out with hematoxylin. For fluorescent stainings AlexaFluor488- and AlexaFluor594-conjugated antibodies (Molecular Probes) were used.

Primary antibodies

<i>Name</i>	<i>Usage</i>	<i>Dilution</i>	<i>Manufacturer</i>
WO-2	Anti-human A β (A β 5-8)	1:5000 (WB)	Prof. Gerd Multhaup, FU Berlin
GFAP	Anti-mouse	1:5000 (WB)	DAKO
Iba1	Anti-mouse	(IHC)	Waco
β -Actin	Anti-mouse	1:2000 (WB)	Sigma
S100A6	Anti-mouse	1:3000 (ICH)	generous gift of R. Pochet
Transferrin	Anti-mouse	1:2000 (WB)	Stressgen
A β N1(D)	Anti-human	1:500 (IHC)	Takaimo Saido, RIKEN Institute, Japan
A β N1(rD)	Anti-human	1:500 (IHC)	Takaimo Saido, RIKEN Institute, Japan
A β N3(pE)	Anti-human	1:250 (IHC)	Takaimo Saido, RIKEN Institute, Japan
4G8	Anti-human	1:1000 (IHC)	Senetec

HRP-linked scndary antibodies

Goat-anti-rabbit immunoglobulins (DAKO, P0448, Denmark)

Goat-anti-mouse immunoglobulins (DAKO, P0447, Denmark)

Rabbit-anti-goat immunoglobulins (DAKO, P0449, Denmark)

Biotinylated secondary antibodies

Rabbit-anti-mouse immunoglobulins (DAKO, E0465 Denmark)

Swine-anti-rabbit immunoglobulins (DAKO, E0353 Denmark)

3.3 TRANSGENIC MICE

APP/PS1KI mice

The generation of APP/PS1KI mice has been described in detail in Casas *et al.* 2004 (Casas *et al.* 2004). In brief, human mutant APP751, harboring the Swedish and London mutations (APP751SL) is expressed under the control of the murine Thy-1 promoter, whereas murine PS1 with two FAD-linked mutations (PS1 M233T and PS1 L235P) is expressed under the control of the endogenous mouse PS1 promoter (“knockin”). All mice named as PS1KI were homozygous for PS1 knock-in mutations; the APP/PS1ki mice harbored one additional hemizygous APP751SL transgene. All animals were handled according to German guidelines for animal care.

mQC, TBA1 and TBA2 mice

For generation of murine thyrotropin-releasing hormone - A β fusion proteins mTRH-A β _{3E-42} and mTRH-A β _{3Q-42} (see Fig. 8) the respective cDNAs were inserted into vector pUC18 containing the murine Thy-1 sequence applying standard molecular biology techniques. Murine QC was isolated from insulinoma cell line β -TC 3. The mQC cDNA was cloned into vector pTG-CAG. All constructs were verified by sequencing. The transgenic mice were generated by male pronuclear injection of fertilized C57Bl6 oocytes (PNI, generated by genOway, Lyon, France). The injected oocytes were then implanted into foster mothers for full term development. The resulting offspring (3 founders of each line) were further characterized for transgene integration by PCR analysis and after crossing to C57Bl6 wildtype mice for transgene expression by RT-PCR (n=3-5 each line). The line with highest transgene mRNA expression was selected for further breeding (named TBA1 and QC mice). TBA1 and QC transgenic appeared healthy and showed no evidence for neurological abnormalities. Only 1 of the 3 founders of the TBA2 PNI gave birth to offspring (TBA2 mouse model). All animals were handled according to German guidelines for animal care

3.4 GENOTYPING

DNA-Isolation from mouse tails

Stock solutions:

1 x Lysis buffer:

- 100 mM Tris/HCl pH 8.5
- 5 mM EDTA
- 0.2 % SDS
- 200 mM NaCl

dissolved in. H₂O (Millipore)

Before use Proteinase K was added (10 $\mu\text{L} \cdot \text{mL}^{-1}$).

Protocol

1. 500 μL of lysis buffer were added to each mouse tail and shaken overnight at 55 °C and 400 rpm in a heating block.
2. Centrifugation for 10 min at 13000 rpm
3. The supernatants were transferred to a new 1.5 mL tube containing 500 μL of isopropanole.
4. Samples were vortexed for DNA precipitation and centrifuged for 10 min at 13000 rpm.
5. Pellet was washed by vortexing in 500 μL of 70% ethanole and again centrifuged for 10 min at 13000 rpm.
6. The supernatant was discarded and rests of ethanole removed by pipetting
Pellet was dried on a heating block at 37 °C
7. Pellet was dissolved in 70 μl H₂O (Aqua ad iniectabilia) (37°C, 30 – 45 min or overnight at 4°C)

Polymerase chain reaction (PCR)

Polymerase chain reaction leads to exponential amplification of a DNA fragment.

General protocol for a total 10µL volume

0,5 µL Primer forward (10 pM stock concentration)

0,5 µL Primer reverse (10 pM stock concentration)

1 µL 10 x PCR-Puffer

1 µL dNTPs (200 µM stock concentration)

5.9 µl H₂O

0.1 µL Taq-Polymerase

1 µL diluted DNA (25 ng of genomic DNA)

PCR genotyping strategy for APP/PS1KI mice

primer sequences:

APP-1: 5`-GTA GCA GAG GAG GAA GAA GTG-3`

APP-2: 5`-CAT GAC CTG GGA CAT TCT C-3`

The PCR on tail DNA was carried out in a volume of 25 µL with a PCR-product of 491 bp length and was run according to the following cycling parameters:

Reaction mix		Reaction conditions		
Genomic mouse DNA	25 ng	step	Temp/time	cycles
Primer	2.5 µL (f.c.: 25 pmol)	denaturing	94°C/300s	1x
dNTPs	2.5 µL (f.c.: 20 µM)	denaturing	94°C/60s	35x
10 x Reaction buffer	2.5 µL	annealing	55°/60s	35x
MgCl ₂	f.c.:1.5 mM	extension	72°C/90s	35x
Taq polymerase	2.5 U	completion	72°C/300s	1x
Reaction volume	25 µL			

Table 1: protocol for APP genotyping (f.c.: final concentration).

PCR genotyping strategy for mQC, TBA1 and TBA2 mice

The screening for detection of the random integration of the transgene was achieved by PCR amplification. Two PCRs were designed (see Figure 4):

- PCR1 is designed to efficiently detect the transgene random integration event. The selected primer pair allows the amplification of a short DNA sequence within the transgene sequence, yielding a specific 505-bp PCR product.
 - PCR2 is designed to assess the integrity of the transgene integration event. The selected primer pair allows the amplification of a DNA sequence extending from 5' region of promoter and 3' region of Thy1 gene yielding a specific 6279-bp 7413-bp PCR product.
- As the Thy1 promoter cassette is derived from mouse genomic sequence, the PCR screen, used to investigate the integrity of the transgene integrity, also lead to the amplification of a 7413-bp product from the endogenous Thy1 gene.

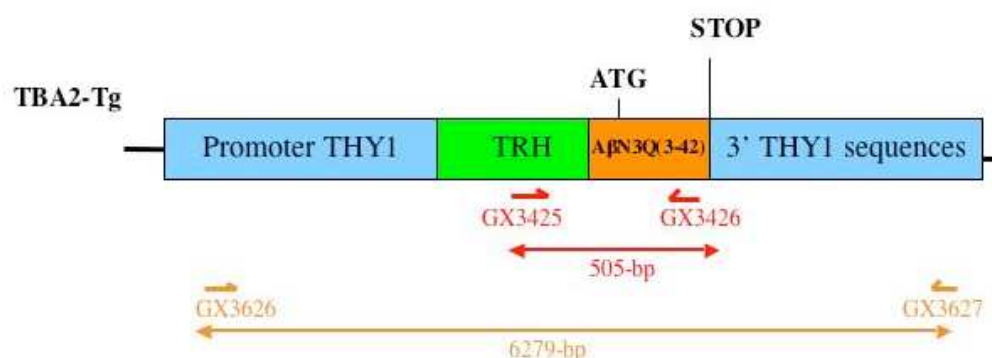


Fig. 9: PCR genotyping methodology: Localisation of primers used for the detection of random integration and transgene integrity. The corresponding amplification product sizes are indicated. Bold line represents plasmid backbone sequences. Half arrows illustrate the primers' localisation. Figures are not depicted to scale. The same structure has the TRH-A β N3E(3-42) transgene construct.

Primer pair	Primer name	Primer sequence 5'-3'	expected PCR size
1	GX3425	5'- AGTAATGAAGTCACCCAGCAGGGAGG -3'	505 bp
	GX3426	5'- TGATCCAGGAATCTAAGGCAGCACC -3'	

Table 2: PCR genotyping TBA1 & 2

Reaction mix		Reaction conditions		
Genomic mouse DNA	40 ng	step	Temp/time	cycles
Primer	0.5µL (f.c.: 2.5 pmol)	denaturing	94°C/180s	1x
dNTPs	20 µM	denaturing	94°C/45s	35x
10 x Reaction buffer	1 µL	annealing	58°/60s	35x
MgCl ₂	2 mM	extension	72°C/60s	35x
Taq polymerase	0.5 U	completion	72°C/300s	1x
Reaction volume	20 µL			

Table 3: Protocol for genotyping by PCR: TBA1 & 2.

Genotyping of mQC mice

Primer pair	Primer name	Primer sequence 5'-3'	expected PCR size
1	mQC3 mQC4	5'-GCCACGGATTTCAGCTGTGC-3' 5'-GAATGTTGGATTGCTGCTC-3'	302 bp

Table 4: PCR genotyping mQC.

Reaction mix		Reaction conditions		
Genomic mouse DNA	100 ng	step	Temp/time	cycles
Primer	2 µL (10 pmol	denaturing	94°C/180s	1x
dNTPs	2 µL (f.c.: 20 µM)	denaturing	94°C/45s	35x
10 x Reaction buffer	2 µL	annealing	58°C/60s	35x
MgCl ₂	1.6 µL (f.c.2 mM)	extension	72°C/60s	35x
Taq polymerase	0.5 U	completion	72°C/300s	1x
Reaction volume	20 µL			

Table 5: Protocol for genotyping by PCR: mQC.

3.5 mRNA QUANTIFICATION FOR TBA1 AND TBA2 MICE

For Real-Time PCR (TBA1 & 2) the following primers were used:

Primer pair	Primer name	Primer sequence 5'-3'	expected PCR size
1	A β 3-42-for A β 3-42-rev	5'-TTGAGGAAAGACCTCCAGC-3' 5'-CATGAGTCCAATGATTGCACC-3'	168 bp

Table 6: Primers for amplification of A β _{3E} and A β _{3E}.

1 μ g of total RNA was reverse transcribed and Real-Time PCR was performed using the fluorescent dye SYBR-Green I according to the following protocol:

Reaction mix		Reaction conditions		
cDNA	1 μ L (1:5 Dilution)	step	Temp/time	cycles
Primer	15 pmol	denaturing	95°C/ 600s	1x
2x Reaction Mix	12.5 μ L	denaturing	94°C/15s	40x
SYBR-Green I	0.5 μ L	annealing	55°C/30s	40x
H ₂ O	8 μ L	extension	72°C/30s	40x
Reaction volume	25 μ L	Melting Curve	55°C - 95°C/ 30s	1x

Table 7: Protocol for mRNA quantification by RT-PCR.

3.6 STAINING OF PARAFFIN-SECTIONS

1. Deparaffinize
2x5 min xylol
10 min 100% ethanol
5 min 95% ethanol
2. Block in methanol
200 mL PBS
2 mL 30% H₂O₂
for 30min
3. Descending ethanol-series
5 min 95% EtOH
1 min 70% EtOH
1 min distilled water
4. microwave treatment 10 min (in 0.01M citrate buffer pH 6.0 (citric acid monohydrate)
5. cool down for 15 min
6. wash 1min in distilled water.
7. wash 15 min PBS + 0,1% Triton-X100
8. wash 1 min with PBS
9. –optional- incubate sections in 88% formic acid for 3 min
10. wash with PBS
11. unspecific block for 1 h in PBS +10% FCS (fetal calf serum)
+4% dry milk (40mg/ml)
12. Discard blocking solution and add primary antibody in PBS including 10% FCS
Incubate over night at room temperature or 4 °C
13. wash 15 min with PBS+ 0,1% Triton-X100
14. Incubation with secondary antibody in PBS including 10% FCS for 1 h at 37 °C
15. wash 15 min with PBS
16. Incubation with ABC-Vectastain-Complex (prepare at least 30 min before use and keep and 4 °C)(Vector Laboratories) for 1.5 h at 37 °C
PBS +10% FCS, +1:100 Lösung A, +1:100 Lösung B
17. wash 15 min with PBS
18. stain with 3,3-diaminobenzidine-tetrahydrochloride (25 mg/mL in 50 mM Tris/HCl pH 7.5,DAB, Sigma)
19. ascending ethanol-series,
1 min 70% ethanol
5 min 95% ethanol
10 min 100% ethanol
10 min Xylol

3.7 HPLC-ASSAY FOR DETERMINATION QC-ACTIVITY IN PLASMA

The QC activity was assessed by quantification of the QC-mediated cyclization of Glutaminyl-beta-naphthylamin to pyroglutamyl-beta-naphthylamin by use of a HPLC based assay. The measurement was carried out using a HPLC system “La chrome”, manufactured by Merck-Hitachi and a RP18 LiChroCART 125-4 column supplied by Merck KGaA. For the separation, a gradient of water and acetonitrile containing 1% TFA each was used p.r.t. as follows:

Time (min)	Eluent A Acetonitrile/TFA(1%)	Eluent B Water/TFA (1%)
0	23	77
8	45	55
10	95	5
15	95	5
20	23	77

Table 8: HPLC-protocol for measurement of QC -activity in tissue lysates and EDTA-plasma.

Detection of glutaminyl-beta-naphthylamine and pyroglutamyl-beta-naphthylamine was performed by use of a Diode Array Detector L7455 manufactured by Hitachi Corp. at a wavelength of 280 nm. All measurements were carried out at room temperature. The concentration of pyroglutamyl-beta-naphthylamine was calculated using a standard curve.

Sample Preparation

Determinations of QC-activity were performed using tissue homogenates from brain, liver, kidney and plasma. The plasma was centrifuged at 4 degrees and 13000 rpm for 10 min and applied for the QC-assay. Besides, the plasma of the control group could be used directly unwatered for measurement (100 µL), while that of the QC-mice had to be diluted at first 1:25 with MOPS-buffer (c: 25 mM, pH 7. 0). Tissue of brain, liver and kidney was mixed in 40fold volume lysis buffer and homogenized by use of a Downs homogenizer. The lysis-buffer (pH 7. 5) consisted of Tris-base (10 mM), EDTA (5mM), Triton (0. 5%) and glycerole (10%). Triton concentrations of 0.5% or less showed to have no influence on protein detection by the Bradford method.

Subsequently, the samples were treated with an ultrasonic stick (16 cycles, intensity 70%) and afterwards centrifuged (25 min, 13000 rpm, 4 °C). The supernatants were taken and immediately used for the measurement (100 µL).

Determination of QC-activity

After the sample preparation, every measurement of pyroglutamyl-beta-naphthylamine was carried out according to the following protocol, which has been identical for measurement of the standard curve with affinity purified QC enzyme and of the time-turnover-graphs with QC from the homogenized tissue samples.

In a 1.5 mL tube, 500 µL substrate solution (Glutaminy-beta-naphthylamine, c: 100 µM, in MOPS-buffer, c: 25 mM, pH 7.0) were mixed with 400 µL N-ethyl-maleimide solution (c: 250 µM in MOPS-buffer, c: 25 µM, pH 7.0) as a cysteine-protease-inhibitor. The mixture was allowed to equilibrate to 30 °C for 10 min in a heating block at 350 rpm. After equilibration, the reaction was started by addition of 100 µL of cell lysate or plasma to a total volume of 1000 µL. The reaction mixture was then incubated for 45 min at 30 °C at 350 rpm. From the total reaction volume, samples (100 µL) were removed after 0, 4, 8, 12, 16, 20, 24, 35 and 45 min. To stop the ongoing conversion from glutaminy-beta-naphthylamine into pyroglutamyl-beta-naphthylamine, these samples were immediately heated for 5 min in boiling water to inactivate the enzyme glutaminy-cyclase. Afterwards, the samples were immediately frozen at -20 °C. The experiment was run in three replicates at the same time. Prior to analysis using HPLC, all samples have been frozen once. For the measurement the samples were thawed out and thereafter centrifuged for 10 min at 13000 rpm at room temperature before starting the measuring process on the HPLC system. Then 25 µL of the sample were diluted 1:1 with water bidest and mixed. This solution was injected completely with a 100 µL Hamilton syringe into the 20 µL sample loop of the HPLC system. Between the measurements, the Hamilton syringe was cleaned two times with water bidest, two times with acetone and thereafter two times with water bidest again. Before drawing the syringe with a new sample the needle was rinsed two times (2x 3 µL) with the new sample.

The resulting peak areas for pyroglutamyl-beta-naphthylamine (R_t : ~6.8 min, the retention time of glutaminy-beta-naphthylamine was found around R_t : ~4.85 min) were converted into concentrations of pyroglutaminy-beta-naphthylamine by use of the standard curve. The resulting figures were plotted in a time (x-axis) - turnover (y-axis) - diagram. The initial velocity of the reaction converting glutaminy-beta-naphthylamine into pyroglutaminy-beta-

naphtylamine was calculated by linear regression mostly over the first 20 minutes of the time-turnover-diagram

3.8 QUANTIFICATION OF $A\beta_{x-42}$ AND $A\beta_{N3(pE)}$ BY ELISA

Brains were weight in frozen state and directly homogenized in a Dounce-homogenizer in 2.5 ml 2% SDS, containing complete protease inhibitor (Roche). Homogenates were sonified for 30 s and subsequently centrifuged at 80.000 g for 1 min at 4 °C. Supernatants were taken and directly frozen at –80 °C. The resulting pellets were resuspended in 0.5 ml 70% formic acid (FA) and sonified for 30 s. Formic acid was neutralized with 9.5 ml 1 M and aliquots were directly frozen at –80 °C. SDS and FA lysates were used in appropriate dilutions for both $A\beta_{x-42}$ and $A\beta_{N3(pE)}$. ELISA measurements. ELISA measurements were performed according to the protocol of the manufacturer (IBL Co., Ltd. Japan). For statistical analyses, $A\beta_{x-42}$ and $A\beta_{3(pE)}$ concentrations resulting from SDS and formic acid extractions were cumulated.

3.9 RNA PREPARATION AND REVERSE TRANSCRIPTION

Deep frozen brain hemispheres stored at -80 °C were homogenized in 1 ml of Trizol reagent per 100 mg tissue using a glas-teflon homogenizer (10 strokes, 600 rpm). RNA extraction was performed according to the protocol of the manufacturer (Invitrogen).

Reverse transcription and DNaseI treatment of the purified RNA samples was carried out using QuantiTect Reverse Transcription Kit (Qiagen, Hilden, Germany) according to the protocol of the supplier.

3.10 QUANTITATIVE RT-PCR

Quantitative real-time RT-PCR was performed using a Stratagene MX3000P Real-Time Cycler. 10 ng of cDNA were used per reaction. For quantification I used the SYBR-green based 2x SensiMix DNA Kit containing ROX as an internal reference dye (peqLab, Germany). As not denoted otherwise, all oligonucleotid primers were purchased as validated Primer Sets from Quiagen (QuantiTect Primer Assays). The following primers were ordered at MWG-Biotech, Germany:

- MCSF-R

for: 5'-GACCTGCTCCACTTCTCCAG-3'

rev: 5'-GGGTTCAGACCAAGCGAGAAG-3'

- MHCII

for: 5'-CTGATGGCTGCTCATCCTGTG-3';

rev: 5'-TTCTGTTTTCTGTATGCTGTCC-3'

Statistical analysis of quantitative Real-Time PCR measurements was done by the use of the Relative Expression Software Tool V1.9.6 (REST) (Pfaffl *et al.* 2002). The expression ratio results of the investigated transcripts are tested for significance by a Pair Wise Fixed Reallocation Randomisation Test and plotted using standard error (SE) estimation via a complex Taylor algorithm (Pfaffl *et al.* 2002). In figures, levels of significance were labelled as follows: *** $P < 0.001$; ** $P < 0.01$; * $P < 0.05$.

3.11 WESTERN-BLOT

Deep frozen brain hemispheres stored at -80 °C were homogenized using a glas-teflon homogenizer at 650 rpm in PBS buffer containing 2% SDS (pH7.4, supplemented with complete protease inhibitor cocktail (Roche)). The amount of buffer was adjusted to the brain weight in a 8:1 ratio. Lysates were centrifuged at 4 °C and 16.000 rpm for 1 h. Proteins contained in SDS-brain lysates of APP/PS1KI and PS1KI mice were separated using SDS/Polyacrylamide-gel-electrophoresis in a 8% SDS-glycine-gel. 20 µg protein were applied per lane. Proteins were transferred using semidry blotting for 25 min at 20 V on PVDF membranes (BioRad) according to the manufacturers protocol.

Membranes were blocked in 10% non-fat dry milk in TBS-T buffer containing 0.05% Tween-20 for 1 hour. Primary antibody incubation was performed overnight in TBS-T buffer at 4 °C followed by a two-hour incubation with HRP-conjugated secondary antibodies (DAKO) at room temperature. Blots were developed using enhanced chemiluminescence.

Developed X-ray films were quantified using Quantity one software package (BioRad) with beta-Actin as a reference gene. Statistics of blot data were calculated using GraphPad Prism v4.03.

3.12 PHOTOMETRIC MEASUREMENT OF PROTEIN CONCENTRATION

Measurement of protein concentration was performed by use of the commercially available Roti-Quant universal solution (C. Roth). Detection of proteins after this method is based on the biuret reaction. Absorbance was measured by use of a photometer at 595 nm. Concentrations of proteins were calculated by comparison with an calibration curve derived from BSA samples with a range in concentration from 0 – 20 mg*mL⁻¹. All samples were measured in a transparent 96-well culture plate. In each well 2 µL of sample were diluted with 200 µL of detection solution Roti-Quant universal and incubated for 30 min at 37 °C before measurement.

3.13 AGAROSE GEL ELECTROPHORESIS

Analytical separation of DNA and RNA was performed by agarose gel electrophoresis under non denaturing conditions. This method works by enforced movement of negative charged nucleic acids directed to the anode in an electrical field. The nucleic acids separate in the gel depending on their size. Agarose concentration was adapted between 0.7 and 3.0% to the size of the nucleic acids to be separated. Gels were prepared in TBE buffer. Ethidiumbromide was added to a final concentration of 1 µg*mL⁻¹. Gels were run under a voltage of 170 V. A suitable DNA ladder was loaded on the gel to enable analysis of the size of the separated nucleic acid fragments. Gels were analyzed under UV-light-transillumination conditions at a wavelength of $\lambda = 366$ nm. Ethidiumbromide intercalates into the double-strand structure of DNA or RNA, which leads to an increased fluorescence of the bound pigment compared to the unbound species. Finally, the gel was pictured for documentation purposes.

3.14 X-RAY EXAMINATION

For conventional x-ray examination the specimen were positioned in a supine position on the examination table of a Siemens Siregraph D X-ray unit. Images were taken in a.p. and lateral projection. Images were obtained using 40 kV and 5 mAs current. The images were transferred to a Powermac G5 running Osirix 2.3.1 for post-processing.

3.15 BEHAVIOUR TESTS

Clasping Test

To test clasping behavior, mice were suspended by the tail for 30 s and the hindlimb-clasping time was scored. A duration of 0 sec clasping was given a score of 0, 1-10 s a score of 1, 10-20 s a score of 2 and a clasping of more than 20 s a score of 3 (Nguyen *et al.* 2005).

Balance Beam

Balance and general motor function were assessed using the balance beam task. A 1 cm dowel beam is attached to two support columns 44 cm above a padded surface. At either end of the 50 cm long beam a 9 x 15 cm escape platform is attached. The animal is placed on the center of the beam and released. Each animal is given three trials during a single day of testing. The time the animal remained on the beam is recorded and the resulting latencies to fall of all three trials are averaged. If an animal remains on the beam for whole 60 s trial or escapes to one of the platforms, the maximum time of 60 s is recorded (Arendash *et al.* 2001; Wirths *et al.* 2006).

String Suspension Task

As a test of agility and grip strength, a 3 mm cotton string is suspended 35 cm above a padded surface in the beam apparatus. The animals are permitted to grasp the string by their forepaws and are released. A rating system from 0 to 5 is used during the single 60-sec trial to assess each animals' performance in this task: 0 = unable to remain on the string; 1 = hangs only by fore- or hindpaws; 2 = as for 1, but attempts to climb onto string; 3 = sits on string and is able to hold balance; 4 = four paws and tail around string with lateral movement; 5 = escape (Moran *et al.* 1995).

Vertical Grip Hanging Task

Animals were tested for neuromuscular abnormalities (balance and muscle strength) by suspending them from wire bars (40 x 20 cm area with 1mm wires 1 cm apart). Latency to fall within 60 s was measured after a mouse was placed on the bars and turned upside down (height 30 cm) (Erbel-Sieler *et al.* 2004).

Rotarod

Motor learning and coordination were tested by the use of an accelerating rotarod (TSE-Systems, Germany). The rotating rod had an axis diameter of 3.5 cm and a black rubber surface. Each mouse was given six daily trials for two consecutive days. The mice were placed on top of the beam facing away from the experimenters view. They had to move forward on the drum (which rotates with increasing speed around the vertical axis), being forced to continuously adjust their timing of movements. At the beginning of each trial, mice were placed on the inactive drum, which was accelerated to a speed of 48 rpm over a trial period of 360 s. The time until the animal fell off the rod was recorded with a cut-off after 360 s (Dere *et al.* 2003). Analysis was carried out using a two-way ANOVA (genotype x training day), followed by Bonferroni post hoc tests.

Forced Swimming Test

The forced swimming test is performed identical to a probe test in the Morris Water Maze (Spittaels *et al.* 1999). In brief, a pool with a diameter of 110 cm is filled with opaque water to a height of 20 cm and is kept at 22 °C. The mice were placed in the middle of the pool for one 60 sec single trial and total swimming distance and swimming speed were measured using a computer automated tracking system (VideoMot2, TSE-Systems).

Open Field

The open field test was used to assess both exploratory behavior and locomotor activity. The mice were tested using an open field box made of grey plastic with 50 x 50 cm surface area and 38 cm-high walls. Monitoring was done by an automated tracking system equipped with a rearing indicator consisting of 32 infrared sensors to detect vertical activity (VideoMot2, TSE-Systems, Germany). The behavioral parameters registered during 5 min sessions were (i) running speed and total traveled distance (ii) the ratio of time spent in the central part (20 x 20 cm) versus total time (iii) rearing episodes: the number of times an animal stood upon its hind legs with forelegs in the air or against the wall (measure of vertical activity) (Dere *et al.* 2003).

T-maze continuous alternation task (T-CAT)

A T-maze was used according to the measures provided by Gerlai (Gerlai 1998). The apparatus was made of black plastic material with a black floor and guillotine doors. Testing of the mice consisted of one single session, which started with 1 forced-choice trial, followed

by 14 free-choice trials. (i) Forced-choice trial: in the first trial, one of the two goal arms is blocked by lowering the guillotine door. After the mouse is released from the start arm, it will explore the maze, enter the open arm and return to the start position. As soon as the mouse returned to the start arm, the guillotine door was lowered and the animal was confined for 5 s. (ii) Free-choice trials: After opening the door of the start arm, the animal is free to choose between both goal arms, as all guillotine doors are open. Once the mouse entered a goal arm, the other goal arm is closed. When the mouse returned to the start arm, the next free-choice trial started after 5 s confinement in the start arm. A test session was terminated after 30 min or after 14 free-choice trials were carried out. Animals that performed less than 8 trials within the given time frame were excluded from the analysis, which however was not the case. The animals were never handled during the task and the experimenter was not aware of the genotype of the tested animals.

Y-Maze

Spontaneous alternation rates were assessed using a triangular Y-shaped maze constructed from black plastic material with arm sizes of 30 cm × 8 cm. During 20 min test sessions, each mouse was randomly placed in one arm and allowed to move freely through the maze (Frenois et al., 2002). Alternation was defined as successive entries into the three arms in overlapping triplet sets. An entry was defined to be successive as soon as a mouse enters an arm with all four paws. The percent alternation was calculated as the ratio of actual to possible alternations. In order to diminish odor cues, the maze was cleaned with a solution containing 30% ethanol, 60% water and 10% odorless soap.

Cross-Maze

Spontaneous alternation rates were assessed using a cross-maze (28) constructed from black plastic material (arm sizes: 30.0 cm length, 8.0 cm width, wall height 15.0 cm). Adjacent arms were in a 90° position. The 4 arms extended from a central space measuring 8.0 cm in square. Thus, the animals visited the arms via a central space. During 20.0 min test sessions, each mouse was randomly placed in one arm and allowed to traverse freely through the maze. Individual arms were signed 1 – 4. An alternation was defined as entry into four different arms on consecutive entries on overlapping quadruple sets (for example 2,3,4,1 or 4,2,3,1 but not 1,2,3,2). An entry was defined to be successive as soon as a mouse enters an arm with all four paws. The percent alternation was calculated as the ratio of actual to overall performed alternations during the period of observation. In order to diminish odor cues, the maze was

cleaned with a solution containing 30% ethanol, 60% water and 10% odorless soap after each trial.

3.16 STEREOLOGICAL QUANTIFICATION OF TOTAL NUMBERS OF NEURONS

Mice were anaesthetized and transcardially perfused as previously described (Schmitz *et al.*, 2004). The brains were carefully removed from the skull, post-fixed for 2 hours and dissected. The left brain halves were cryoprotected in 30% sucrose, quickly frozen and cut frontally into series of 30 µm thick sections. Every tenth section was systematically sampled, stained with cresyl violet and used for stereological analysis of the hippocampal volume and the number of CA1 neurons. The hippocampal cell layer CA1 was delineated on cresyl violet-stained sections. Using a stereology workstation (StereoInvestigator; MicroBrightField, Williston, VT, USA) and a 100x oil lens, all neurons whose nucleus top came into focus were counted using the Optical Fractionator. In addition, volumes of the investigated brain regions were calculated from the delineated areas with Cavalieri's principle.

3.17 HISTOLOGICAL STAININGS

Cresylviolet staining

- necessary solutions:

1A: stock solution 1M sodium acetate

1B: working solution: 40 mL of 1A + 9.6 mL acetic acid (100%) adjusted to a total volume of 1 L.

2: cresyl violet is supplemented to 1 L of 1B and stirred for 30 min. Solution is stirred overnight at room temperature. Before use the solution was filtered.

3A: stock solution: 2% triton x-100 (20 mL are added to 980 mL mQ-water and stirred for 1 h at room temperature)

3B: working solution: 2.5 mL 3A + 50 mL mQ-water + 150 mL ethanol (100%)

- staining protocol:

1. cryo-sections were mounted on microscope slides and are allowed to dry on air for at least 2 h.
2. 20 min in 1B (2 cuvettes)
3. 20 min in 3B
4. 20 min in 1B (2 cuvettes)
5. 2 x 7 min in 2 (2 cuvettes)
6. 3 x 1 min in buffer 1B (3 cuvettes)
7. 3 min in 100% ethanol
8. 2 x 5 min xylene
9. embedding in DEPEX or other suitable mounting medium

Hematoxylin staining

The H&E staining is a common staining in diagnostic histopathology

Hematoxylin stains nuclear blue, whereas the matrix of hyaline cartilage, myxomatous and mucoid material appears pale blue.

Solution:

- Hematoxylin (Mayers hemalaun solution)

1. sections were deparaffinized in xylene and rehydrated in a descending graded alcohol row

2. washing in aqua dest. (2 min)
3. incubation in hematoxylin (5 min)
4. rinse in aqua dest. (30 s while moving the slide rack)
5. rinse in tap water (5 min)
6. dehydration in

100% ethanol (5 min)
100% ethanol (5 min)
Xylene (2x 10 min)
7. embedding with a quick hardening mounting medium

3.18 PLASMA CHOLESTEROL MEASUREMENT USING GAS CHROMATOGRAPHY

For extraction of plasma cholesterol 50 μ L of plasma were mixed with 1 mL 1 N ethanolic NaOH, stirred for 1 h at 50 °C and 1 mL H₂O was added. The aqueous phase was extracted twice with 3 mL cyclohexan. Samples were centrifuged for 20 min at 6000 rpm and room temperature. The unified organic phases were evaporated in a stream of N₂ at 65 °C. For sterol analysis 50 μ g 5 α -cholestane (Serva) and 1 μ g epicoprostanol (sigma) were added as internal standards. Samples were evaporated under nitrogen at 65 °C, dissolved in n-decan and transferred into a micro-vial for gas-liquid chromatography-flame ionization detection (GC-FID) analysis of cholesterol. Sterols were derivatized to trimethylsilyl- (TMSi) ethers by addition of 20 μ L of TMSi-reagent (pyridine:hexamethyldisilazane-trimethylchlorosilane; 9:3:1, by volume; all reagents were supplied by Merck) into each microvial and incubated for 1 h at 60 °C.

To quantify cholesterol in plasma samples, cholesterol and 5 α -cholestane-TMSi ethers were separated on a cross-linked methyl silicone DB-XLB 122-1232 fused silica capillary column (J and W, Folsom) (30 m x 0.25 mm i.d. x 0.25 μ m film thickness) in a HP 6890 series gas chromatograph (Hewlett Packard). The oven temperature was initially kept at 150 °C for 3 min, then increased by 30 °C * min⁻¹ to a final temperature of 290 °C. The concentration of cholesterol was calculated by one-point calibration using 5 α -cholestane as a standard. The peak area of cholesterol is divided by the peak area of 5 α -cholestane and multiplied by the amount of 5 α -cholestane added to the sample (50 μ g). This calculation method was validated against standard curves for cholesterol and showed a high validity. The identity of cholesterol was proven by comparison with the mass spectrum of authentic cholesterol as a standard (Sigma).

4 RESULTS

4.1 DEFICITS IN WORKING MEMORY AND MOTOR PERFORMANCE DECLINE IN THE APP/PS1KI MOUSE MODEL FOR ALZHEIMER'S DISEASE ARE PARALLELED BY EXTENSIVE NEURON LOSS AND HIPPOCAMPAL SHRINKAGE

4.1.1 PHENOTYPICAL CHARACTERIZATION

APP/PS1KI mutant mice did not show any apparent abnormalities until 6 months of age (ANOVA, $P < 0.0001$). At this time point, a progressive and significant decrease in the body weight compared to their PS1KI littermates is apparent ($P < 0.05$), which becomes highly significant at the age of 9 and 12 months ($P < 0.01$ and $P < 0.001$ respectively, Fig. 10, B). Furthermore, most of the APP/PS1ki mice start to develop a marked and rigid thoracolumbar kyphosis, which is a type of spinal deformity with an increased spine curvature starting at the age of approximately 6 months (Fig. 10, A). X-ray analyzes of PS1KI and APP/PS1KI littermates revealed no evidence of abnormal vertebral anatomy or bony deformity, but clearly demonstrated a thoracolumbar kyphosis in 12 month-old APP/PS1KI mice (Fig. 10, C - F).

A characteristic clasping phenotype has been previously shown in aged APP/PS1KI mice, which means that they show an unusual simultaneous retraction of both fore- and hindlimbs. (Wirh's *et al.* 2006) Quantitative measurement of this behavior by suspending the animals by their tail and evaluating the clasping score, revealed a significant increase in the foot-clasping time already at 6 months of age in the APP/PS1KI mice ($P < 0.001$), with no differences in young animals at the age of 2 months (ANOVA, $P < 0.0001$; Fig. 10, G).

In addition, APP/PS1KI mice showed evidence for an abnormal gait. Measuring the average stride length in a foot printing test showed no differences in young animals at the age of 2 months (ANOVA, $P < 0.0001$). However, analysis of 6 and 9 month-old animals revealed a significantly reduced stride length in the APP/PS1KI mice ($P < 0.01$ and $P < 0.001$ respectively, Fig. 10, H - I).

Paraphenylene diamine stained gastrocnemius muscle sections were analyzed by light microscopy. There was no apparent neurogenic muscle fiber atrophy; no spheroids were detected in the distal preterminal nerve fiber branches of any of the mouse lines investigated (not shown).

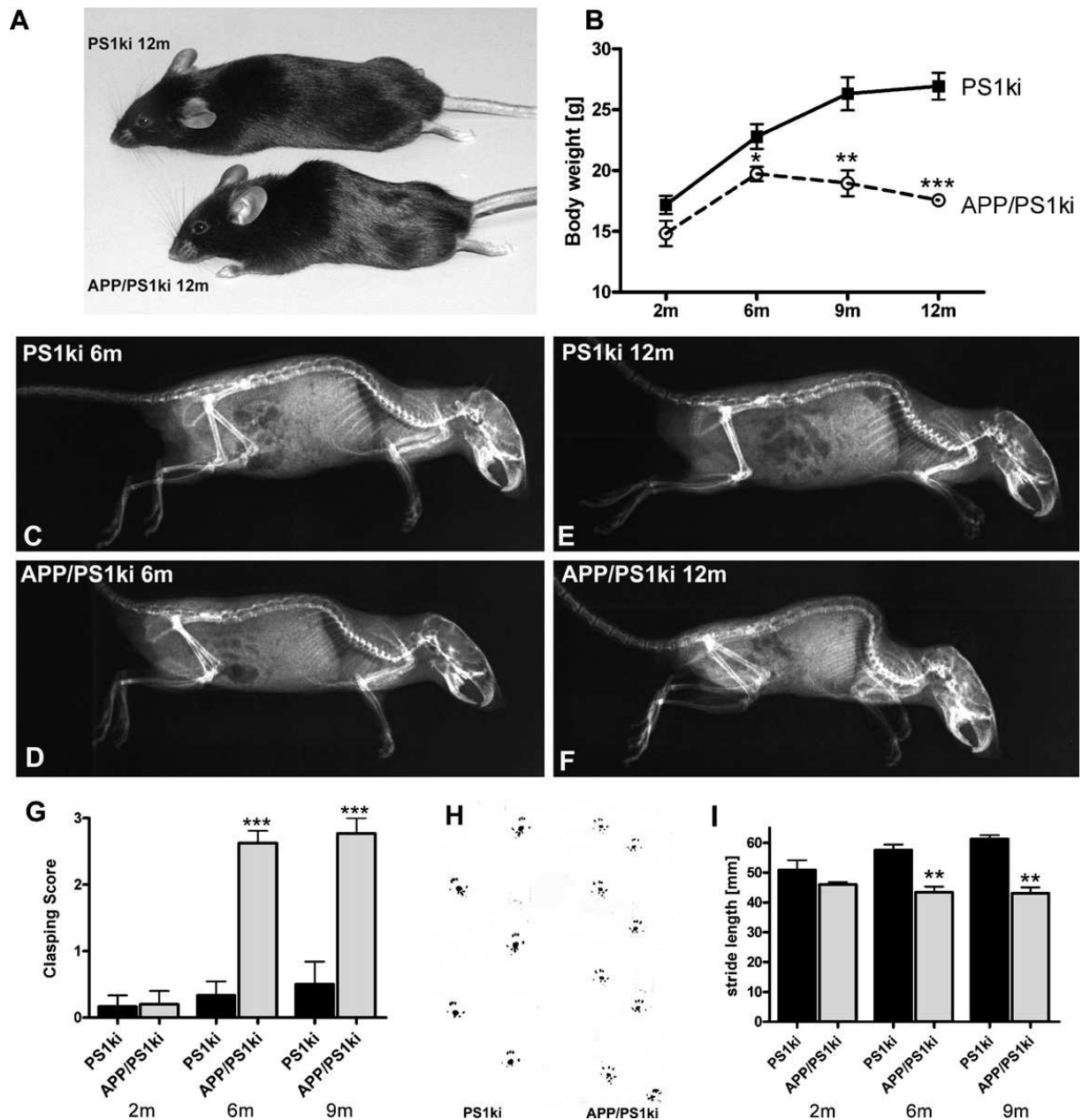


Fig. 10: APP/PS1KI mice show an age-dependent development of a thoracolumbar kyphosis (A). Additionally they have a reduced body weight compared to their age-matched PS1ki littermates (B). X-ray examination further highlights the thoracolumbar kyphosis, which becomes very robust in 12 month-old APP/PS1KI animals (C – F). Quantification of the clasping phenotype revealed highly significant differences between APP/PS1KI and PS1KI littermates already at 6 months of age (G). Representative footprinting pattern of 6 month-old APP/PS1KI and PS1KI mice (H)(experiment H was conducted by Dr. Stephanie Schaefer). Quantitative analysis revealed a significantly reduced stride length already at 6 months of age in the APP/PS1KI mice (I).

4.1.2 APP/PS1KI MICE ARE STRONGLY IMPAIRED IN SENSORY-MOTOR TASKS

For a more detailed characterization of the abovementioned clasping and rearing phenotypes, different sensory-motor tasks were performed using APP/PS1KI and PS1KI mice at the age of 2, 6, 9 and 12 months. The balance beam task analyzes the ability of mice to remain on a thin wooden dowel. Whereas PS1KI mice, as well as young (2 month-old) APP/PS1KI mice were able to stay on the dowel and often walked freely around it without any disturbance, aged APP/PS1KI mice showed a significant impairment in this task starting at the age of 6 months ($P < 0.05$). This phenotype was even more pronounced at 9 and 12 months of age (both $P < 0.001$; Fig. 11, A). A decreased latency to fall was detected between 6 and 12 months of age ($P < 0.05$) and 9 and 12 months of age in the PS1KI mice ($P < 0.05$), which might be attributed to the strong increase in body weight in the aged PS1KI mice (Kruskal-Wallis-Test, $P < 0.0001$; Fig. 10, B).

The string suspension paradigm is a task which measures the ability of mice to hold on to a wire using their forepaws. APP/PS1KI mice showed a significantly poorer performance than the PS1ki mice at 6, 9 and 12 months of age (all $P < 0.001$, Fig. 11, B), whereas young mice at 2 months of age did not show any impairment ($P > 0.299$). No differences were detected during aging in the PS1KI mice (ANOVA, $P < 0.0001$).

The vertical grip hanging task is a measure for neuromuscular abnormalities and tests the ability of mice to hang upside down from wire bars. This task also revealed a significantly decreased latency to fall in the APP/PS1KI mice already at 6 months of age ($P < 0.05$), which persisted at 9 months ($P < 0.05$) and becomes highly significant at 12 months of age ($P < 0.001$, Fig. 11, C). There were no difference in young APP/PS1KI mice ($P = 0.309$) or in PS1KI mice during aging (ANOVA, $P < 0.0001$).

The rotarod task is another accepted measure of impaired motor performance in mice. Abnormal motor function was revealed already at 6 months of age in this experimental paradigm. A genotype x training day ANOVA was calculated for the 2 month-old animals and revealed a significant effect of the training day ($F_{(4, 45)} = 13.36$, $P < 0.0001$), as well as a tendency towards a genotype effect, which was, however, not significant at that time point ($F_{(1, 45)} = 3.84$, $P = 0.056$). At 6 months of age, a significant effect of genotype ($F_{(1, 55)} = 17.25$, $P < 0.0001$) and training day ($F_{(4, 55)} = 4.78$, $P = 0.022$) was detected. Analysis of data presented in Fig. 11, D revealed that APP/PS1KI and PS1KI mice at 2 months of age showed a quite similar improvement during motor training. Six-month-old PS1KI mice showed on average a prolonged latency to fall than the age-matched APP/PS1KI mice, however, both

groups improved their latency to fall over the 5 days training period (Fig. 11, E). Combining the rotarod data of the 2 and 6 month-old groups reveals a significant effect of the genotype ($F_{(3,100)} = 14.80$, $P < 0.0001$), as well as a significant effect of the training day ($F_{(4, 100)} = 17.39$, $P < 0.0001$)

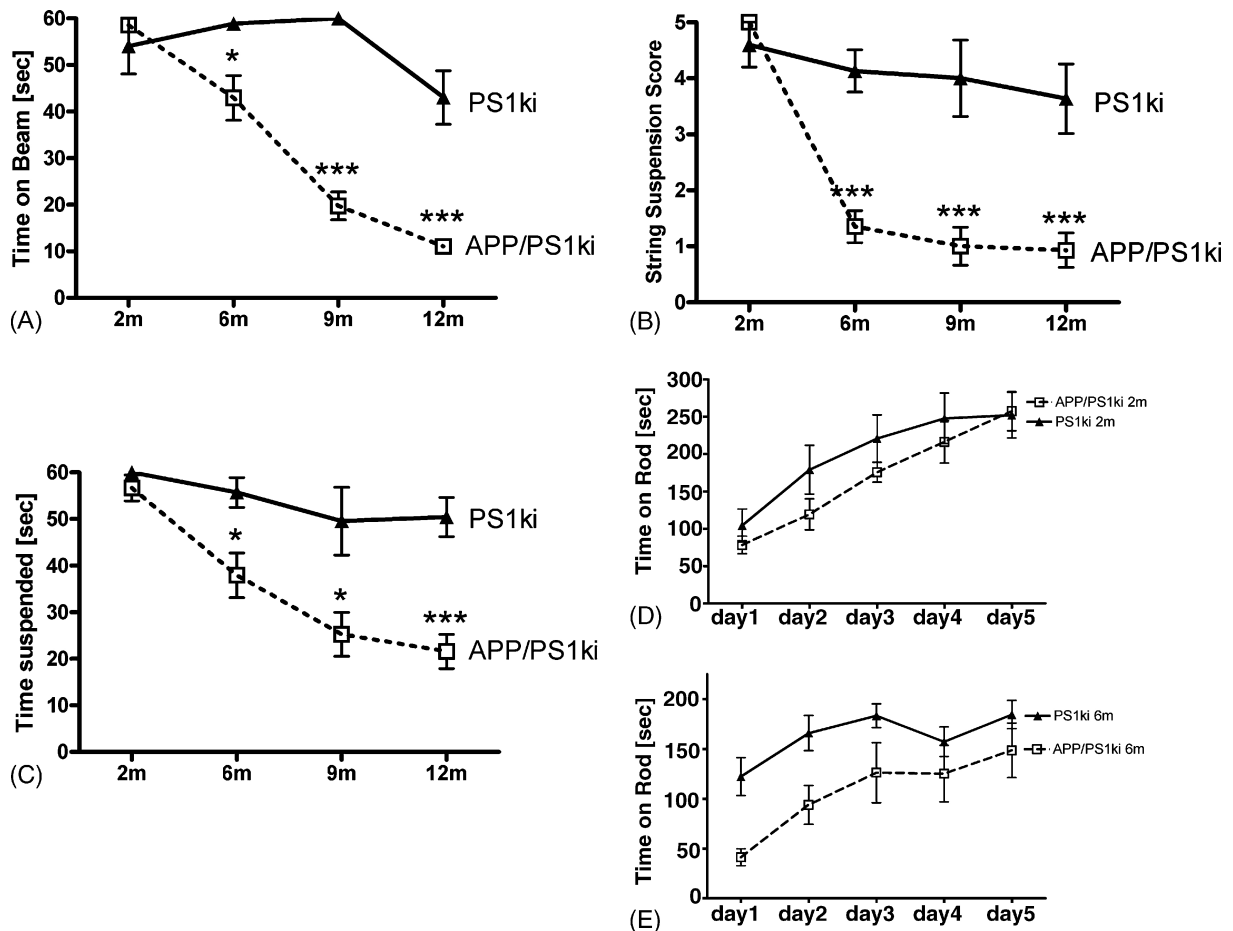


Fig. 11: Aged APP/PS1KI mice show highly significant impairment in the balance beam task (A), the string suspension task (B), as well as the grip hanging task (C) starting at the age of 6 months. Analysis of rotarod performance revealed no genotype effect at 2 months of age (D) but showed a significant genotype effect in 6 month-old APP/PS1KI mice (E).

4.1.3 FORCED SWIMMING TEST

Analysis of swimming distance and speed in the forced swimming test revealed that both parameters were significantly reduced in aged APP/PS1KI mice (ANOVA, $P < 0.0001$), without significant differences in young APP/PS1KI mice at 2 months of age ($P = 0.82$). Regarding swimming distance, impairment was detectable at 6 months ($P < 0.001$), becoming even more severe at 9 and 12 months of age (both $P < 0.001$; Fig. 12, A). The same held true

for the swimming speed, which was also significantly reduced in APP/PS1KI mice older than 2 months of age (all data, $P < 0.001$; Fig. 12, B). Additionally, some of the aged APP/PS1KI mice displayed alterations in their swimming behavior, often showing circulating and tumbling agitations in contrast to their PS1KI littermates, which always showed a straight way of swimming in this task (Fig. 12; C – D).

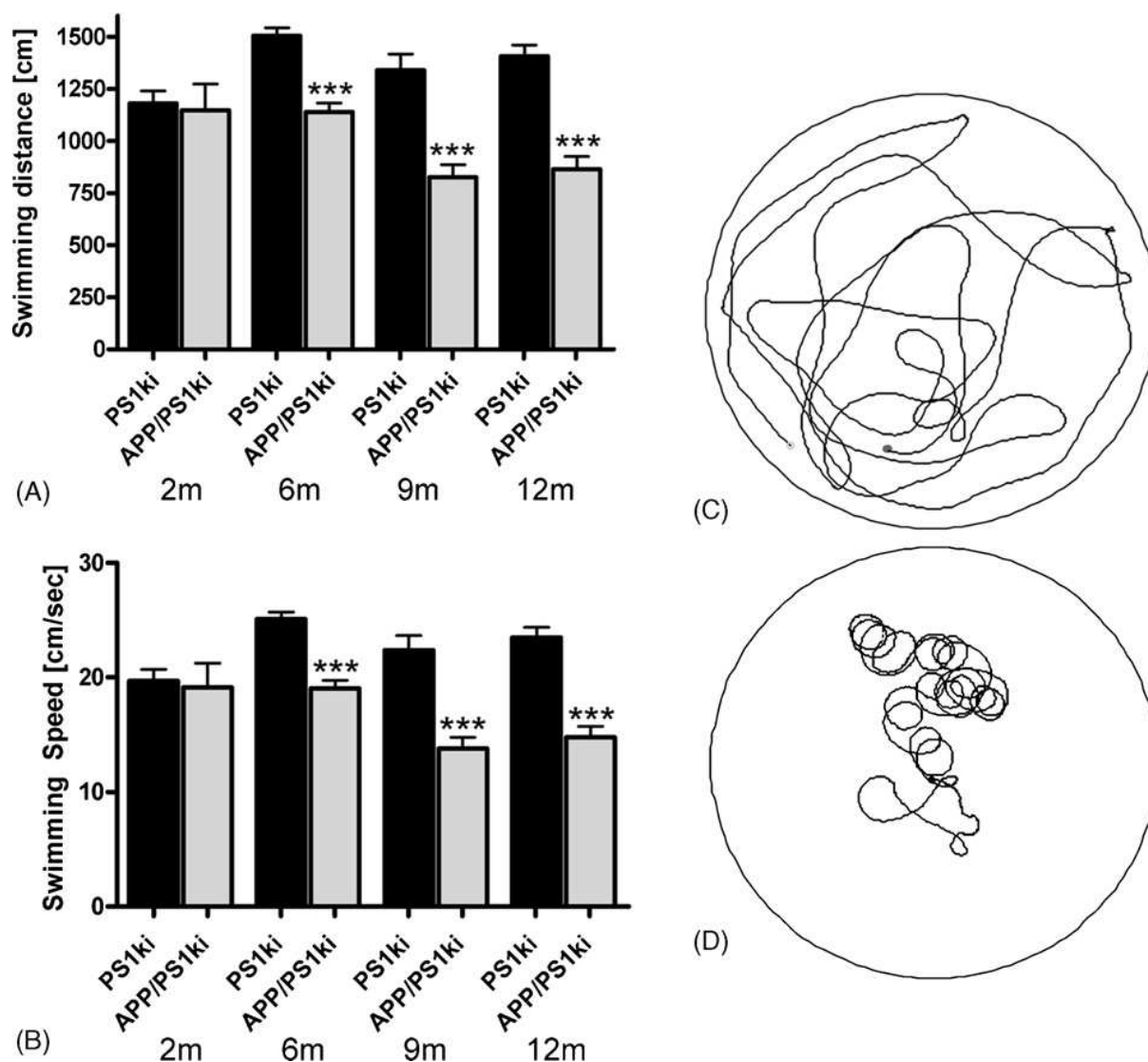
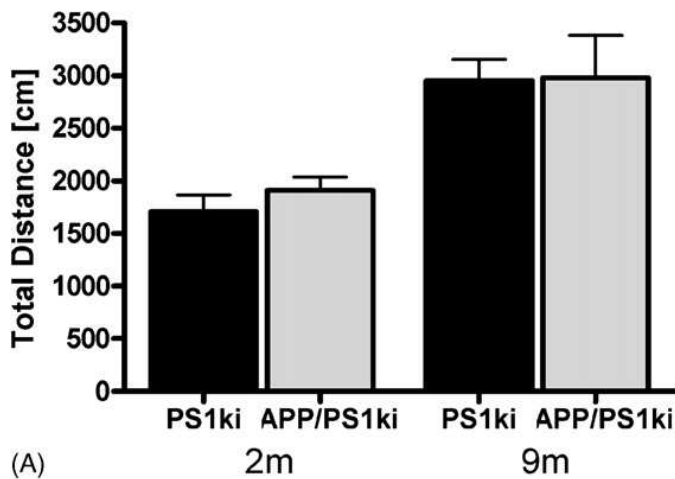


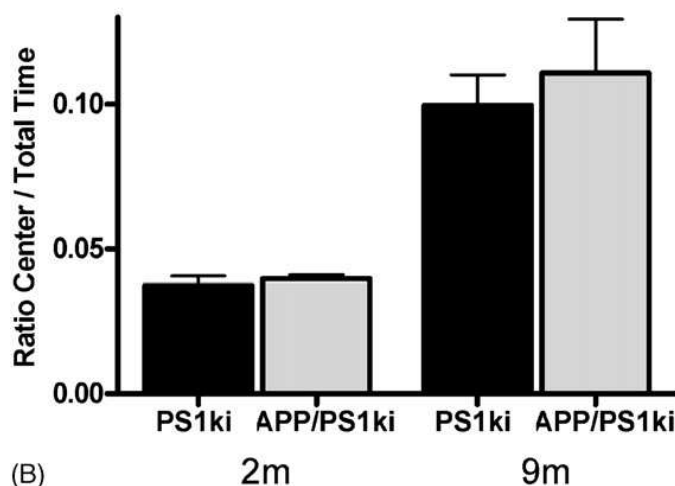
Fig. 12: Forced Swimming test. APP/PS1KI mice are strongly impaired in the forced swimming test starting at the age of 6 months. This becomes evident by a significantly reduced swimming distance (A), as well as a reduced swimming speed during the 60 sec single trial (B). Aged (12 months) PS1KI mice show a normal swimming pattern (C), whereas APP/PS1KI mice show a characteristic tumbling and circulating swimming behavior (D).

4.1.4 LOCOMOTOR AND EXPLORATORY BEHAVIOUR

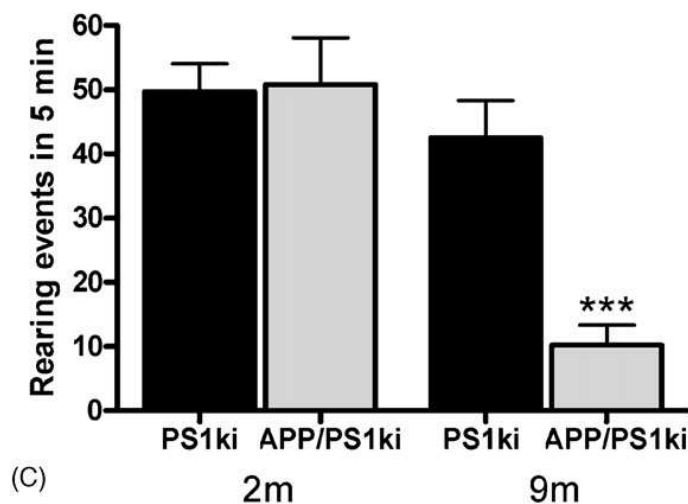
The exploratory and spontaneous locomotor activity of APP/PS1KI mice was compared to PS1KI mice at the age of 2 and 9 months in the open field paradigm (ANOVA, $P < 0.0001$). No significant differences were observed in the distance traveled during the 5 min trial



(A)



(B)



(C)

between APP/PS1KI and PS1KI mice at either age ($P > 0.05$; Fig. 13, A). The mean movement speed was also unchanged between APP/PS1KI and PS1KI mice ($P > 0.05$, not shown). The ratio of distance traveled in the center of the arena versus the total distance can be used as a measure of anxiety-related behavior (Paylor *et al.* 1998). No differences in the center/total distance ratio could be detected between APP/PS1KI and PS1KI at either age (ANOVA, $P < 0.001$; t -test both $P > 0.05$ (Fig. 13, B)). Interestingly, the 9 month-old APP/PS1KI mice showed a dramatic reduction in the rearing frequency, pointing again to an impaired motor behavior ($P < 0.001$; Fig. 13, C).

Fig. 13: Open field. There is no significant difference in the exploratory behavior between APP/PS1KI and PS1KI mice at the analyzed time points. Neither the total traveled distance (A) nor the center/total time ratio (B) was altered between both groups at 2 and 9 months of age. However, APP/PS1KI mice at 9 months of age showed a significantly reduced frequency of rearing events, pointing to impaired motor performance (C).

4.1.5 AGE-DEPENDENT WORKING MEMORY IMPAIRMENT IN APP/PS1KI MICE

Two different paradigms were used to assess whether APP/PS1KI mice are impaired regarding working memory in comparison with their PS1KI littermates. In the Y-maze, no difference between the percentages of alternation was detected in 2-month-old APP/PS1KI mice (ANOVA, $P = 0.0037$). However, at 6 months of age APP/PS1KI mice showed a significantly

reduced alternation percentage ($P < 0.05$), indicating impaired working memory (Fig. 14, A). This deficit became even worse at the age of 12 months ($P < 0.01$). The observed deficiency was obviously not due to a lack of explorative behavior, as APP/PS1KI mice at 6 months of age showed an even higher frequency of total arm entries within the given time frame ($P < 0.05$; Fig. 14, B).

The T-maze continuous alternation task (T-CAT) revealed similar results (ANOVA, $P = 0.0003$). Whereas no differences were obvious at 2 months of age, a significantly reduced alternation rate was observed in 6 and 12 month-old APP/PS1KI mice (both $P < 0.01$). At these time points the APP/PS1KI mice alternated even below chance level (Fig. 14, C). Mean session duration to perform the free-choice trials was not different between APP/PS1KI and PS1KI mice at each time point analyzed (not shown).

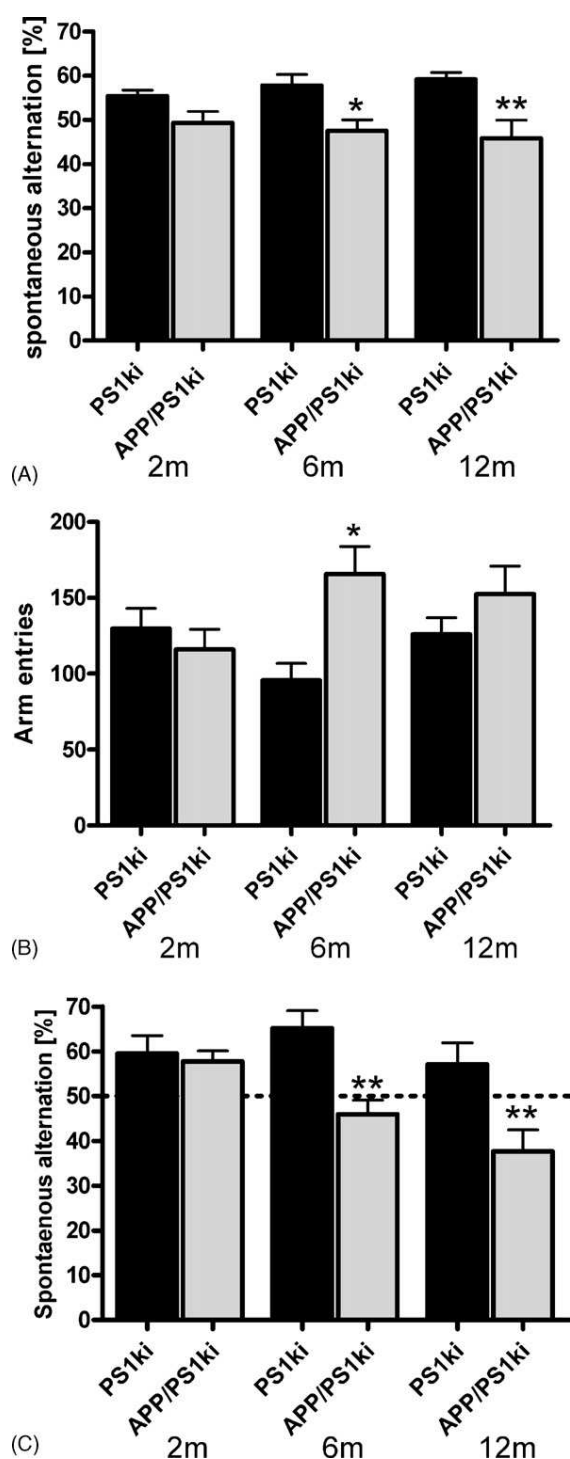


Fig. 14: Working memory using Y-maze and T-maze continuous alternation task (T-CAT). Analysis of spontaneous alternation in the Y-maze revealed significantly reduced alternation frequencies in the APP/PS1KI mice at 6 and 12 months with no difference at 2 months of age (A). This is not due to a lack of explorative behavior, as APP/PS1KI mice at this age showed a higher frequency of total arm entries (B). The T-CAT also revealed a significantly reduced alternation behavior at the age of 6 and 12 months in the APP/PS1KI mice, with no disturbance in 2 month-old mice (C).

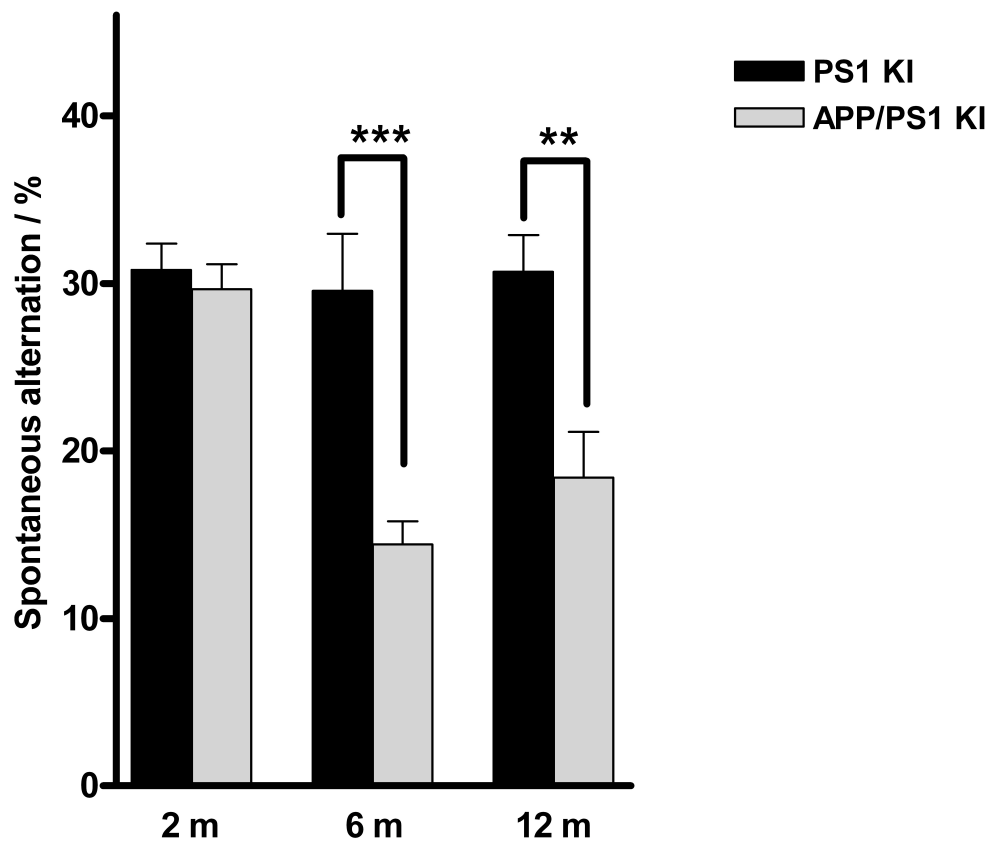


Fig. 15: Working memory test using cross-maze task. Analysis of spontaneous alternation in the cross-maze revealed significantly reduced alternation frequencies in the APP/PS1KI mice at 6 and 12 months with no difference at 2 months of age (N=6-14, unpaired t-test (two-tailed), **: 0.001<p<0.01; *: p<0.001, data shown as mean \pm s.e.m.).**

The finding of strongly impaired working memory performance shown in Y-maze and T-maze task is firmly underlined by the results from the cross-maze-task (Fig. 15). The cross-maze, built up from four arms arranged in rectangular angles instead of three arms with angles of 120°, differs from the Y-maze merely by the shape of the maze. Because the higher number of arms, this task places higher demands to mice in exploring the maze's arms in an optimal alternating order. Therefore, the results from the crossmaze are very similar to the Y-maze, but show an even higher level of statistical significance. While no difference in working memory performance was observable at two months of age between PS1KI and APP/PS1KI mice, at six months of age the latter are significantly impaired in this respect (p=0.0001). At 12 months of age working memory performance of APP/PS1KI mice was also strikingly worse compared to age-matched PS1KI mice (p=0.0021). The increase in working memory performance comparing twelve-month-old APP/PS1KI mice to six-month-old ones was statistically not significant (p=0.1607).

4.1.6 CA1 NEURON LOSS AND HIPPOCAMPAL ATROPHY

Neuronal loss was quantitatively assessed by design-based stereology. I found a 33% loss of pyramidal cells within the pyramidal layer of CA1 in the hippocampus in 6-month-old APP/PS1KI mice compared to 6-month-old PS1KI littermate control mice ($P = 0.003$; Fig. 16, A). Previously it has been shown that 2-month-old APP/PS1KI mice showed a normal number of CA1 neurons and a 50% reduction at 10 months of age (Casas *et al.*, 2004). In addition, 6-month-old APP/PS1KI mice exhibited a decreased volume of the CA1 pyramidal cell layer of 30% ($P = 0.022$; Fig. 16, B), and a total hippocampal atrophy of 18% ($P = 0.019$; Fig. 16, C).

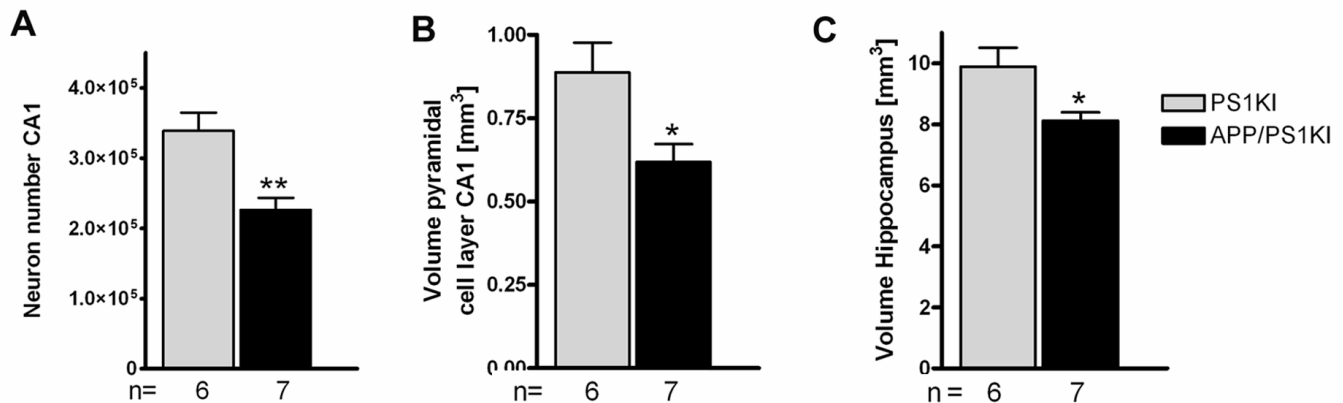


Fig. 16: (A) Stereological cell counting of CA1 neurons of 6-month-old APP/PS1KI ($n = 7$) and PS1KI ($n = 6$) mice. Compared to age-matched PS1KI mice, six month old APP/PS1KI mice show a neuron loss in CA1/2 region of the hippocampus of 33%. (B) A significant difference in the volume of the CA1 pyramidal layer was detected at 6 months, corresponding to a reduction of 22% ($n = 6 - 7$ per group). (C) This results in an overall hippocampus volume reduction of 18%. Values are given as means \pm s.e.m. ** $P < 0.01$; * $P < 0.05$, unpaired t-test.

At 12 months of age, APP/PS1KI mice show a further slightly decline in neuron numbers and volume figures of CA1 region and total hippocampus as well, however no significant differences compared to six month old APP/PS1KI mice were detected. In detail, neuron numbers of APP/PS1KI mice showed a decline of 42% ($P = 0.0003$) at 12 months of age, while CA1 and hippocampal volumes exhibited a loss of 25% ($P = 0.016$) or 22% ($P = 0.013$), respectively (Fig. 17 A-C).

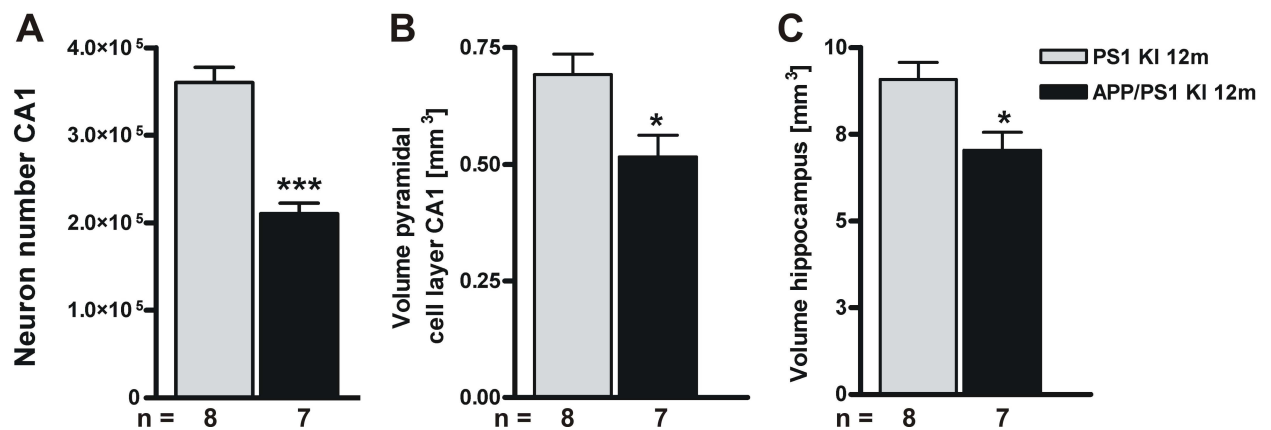


Fig. 17: (A) Stereological cell counting of CA1 neurons of 12-month-old APP/PS1KI ($n = 7$) and PS1KI ($n = 8$) mice. Compared to age-matched PS1KI mice, six month old APP/PS1KI mice show a neuron loss in CA1/2 region of the hippocampus of 42%. (B) A significant difference in the volume of the CA1 pyramidal layer was detected at 6 months, corresponding to a reduction of 25% ($n = 7 - 8$ per group). (C) This results in an overall hippocampus volume reduction of 22%. Values are given as means \pm s.e.m. *** $P < 0.001$; * $P < 0.05$.

4.2 PATHOLOGY-DEPENDENT DEVELOPMENT OF INFLAMMATION IN AN APP/PS1KI MOUSE MODEL OF ALZHEIMER`S DISEASE

Besides rare exceptions no significant upregulation in expression of any of the genes of interest could be detected between 2-month-old APP/PS1KI and PS1KI mice. However, I observed a significant upregulation of GFAP and a statistical trend pointing to an increased expression of toll like receptor 2 ($P=0.08$). Therefore APP/PS1KI mice appear not to be inflicted by severe inflammation in the brain, because at this early timepoint of the AD related pathological process is still in its very beginning. This fits well to the behavioural phenotype of these mice at two months of age, where no deficits in working memory performance, signs of axonal degeneration or motor disturbances are present (Wirths *et al.* 2007; Wirths *et al.* 2006). Interestingly, expression of calcium homeostasis related protein S100A6 was found to be significantly downregulated 0.5-fold. Osteopontin showed only a trend of deterioration to an extent of (0.5x; $P= 0.08$) compared to two month old PS1KI mice.

In contrast, at six months of age, where pathology of AD is already extensively present, I observed significant upregulation in a broad set of inflammation markers. Expression of GFAP mRNA revealed a strong 9-fold increase compared to age-matched PS1KI controls, indicating a severe astrogliosis in brains of APP/PS1KI mice. Occurrence of astrogliosis was also underlined by overexpression of S100A6 (2.6x, $P=0.003$) that is often used as a marker

for activated astrocytes. Proteins characteristic for activated microglia cells like Macrophage scavenger 2 (7.8x, $P=0.005$) and toll like receptor family – I measured Tlr2 (6.1x, $P=0.001$), Tlr4 (1.9x, $P=0.016$), Tlr7 (3.1, $P<0.001$) and Tlr9 (2.3x, $P=0.004$), revealed all prominently upregulated expression patterns. I detected also an increase in the expression of microglia associated cytokines like CD11 β (2.4x, $P=0.002$), F4/80 (3.8x, $P<0.001$), interleukin-1 β (1.8x, however by a P -value of 0.194 not significant). Interestingly, the expression of interleukin-6 (1.0x, $P=0.912$) and interleukin-10 (0.8x, $P=0.336$) remained unchanged. Tumor necrosis factor (TNF- α) was not upregulated compared to PS1KI mice at 6 months of age, while transforming growth factor (TGF- β) revealed a massively increased 2.7-fold expression ($P<0.001$) at this time point. The expression of cell surface glycoprotein major histocompatibility complex (MHC-II) remained unchanged, although a tendency of age dependent diminished expression may be assumed from the data. Macrophage colony stimulating factor's (M-CSF-R) expression was elevated 2.6-fold ($P<0.001$). The same was valid for the family of Metallothioneins (Mt1 (2.0x, $P=0.002$), Mt2 (2.5x, $P=0.004$), Mt3 (1.5x, $P=0.005$), for the proapoptotic factor FAS (1.8x, $P=0.004$) and for osteopontin (2.7x, $P=0.001$). A strong upregulation of mRNA was also found for iron regulatory proteins transferrin (2.4x, $P=0.001$) and ferritin light chain (Ftl, 1.8x; $P=0.001$).

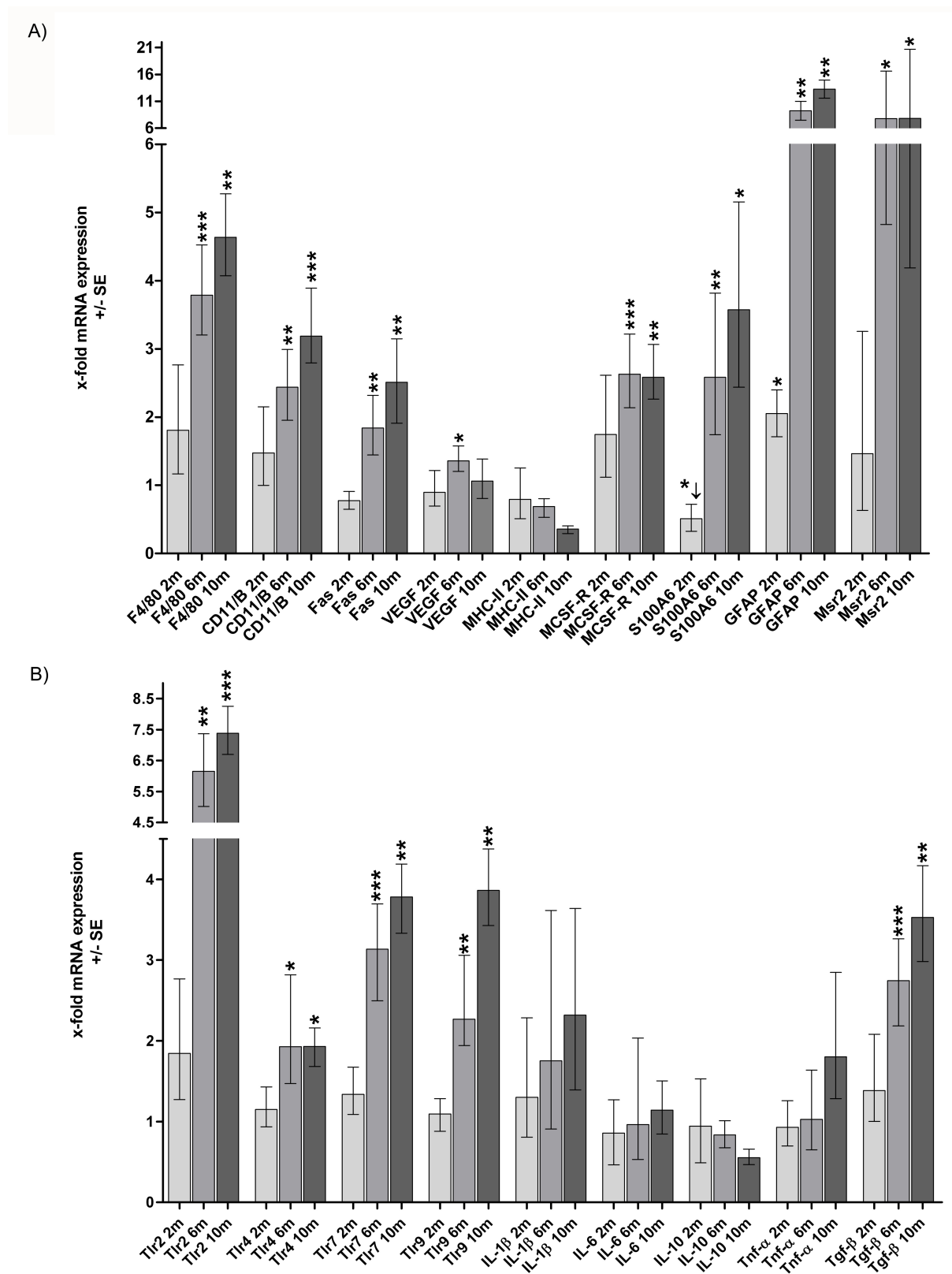


Fig. 18: Gene expression for various inflammation-associated genes are shown as a ratio of mRNA levels in APP/PS1KI mice compared to age-matched PS1KI control animals. Levels of significance refer to the expression ratio of APP/PS1KI mice to PS1KI mice at same age: *** $P < 0.001$; ** $P < 0.01$; * $P < 0.05$. For real-time RT-PCR analysis I used male animals of two (4 PS1KI, 4 APP/PS1KI), six (4 PS1KI; 5 APP/PS1KI and ten months of age (4 PS1KI; 4 APP/PS1KI).

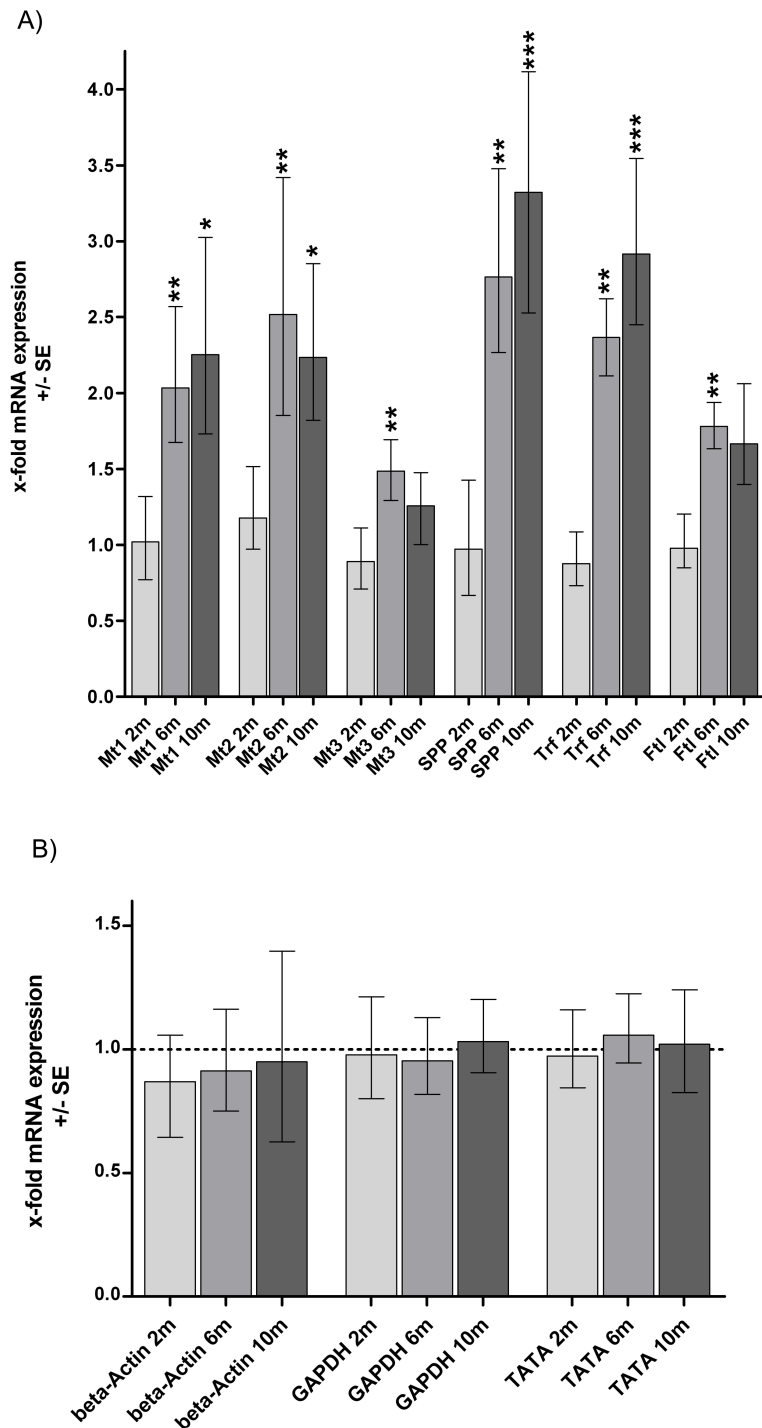


Fig. 19: A) Gene expression for various genes of antioxidant or other neuroprotective relevance is shown as a ratio of mRNA levels in APP/PS1KI mice compared to age-matched PS1KI control animals. Levels of significance refer to the expression ratio of APP/PS1KI mice to PS1KI mice at same age: *** $P < 0.001$; ** $P < 0.01$; * $P < 0.05$. B) Expression of reference genes used in statistical calculations is shown as a ratio of mRNA levels in APP/PS1KI mice compared to age-matched PS1KI control animals. The expression of all three housekeeping genes that were used to form an housekeeping index as a basis for gene expression calculations by use of REST software remained highly stable and does not differ between APP/PS1KI and PS1KI mice at any timepoint. For real-time RT-PCR analysis I used male animals of two (4 PS1KI, 4 APP/PS1KI), six (4 PS1KI; 5 APP/PS1KI and ten months of age (4 PS1KI; 4 APP/PS1KI).

Immunohistochemically analysis of exemplary chosen proteins gave evidence for accumulation of markers for activated astrocytes like GFAP, S100A6, microglia inflammation marker Iba1 and for iron metabolism implied transferrin on the protein level at six months of age (fig. 20 and 21).

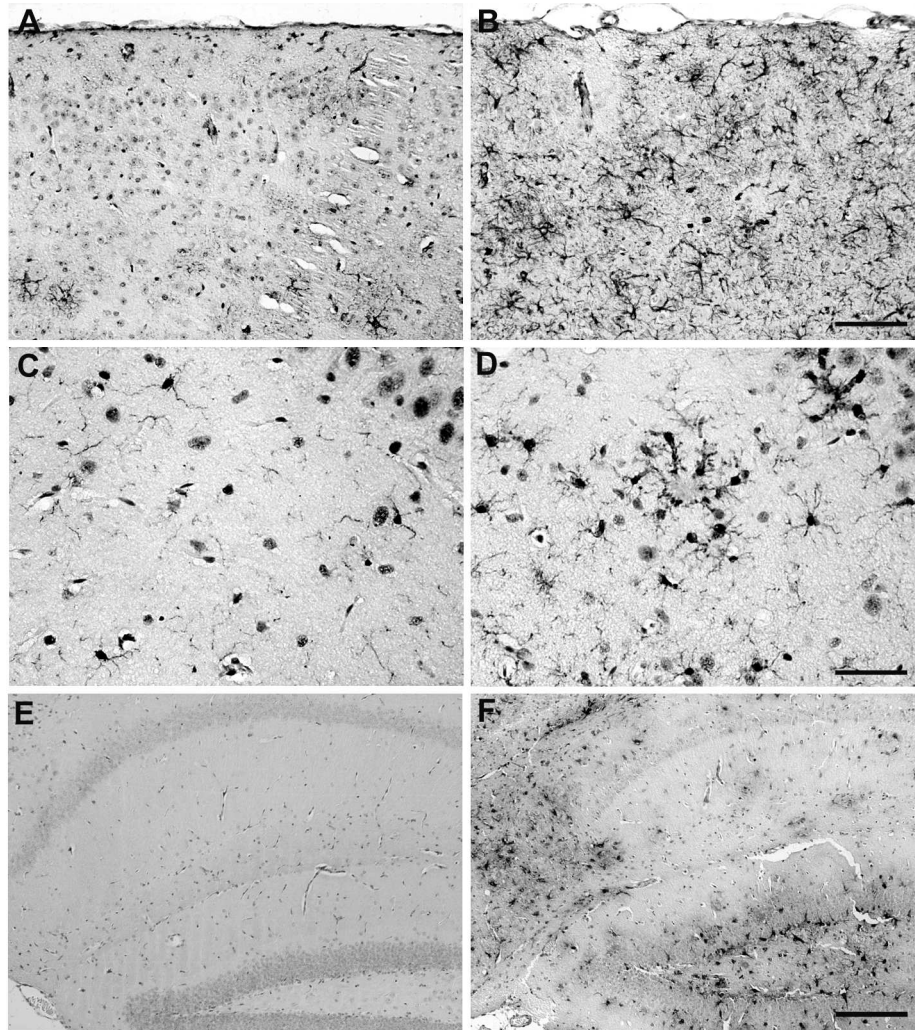


Fig. 20: Immunohistochemical stainings were used to verify the increased expression of inflammatory on the protein level. Representative stainings against GFAP in the cortex (A, B), against the microglia marker Iba1 in the cortex (C, D), as well as against S100A6 in the hippocampus (E, F) are shown at six months of age in PS1KI (A, C, E) and APP/PS1KI (B, D, F) mice. Scale bars: 100 μ m (A, B); 50 μ m (C, D); 200 μ m (E, F).

GFAP was significantly increased at two ($P=0.0011$; $t=8.415$, $df=4$) and six ($P=0.0017$; $t=7.527$, $df=4$) months of age between APP/PS1KI and PS1KI mice, indicating massive

astrogliosis. Besides, GFAP load was also significantly higher in six-month-old APP/PS1KI mice compared to two-month-old mice of equal genotype ($P=0.0041$; $t=5.911$, $df=4$). Transferrin was significantly increased comparing six-month-old APP/PS1KI mice to six-month-old PS1KI control ($P=0.0136$; $t=4.208$, $df=4$) and two-month-old APP/PS1KI mice ($P=0.0049$; $t=5.633$, $df=4$) as well.

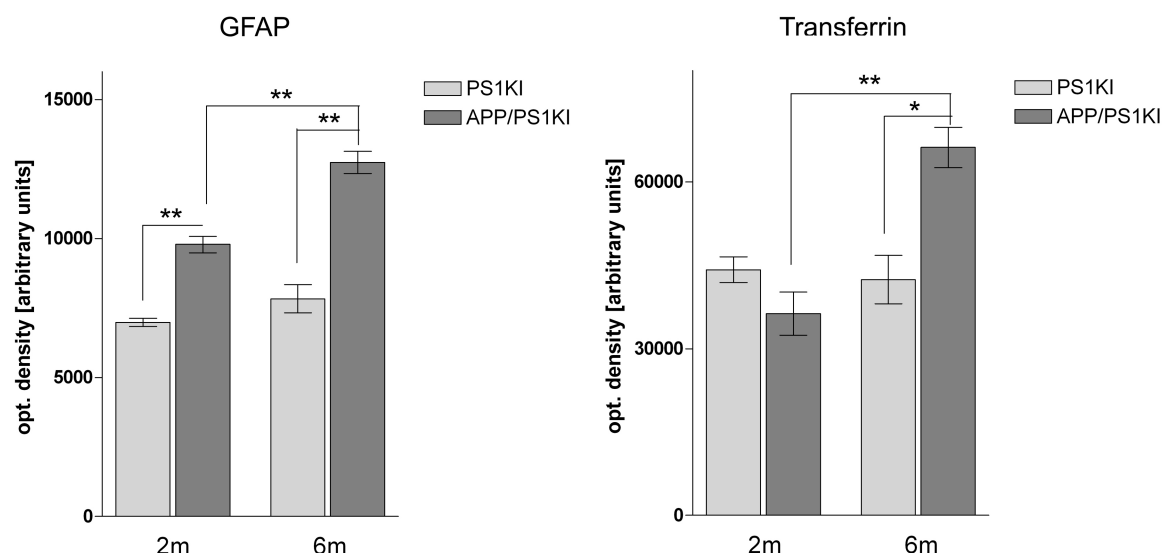


Fig. 21: Exemplary quantitative western blot analysis of GFAP and transferrin normalized to beta-actin as a reference gene. GFAP was significantly increased at two ($P=0.0011$; $t=8.415$, $df=4$) and six ($P=0.0017$; $t=7.527$, $df=4$) months of age between APP/PS1KI ($n=3$) and PS1KI ($n=3$) mice, indicating massive astrogliosis. Besides, GFAP load was also significantly higher in six-month-old APP/PS1KI mice compared to two-month-old mice of equal genotype ($P=0.0041$; $t=5.911$, $df=4$). Transferrin was significantly increased comparing six-month-old APP/PS1KI ($n=3$) mice to six-month-old PS1KI ($n=3$) control ($P=0.0136$; $t=4.208$, $df=4$) and two-month-old APP/PS1KI mice ($P=0.0049$; $t=5.633$, $df=4$) as well. Levels of statistical significance (unpaired t-test) were given as $**P < 0.01$; $*P < 0.05$. Data are plotted \pm SE.

At 10 months of age, expression of all observed genes remained unchanged in means of statistical significance or showed only a slight increase in their mean expression. No significant decrease in expression of any gene was detected by real time RT-PCR of APP/PS1KI mice compared to age-matched PS1KI control mice. In most cases the difference in mRNA expression seemed to be more incisive comparing 2 and 6 month old animals than between 6 and 10 months of age. This indicates that 6 months represent a critical time point in this animal model.

In detail, I observed upregulation of cytokines in 10 m old APP/PS1KI animals compared to PS1KI animals of same age as follows: Tlr2 mRNA expression was 7.4-fold elevated

($P<0.0001$), Tlr4 1.9x ($P=0.016$), Tlr7 3.8x ($P=0.004$) and Tlr9 3.9x ($P=0.004$). CD11/B mRNA levels were found to be 3.2-fold higher in APP/PS1KI animals compared to control group, IL1 β 2.3x – however with an only trend indicating p-value of 0.073. Interleukin-6 and interleukin-10 again were detected to remain unchanged.

Tumor necrosis factor TNF- α by mean appeared to be upregulated in 10m old APP/PS1KI mice relative to age-matched controls, however there was no statistically significant difference ($P=0.205$). Messenger RNA-levels of MHC-II seemed to be diminished at 10 m of age, however no statistical significance could be found here neither ($P=0.149$).

Transforming growth factor TGF- β showed a 3.5x upregulation in mRNA expression at 10 months of age ($P=0.004$). The same was found for MCSF-R (2.6x, $P=0.004$).

Levels of metallothionein mRNA in brains of 10 m old mice remained stable or showed only minor changes in relation to 6 month old mice compared to their age-matched PS1KI littermates (MT1: 2.3x, $P=0.015$; MT2: 2.2x, $P=0.028$). Interestingly, according to MT3 mRNA expression, statistical significance between APP/PS1KI and PS1KI mice was no longer evident at 10 months of age, though mean expression of this gene was only slightly decreased at this time point (1.3x, $P=0.804$ at 10 months instead of 1.5x, $P=0.005$ at 6 months. In 10-month-old APP/PS1KI mice Transferrin (2.9x, $P<0.001$), S100A6 (3.6x, $P=0.016$), osteopontin (3.3x, $P<0.001$) and GFAP (12.9x, $P=0.004$) mRNA also met strong upregulations.

4.3 CHOLESTEROL METABOLISM IN APP/PS1KI MICE

I measured the plasma cholesterol levels in wildtype, PS1KI, APP^{SL} and APP/PS1KI mice at two and six months of age. Cholesterol levels mice were determined by GC. There was no detectable difference in plasma cholesterol between APP single transgenic (2 m, 80.16 ± 5.7 mg/dL; 6 m, 78.88 ± 4.8 mg/dL) and wildtype control mice (2 m, 86.85 ± 5.3 mg/dL; 6m, 83.32 ± 4.1 mg/dL). Furthermore, the levels of young wildtype mice did not differ from the levels of the 3-months group in the first set of mice, verifying that both enzymatic as well GC determination of plasma cholesterol gives comparable results. PS1 knock-in mice revealed also no significant change between 2 (125.4 ± 4.7 mg/dL) and 6 months (121.5 ± 10.0

mg/dL), whereas APP/PS1KI mice showed a significant decrease between 2 (116.6 ± 5.6 mg/dL) and 6 months (92.13 ± 5.5 mg/dL) ($P = 0.013$) (Fig. 22). Both PS1KI and APP/PS1KI mice have higher basal cholesterol levels than APP single transgenic or wildtype mice. This is due to a different genetic background. Whereas wildtype and APP single transgenic mice are on C57BL/6-background, the knock-in lines have C57BL/6 50% - CBA 25% - 129SV 25% (Casas *et al.* 2004).

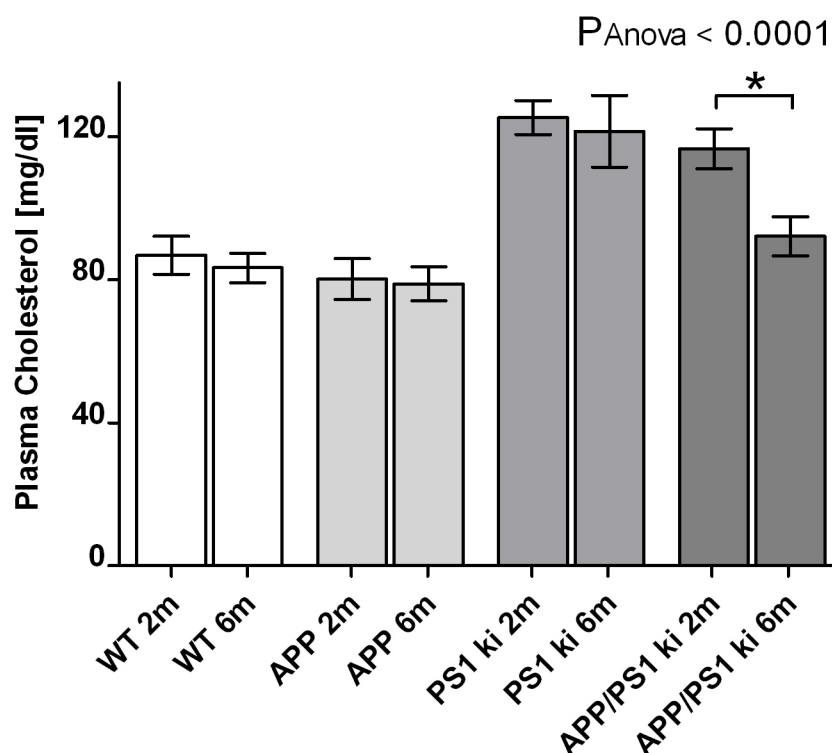


Fig. 22: Measurement of plasma cholesterol concentrations in wildtype (2m: N=7, 6m: N=6), PS1KI (2m: N=6, 6m: N=5), APP751SL (2m: N=5, 6m: N=5) and APP751SLxPS1KI mice (2m: N=6, 6m: N=5), * <0.05 , Mann-Whitney t-test.

4.4 24-(S)-HYDROXY-CHOLESTEROL AS A PREDICTIVE BIOMARKER IN ALZHEIMER`S DISEASE?

In this study I measured the levels of total cholesterol and 24(S)-hydroxycholesterol in plasma of wildtype, APP751^{SL}, PS1KI transgenic mice and in the APP751SLxPS1KI species. Only animals of female gender have been studied, because female mice show an accelerated progression of the disease compared to male mice and proved to show a significant loss of hippocampal CA1 neurons of already 33% at 6 months-of-age. Mean values \pm SD of the ratio

between 24(S)-hydroxycholesterol to cholesterol in plasma at two months respectively six months-of-age (values in brackets) were the following (see Fig. 23):

wildtype = 38.6 ± 9.5 (55.4 ± 40.7), PS1KI = 62.1 ± 11.7 (59.4 ± 8.1), APP751^{SL} = 41.2 ± 15.7 (43.5 ± 16.1) and APP751^{SL}xPS1KI = 50.4 ± 12.9 (48.7 ± 3.5). Levels of significance of cholesterol corrected 24(S)-hydroxycholesterol levels resulted in $p = 0.53$ for wildtype, $p = 0.79$ for PS1KI, $p = 0.84$ for APP751^{SL} and $p = 0.93$ for APP751^{SL}xPS1KI genotype.

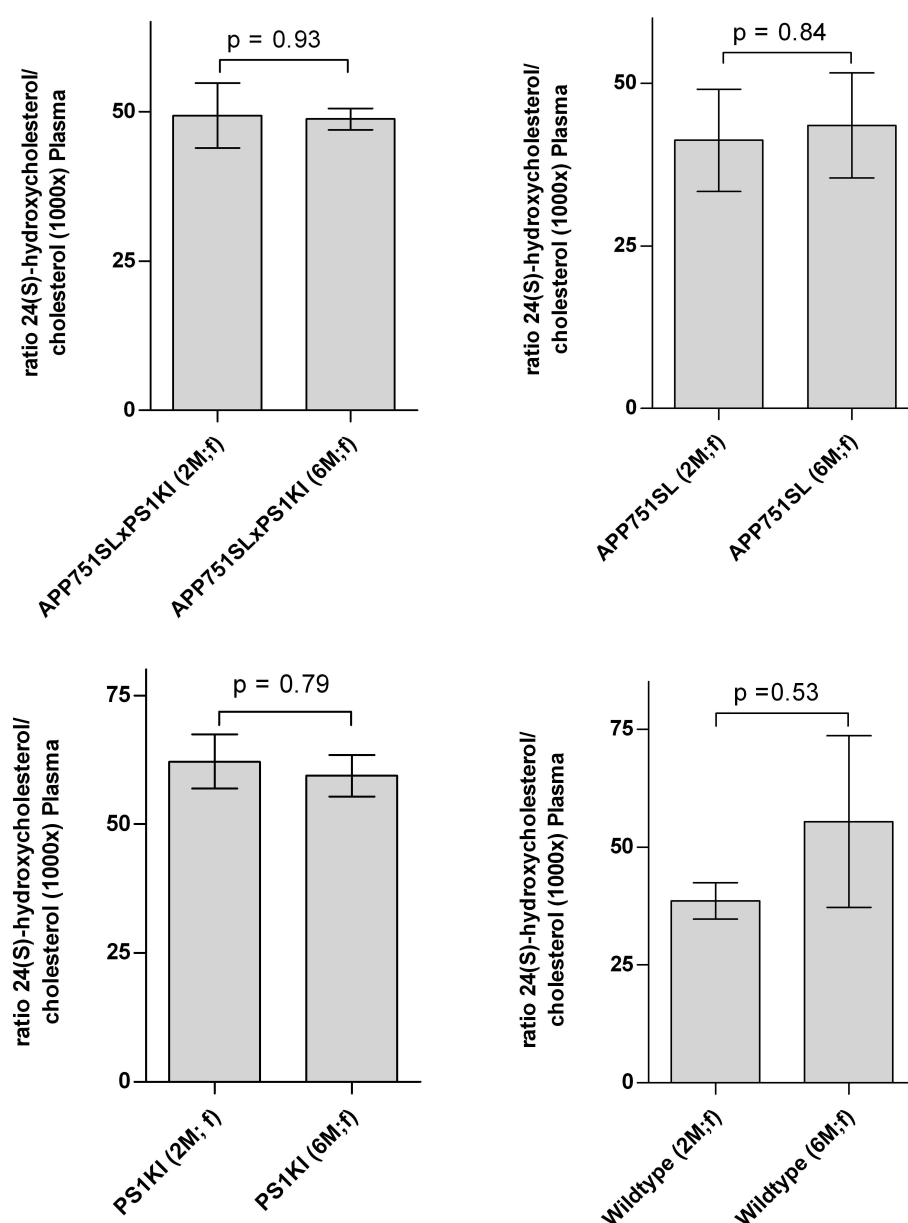


Fig. 23: Ratio of 24(S)-hydroxycholesterol to total cholesterol in plasma of wildtype (2m: N=7, 6m: N=6), PS1KI (2m: N=6, 6m: N=5), APP751SL (2m: N=5, 6m: N=5) and APP751SLxPS1KI mice PS1KI (2m: N=6, 6m: N=5) (f = female). The ratios were measured at the age of two (2M) and six months (6M). There was no significant difference in the ratio of 24(S)-hydroxycholesterol to total cholesterol comparing any group at any timepoint.

4.5 IN VIVO FORMATION OF PYROGLUTAMATE A β in APP/PS1KI, TBA1 and TBA2 MICE

4.5.1 DOMINANT AGGREGATION OF β -AMYLOID STARTING WITH PYROGLUTAMATE AT POSITION 3 IN THE APP/PS1KI MOUSE MODEL

It was previously shown that approximately 85% of all A β peptides in the APP/PS1KI mouse brain are comprised of peptides ending with residue 42 at the C-terminus (Casas *et al.* 2004), and in addition that a variety of different N-modified A β peptides accumulate in this model (Casas *et al.* 2004; Wirths *et al.* 2006). Accordingly, the immunohistochemical staining pattern of N-modified A β peptides in the hippocampus has been studied in the present study in greater detail. Strong immunoreactivity was detected already at 2 months of age in hippocampal CA1 neurons in APP/PS1KI mice with an antibody directed against A β _{N1(D)}, detecting only A β peptides starting at position 1 (Fig. 24 A, B). PS1KI control animals were constantly negative (not shown). Interestingly there is some heterogeneity among the intraneuronal A β peptides, which could be demonstrated by strong immunoreactivity with antibodies against racemized aspartate at position 1 (A β _{N1(rD)}) (Fig. 24 D, E), and cyclized glutamate (pyroglutamate) at position 3 (A β _{N3(pE)}) (Fig. 24 G, H). Quantification of N-modified A β peptides in CA1 neurons revealed that all 3 different peptides showed a strong intraneuronal accumulation between 2 and 6 months of age, however, with varying degrees. The amount increased as follows: A β _{N1(D)} by 301%, A β _{N1(rD)} by 297%, and A β _{N3(pE)} by 435%. In addition the total A β load of N-modified A β peptides was assessed in the hippocampus of 2- and 6-month-old APP/PS1KI mice. The amount showed an age-dependent increase for A β _{N1(D)} by 529%, for A β _{N1(rD)} by 486%, and for A β _{N3(pE)} by 1076%. As previously published, the spatial pattern of plaque deposition did not correlate with the observed CA1 neuron loss (Fig. 24).

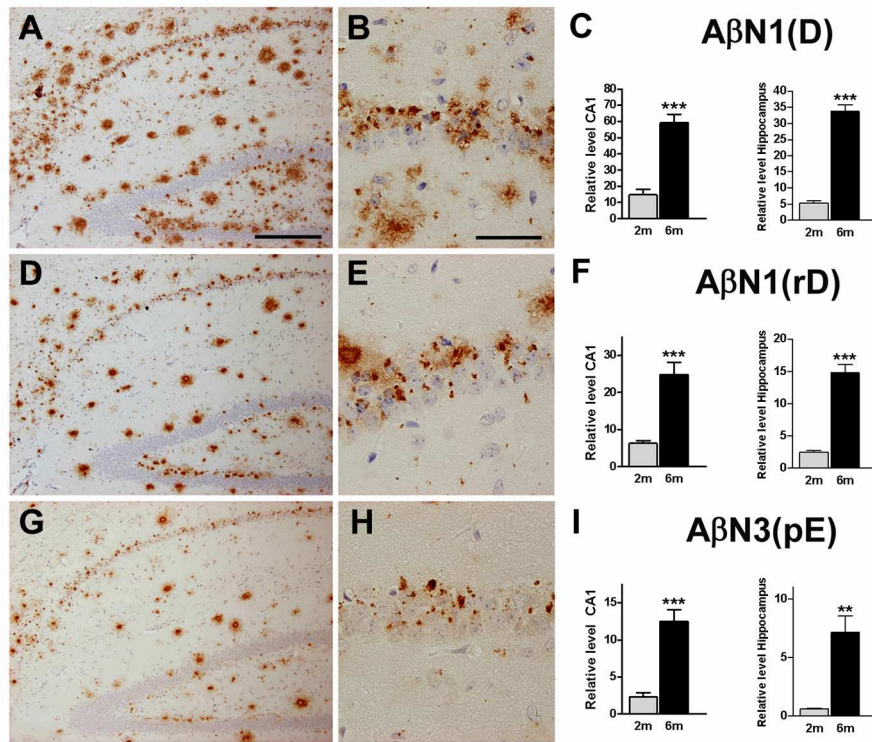


Fig. 24: Representative hippocampal sections of 6-month-old APP/PS1KI mice treated with antibodies against N-modified Aβ forms including peptides starting with L-aspartate AβN1(D) (A, B), racemized aspartate AβN1(rD) (D, E), and AβN3(pE) against pyroglutamate at position 3 (G, H). Quantitative analysis revealed a significant increase of all Aβ peptides in CA1 pyramidal neurons and in total hippocampus (C, F, I) at 6 months compared with 2-month-old APP/PS1KI mice ($n = 5$ per group). Values are given as means \pm s.e.m., (C, F, I); *** $P < 0.001$; ** $P < 0.01$; * $P < 0.05$, unpaired t-test. Scale bars: 200 μ m (hippocampus: A, D, G) and 33 μ m (CA1: B, E, H).

Quantification of total brain Aβ_{x-42} and Aβ_{N3(pE)} peptides using specific ELISAs revealed a related finding. Total Aβ_{x-42} peptides were found already in a considerable amount at 2 months of age (35191 ± 446 pg/mg w.w) and increased significantly up to the age of 6 months (58063 ± 7014 pg/mg w.w.; $P < 0.05$; + 65%). Quantification of the N-modified peptide Aβ_{N3(pE)} disclosed a much more dramatic increase in the APP/PS1KI mice between 2- (2.12 ± 0.01 pg/mg w.w.) and 6-month-old animals (91.32 ± 13.08 pg/mg w.w.; $P = 0.0022$; + 4200%) (Fig. 25, A – B), thereby corroborating the results of the immunohistochemical quantification in the CA1 granular cell layer and hippocampus.

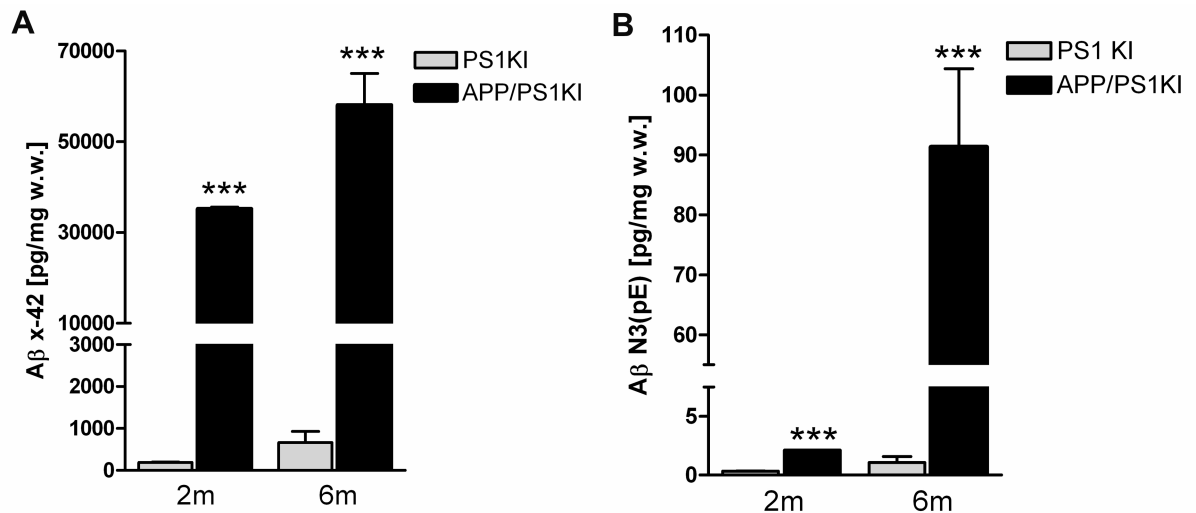


Fig. 25: ELISA analysis of (A) Aβ_(x-42) and (B) Aβ_{N3(pE)} in the brain of APP/PS1KI (2m: N=3, 6m: N=4) and PS1KI PS1KI (2m: N=3, 6m: N=3) mice at 2 and 6 months of age. Values are given as means ± s.e.m., ****P* < 0.001, unpaired t-test.

4.5.2 Target Gene expression in heterozygous and homozygous transgenic mice with Ubiquitous Overexpression of Glutaminyl-Cyclase (QC)

The mQC mouse model was designed for analyzing the impact of glutaminyl cyclase on the neuropathological development of transgenic mice models for Alzheimer's disease. Therefore, mQC transgenic mice were prepared for later crossing with different Alzheimer's disease mouse models, that have been overexpressing the direct substrates of QC Aβ_{N3E-42} and Aβ_{N3Q-42}.

Purpose of the project was to verify the overexpression of mQC in mQC-transgenic mice by determination of the activity and the expression of the enzyme glutaminyl cyclase in heterozygous and homozygous genotypes of this mouse model. Ubiquitous expression is driven in the mQC-model by the chicken-beta-actin CAG promoter and mice were bred on a C57BL6 background. Generation of transgenic mice was performed at Genoway Germany GmbH, Hamburg.

Activity of glutaminyl cyclase was determined in EDTA-plasma in an HPLC based assay (see materials and methods chapter 3.7). I analyzed animals homozygous and heterozygous for

mQC and used wildtype C57BL6 animals as a control group that showed only endogenous mQC activity. I analyzed the activity of glutaminyl cyclase EDTA-plasma of two month old female (N = 1) and male (N = 2) homozygous transgenic animals and two wildtype controls with an equal genetic background. All homozygous animals were sacrificed at 2 months of age. In addition 2 m old female heterozygous (N = 2) and wildtype (N = 2) mice were analyzed. Besides the analysis of mQC-activity, the expression of QC-mRNA in kidney and brain was examined by real-time RT-PCR.

4.5.2.1 QC-ACTIVITY IN EDTA-PLASMA AND TISSUE HOMOGENATES

The aim of the study was to verify the ubiquitous overexpression of the mQC cDNA in the transgenic mQC-mouse-model (heterozygous (He) and homozygous (Ho) transgenic animals). The results proof an overexpression of the target gene in both homozygous and heterozygous transgenic mice compared to wiltype mice that express mQC only at endogenous levels.

Determination of mQC activity was assessed in a HPLC based assay in EDTA-Plasma, while in tissue homogenates this assay could not be applied probably due to the high lipid content in tissue that interfere with the sample preparation.

In EDTA-Plasma, 2-month-old heterozygous female mQC mice displayed a 21-fold higher specific QC activity compared with wildtype littermates, while homozygous 2-month-old mice even displayed a 37-fold increased mQC activity in EDTA-plasma. Males were generally seen to show 2 – 3-fold higher levels of mQC-activity compared to females in EDTA plasma. The expected double increase between homozygous and heterozygous 2 m old animals was – in contradiction to female mice - not observed in male mice, where homozygous and heterozygous mice turned out to display similar levels of mQC activity. Small group sizes may show their impact here. Though, homozygous and heterozygous mQC-mice proved to own a highly increased QC-activity in EDTA-plasma, giving clear evidence for expression of the transgen in these mice.

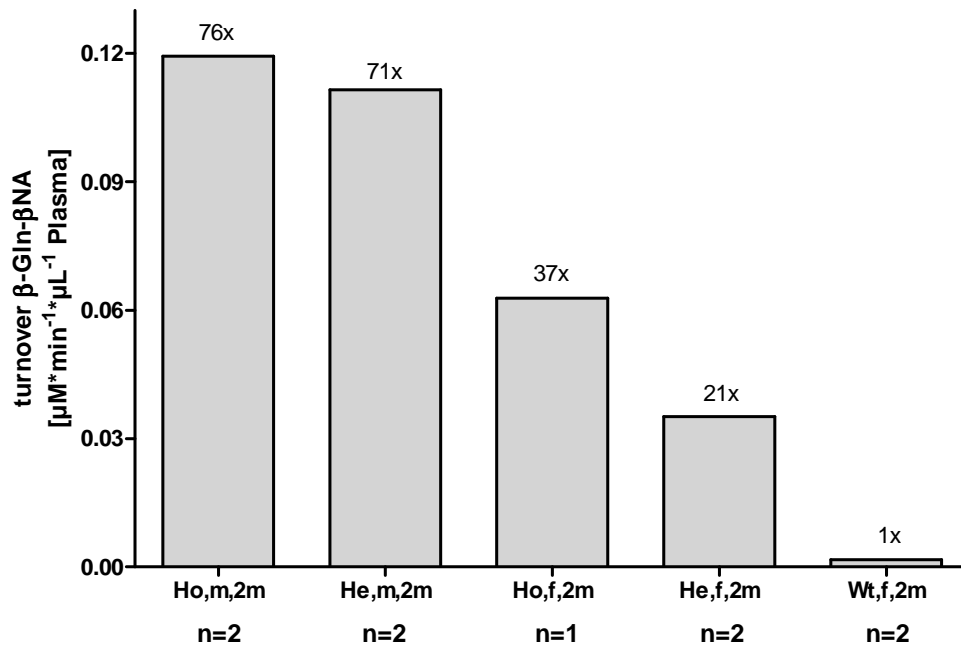


Fig. 26: Activity of glutaminyl cyclase activity in EDTA-plasma of homozygous (Ho), hemizygous (He) mice transgenic for QC and wildtype as reference species (WT). All mice were bred on a pure C57BL6 background.

4.5.2.2 EVALUATION OF QC-TRANSCRIPT LEVELS USING REAL-TIME RT-PCR

In brain and kidney, QC mRNA concentrations were strongly increased compared to control group (Fig. 27, 28). Compared to female wildtype animals of 2 months of age, age-matched heterozygous mQC-transgenic mice showed a 4.4-fold increase in mQC expression, while heterozygous male mice revealed even higher expression of mQC with a 7.7-fold mRNA level. Homozygous male mQC-mice of 2 months of age showed a 11.3-fold overexpression of mQC-mRNA, which is a 1.47-fold increase compared to heterozygous male animals. Homozygous females were determined to have a 6.3-fold higher mQC-mRNA expression compared to wildtype female animals, which is a 1.43-fold increase compared to heterozygous female animals. Therefore, gender-matched expression ratios between homozygous and heterozygous animals showed to be highly stable. Homozygous animals seem to have an estimated 40% increase in mQC mRNA-expression compared to heterozygous mice.

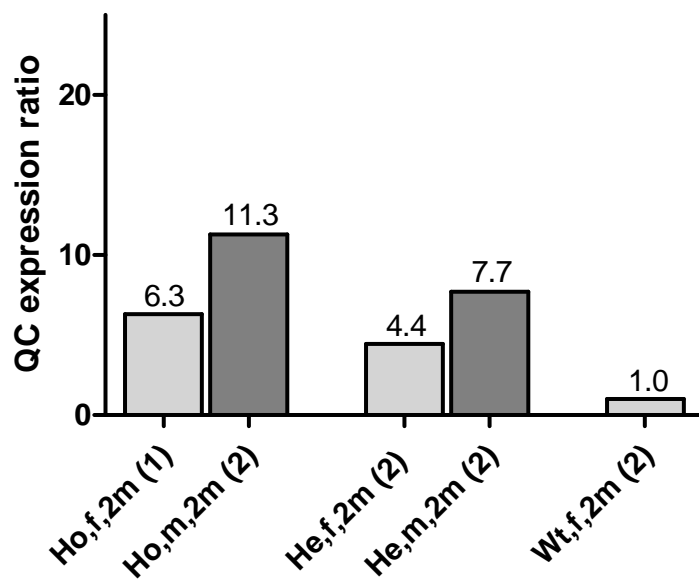


Fig. 27: Analysis of expression of glutaminyl cyclase in brain of homozygous, heterozygous mQC-transgenic and wildtype mice. Group sizes are shown in brackets behind bar denotations. Data are corrected with expression of HRPT as a housekeeping gene.

Conclusively, expression analysis in the brain clearly proves overexpression of mQC in mQC-transgenic mice.

4.5.2.3 QC-EXPRESSION IN THE KIDNEY

In the kidney expression of heterozygous female mQC-transgenic mice relative to wildtype animals was observed to be 326-fold increased, while this ratio was determined to be only 94-fold increased in heterozygous male mice. Mice homozygous for mQC revealed to have generally higher levels of mQC-expression than gender-matched heterozygous littermates. Though no stable ratio of expression was found between gender-matched homozygous and heterozygous mQC-mice, as has been described for the brain mRNA expression.

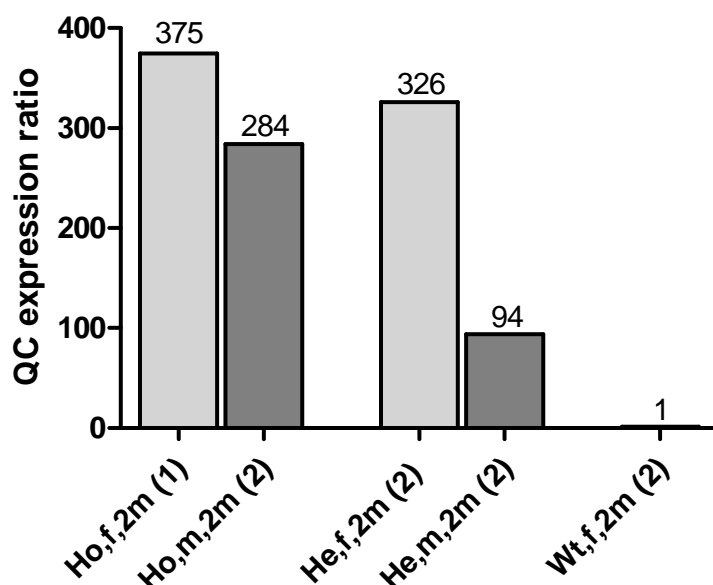


Fig. 28: Analysis of expression of glutaminyl cyclase in kidney of homozygous and heterozygous mQC transgenic and wildtype mice. Group sizes are shown in brackets behind bar denotations. Data are corrected with expression of HRPT as a housekeeping gene.

Homozygous female mQC-mice showed a 375-fold increase in mQC mRNA expression, while male littermates revealed only a 284-fold increase. This was nearly three times as high as expression determined in heterozygous males. Comparison of expression between homozygous and heterozygous females revealed only a minor increase in mQC expression in homozygous animals.

4.5.3 *IN VIVO* FORMATION OF PYROGLUAMATE A β IN TBA1 AND TBA2 MICE

In addition to A β starting with aspartate at position 1 (A β_{1D}), the majority of amyloid A β peptides in Alzheimer's disease (AD) brain exhibit a large heterogeneity at their N-terminus. The dominant species starts at position 3 with pyroglutamate (A $\beta_{3(pE)}$), which can be converted enzymatically using either N-terminal glutamate (A β_{3E}) or glutamine (A β_{3Q}) as substrate (Fig. 7). Two novel mouse models that express A β_{3-42} peptides under the control of the Thy-1 promoter were generated. The TBA1 line expresses A β with N-terminal glutamate (A β_{3E-42}), whereas the TBA2 line expresses A β with N-terminal glutamine (A β_{3Q-42}). Both transgenic A β peptides were expressed as fusion proteins with the pre-pro-sequence of murine thyrotropin-releasing hormone (mTRH) (Fig. 29b), for transport via the secretory

pathway (Cynis *et al.* 2006). The mRNA expression levels of the transgenic constructs in the brain of TBA1 and TBA2 mice were similar (Table 9).

Mouse line	Expression level compared to TBA1	Standard error	p-value
TBA1-QC	0.958	0.775 – 1.162	0.760
TBA2	1.503	0.913 – 1.423	0.054

Table 9: mRNA expression ratio of the transgenic construct in TBA1 mice (n = 4) compared with double-transgenic TBA1-QC (n = 3) and TBA2 mice (n = 4). The results of the expression ratio of the transcripts were tested for significance by a Pair Wise Fixed Reallocation Randomisation Test, and did not show a significant difference between the different mouse lines. The results were normalized to β -Actin mRNA levels.

Protein quantification of $A\beta_{x-42}$ and $A\beta_{3(pE)}$ levels in brain lysates of wildtype (WT), murine glutamyl cyclase transgenic (QC), TBA1, TBA1-QC double-transgenic, and TBA2 mice revealed significant differences (Fig. 29 c-e). While WT and QC transgenic mice generated low amounts of murine $A\beta_{x-42}$ (WT, 1.29 ± 0.91 ; QC, 1.36 ± 0.61 pg/mg w.w.), TBA1 mice elicited 32.57 ± 2.27 pg/mg w.w. $A\beta_{x-42}$, which was significantly more compared to WT mice ($P < 0.0001$). A trend of increased $A\beta_{x-42}$ was detected in TBA1-QC double-transgenic mice with 53.29 ± 10.13 pg/mg w.w., which, however, did not reach statistical significance in comparison to TBA1 single-transgenic mice ($P = 0.06$). TBA2 showed a 12-fold elevation of $A\beta_{x-42}$ (410.2 ± 21.52 pg/mg w.w) compared to TBA1 ($P < 0.0001$) and to TBA1-QC double-transgenic mice ($P < 0.0001$) (Fig. 29 c). In WT and QC mice $A\beta_{3(pE)}$ was undetectable by ELISA (Fig. 29 d). However, there was a significant difference between TBA1 (1.89 ± 0.16 pg/mg w.w.), and TBA1-QC double-transgenic mice (2.34 ± 0.14 pg/mg w.w.). The TBA1-QC double-transgenic mice elicited a 1.2-fold increased amount of $A\beta_{3(pE)}$ ($P < 0.05$). This finding indicates that QC catalyzes N-terminal glutamate to pyroglutamate formation *in vivo*. The TBA2 mice showed significantly higher $A\beta_{3(pE)}$ levels (53.23 ± 4.59 pg/mg w.w) than TBA1 (28-fold more; $P < 0.0001$). The ratios of $A\beta_{3(pE)}$ to total $A\beta_{x-42}$ revealed similar results. TBA1 mice had a ratio of 0.06 ± 0.005 compared to TBA1-QC double-transgenic mice with 0.05 ± 0.005 ($P = 0.25$). TBA2 mice showed a increased ratio of 0.11 ± 0.015 ($P < 0.0001$) (Fig 29 e).

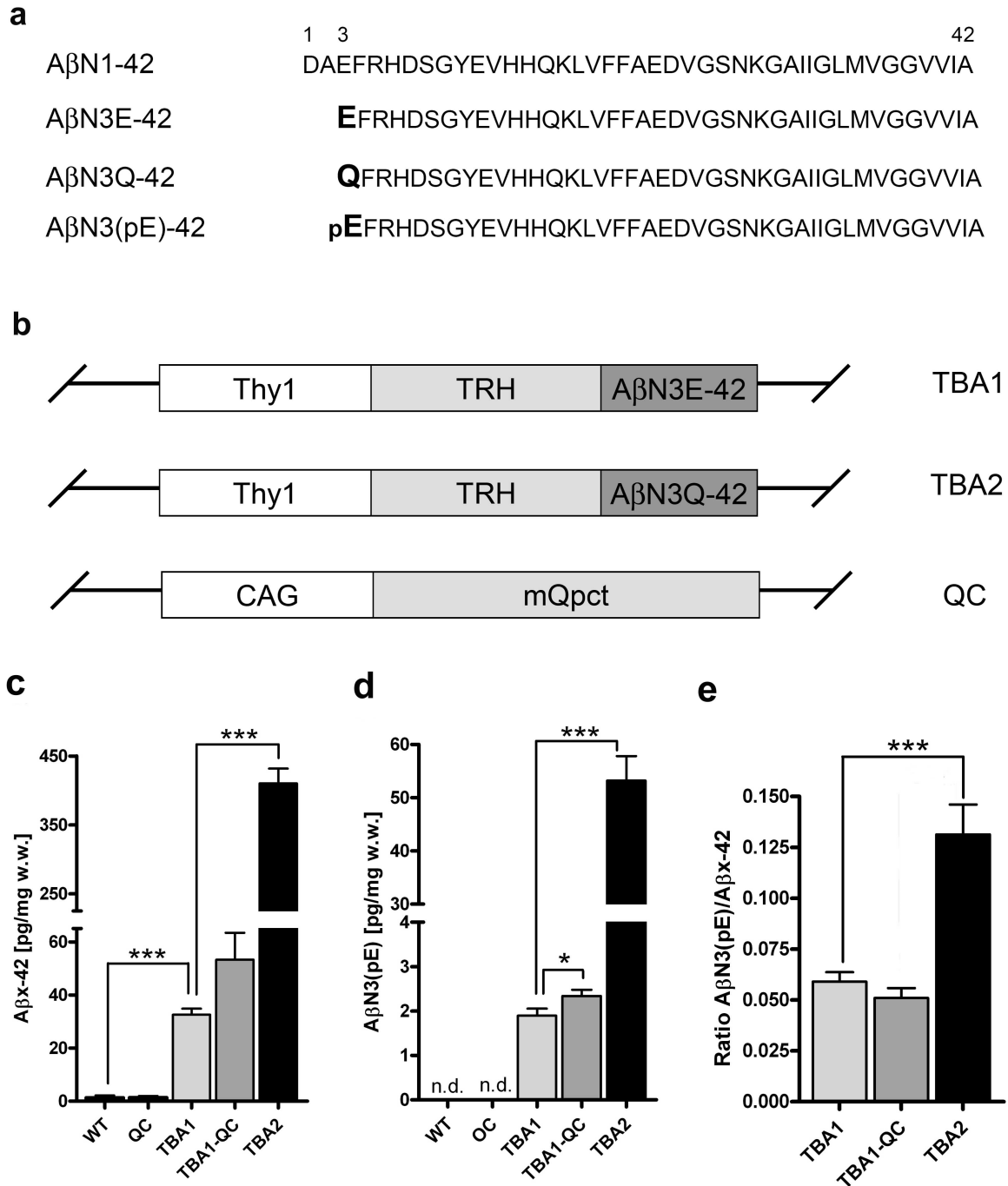


Fig. 29: Constructs to generate the transgenic mice and expression profile in brain at 2 months of age. (a). A β ₁₋₄₂ starts at position 1 with aspartate (D), A β _{3E-42} at position 3 with glutamate (E), and A β _{3Q-42} with glutamine (Q). Both N-truncated A β _{3E-42} and A β _{3Q-42} peptides can be converted by QC activity to generate A β _{3(pE)-42} (Fig. 7). **(b)** Schematic drawing of the transgenic vectors. TBA1 and TBA2 transgenic mice express either A β _{3(E)-42} or A β _{3(Q)-42} under the control of the Thy1 promoter and are fused to the signal peptide of TRH. QC transgenic mice express the murine QC minigene (mQpct) under the control of the CAG promoter. **ELISA analysis of (c - e)** ELISA measurements of A β _{x-42} and A β _{3(pE)} in brain hemisphere lysates of WT (N=6), QC (N=6), TBA1 (N=9), TBA1/QC (N=9), and TBA2 (N=4) mice. **(c)** Significant increase in A β _{x-42} levels was found in TBA1 mice, compared to WT controls ($P < 0.0001$). TBA2 showed the highest levels of A β _{x-42} compared to TBA1 ($P < 0.0001$, unpaired t-test) and TBA1-QC double-transgenic mice ($P < 0.0001$, unpaired t-test). **(d)** TBA1-QC double-transgenic mice had increased levels compared to TBA1 expression alone. TBA2 mice showed the highest levels of A β _{3(pE)} compared to TBA1 ($P < 0.0001$, unpaired t-test) and TBA1-QC double-transgenic ($P < 0.0001$, unpaired t-test) mice. **(e)** The same was true for the ratios of A β _{3(pE)} to total A β _{x-42}. All mice were 2 months of age. Values are given as means \pm s.e.m., * $P < 0.05$. *** $P < 0.001$.

The TBA2 transgenic mice revealed obvious macroscopic abnormalities, including growth retardation, cerebellar atrophy, premature death (Fig. 31), and a striking neurological phenotype characterized by loss of motor coordination and ataxia (video material, data not shown). The body weight at 2 months of age was significantly reduced in TBA2 mice (females, 12.20 ± 0.95 g; males, 17.60 ± 0.51 g), compared to WT control littermates (females, 19.90 ± 0.40 g; males, 24.43 ± 1.23 g; both significance: $P < 0.001$).

Only one TBA2 founder mouse was fertile and was studied in more detail (named TBA2 line). The offspring showed a strong transgene $A\beta$ expression in CA1 at 2 months of age, however, the accumulation of $A\beta_{3(pE)}$ was low (Fig. 32 b). It is suggestive that accumulation of $A\beta_{3(pE)}$ is age-dependent, because it was found to be present at 6 months of age in another infertile founder after pronuclear injection of the TBA2 construct. This infertile TBA2 founder revealed a dramatic loss of neurons in the CA1 layer, which correlated well with abundant deposition with $A\beta_{3(pE)}$ (Fig. 30 a-c).

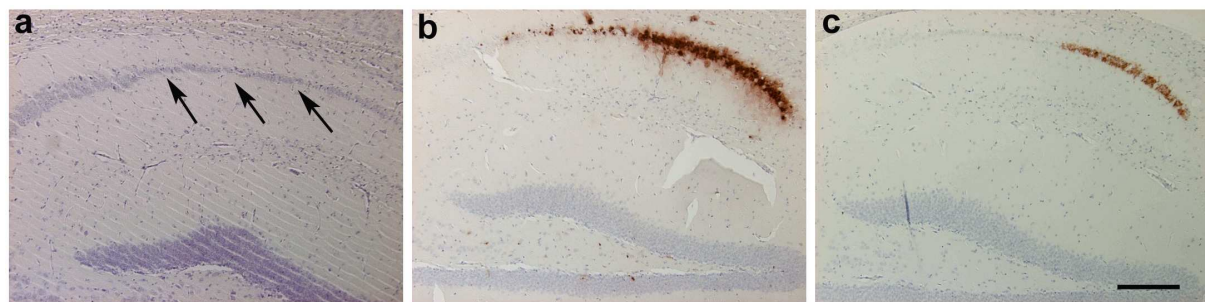


Fig. 30: Immunohistochemical staining of the hippocampus of the infertile TBA2 founder mouse, which died at 6 months of age. (a) Haematoxylin staining demonstrating thinning of the CA1 pyramidal cell layer (arrows). (b) Immunostaining with 4G8 revealed strong $A\beta$ accumulation in the CA1 pyramidal layer of the hippocampus. (c) The same staining pattern was observed with an antibody against $A\beta_{3(pE)}$. Scale bar: a-c, 200 μ m.

It may be hypothesized that the lack to detect $A\beta_{3(pE)}$ associated neurodegeneration in CA1 neurons in the fertile TBA2 line is due to the premature death phenotype at approximately 3 months of age.

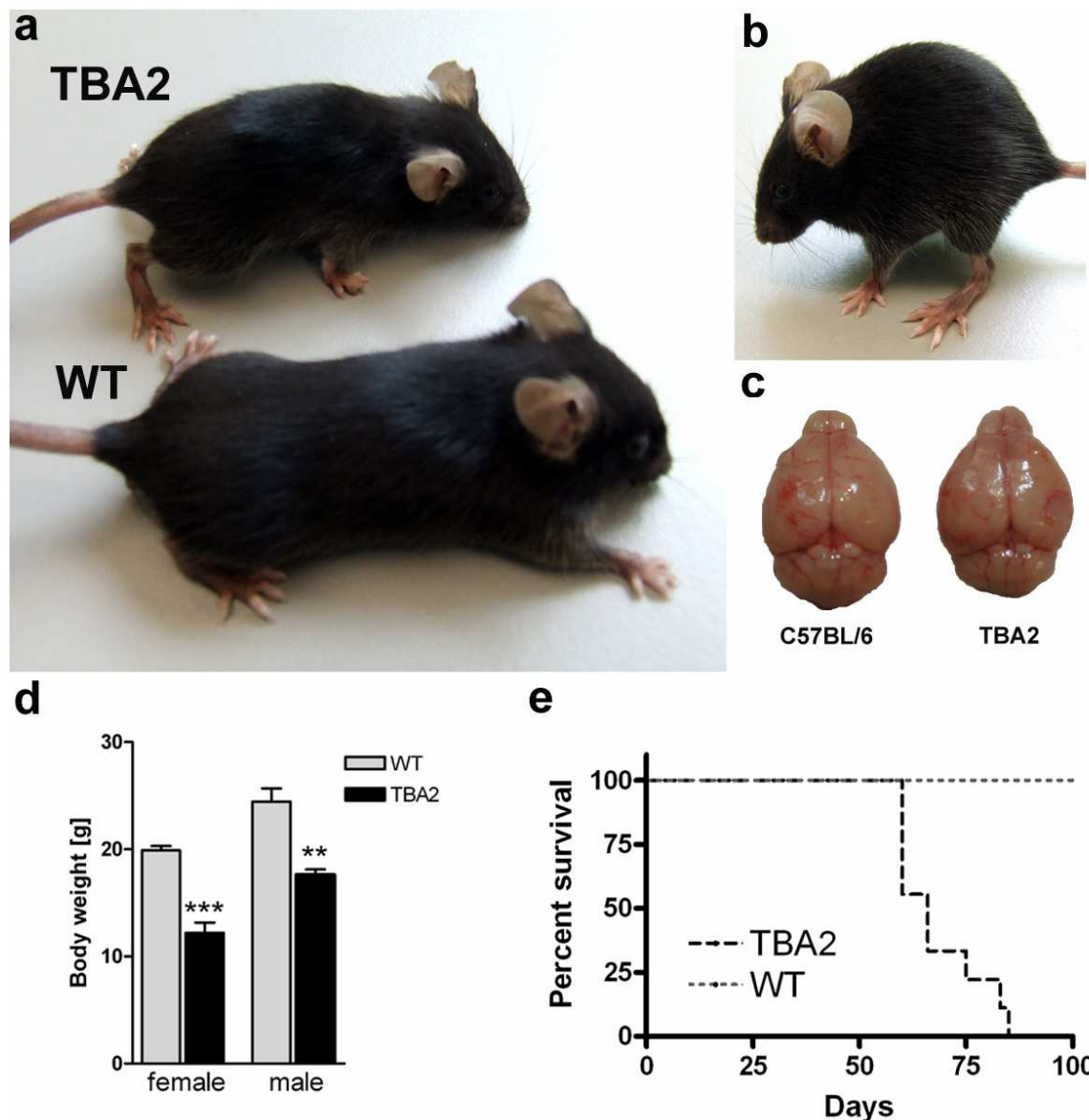


Fig. 31: Characterization of TBA2 transgenic mice. (a, b) Picture of wildtype (WT) and TBA2 mice showing that TBA2 mice are generally smaller and that they display a crooked posture (b). (c) Macroscopic inspection of TBA2 brains revealed that an atrophic cerebellum as compared to age-matched WT littermates (2 months-old mice). (d) Both female (N=4) and male (N=4) TBA2 mice showed a reduced body weight compared to their age-matched WT littermates (2 months-old mice, N: 3 female, 4 males)) (unpaired t-test). (e) TBA2 (N=9) mice displayed a significantly reduced survival rate compared to WT littermates (N=6) ($P = 0.0002$; Logrank Test). Values are given as means \pm s.e.m., *** $P < 0.001$.

The neurological phenotype of the TBA2 line resembles that of mouse models with Purkinje cell degeneration (for example(Burright *et al.* 1995)). Consistently, TBA2 brain sections showed strong immunoreactivity using antibody 4G8 against A β (epitope 17-24) predominantly in CA1 pyramidal neurons and in Purkinje cells (Fig. 32). Neurons in other brain areas were also positive, but the immunoreactivity was less abundant. Diffuse plaques were observed in cortex, hippocampus, cerebellum, thalamus and other subcortical areas, but were less prominent compared to intraneuronal staining (not shown). While low number of

plaques was detected in the cerebellar molecular, piriform and granular layers, most A β immunoreactivity was found associated with Purkinje cells (Fig. 32 e, f). Many, but not all, Purkinje cells were positive for A β _{N3(pE)} (Fig. 32 f, g). Neuropathological analysis of TBA2 mice demonstrated neurodegeneration of Purkinje cells by several observations: (i) The Purkinje cells were positive for ubiquitin, a marker for protein degradation (Fig. 32 l). (ii) Abundant micro- and astrogliosis was observed in the cerebellar molecular layer (Fig. 32 h-k). (iii) Loss of calbindin-positive Purkinje cells. Interestingly, extracellular A β deposition was observed, which was associated with the site of Purkinje cell loss (Fig. 32 m, n). The neuropathological observations correlate well with the age-dependent neurological and cerebellar atrophy deficits in the TBA2 model (Fig. 31 c). No staining was observable using antibodies against hyperphosphorylated Tau (AT8 and PS199) or activated caspase-3 (a marker for apoptosis).

5 DISCUSSION

5.1 DEFICITS IN WORKING MEMORY AND MOTOR PERFORMANCE DECLINE IN THE APP/PS1KI MOUSE MODEL FOR ALZHEIMER'S DISEASE ARE PARALLELED BY EXTENSIVE NEURON LOSS AND HIPPOCAMPAL SHRINKAGE

The objective of the present study was the characterization of a behavioral correlate to a previously described age-dependent axonal degeneration and hippocampal neuron loss in a mouse model expressing human mutant APP on a homozygous PS1 knock-in background (Casas *et al.* 2004; Wirths *et al.* 2006), which has not been previously behaviorally characterized. It has been shown in this work that APP/PS1KI, in contrast to PS1KI mice, display a severe progressive neurological phenotype characterized by wasting, growth retardation, gait disturbances and the development of a thoracolumbar kyphosis, which is a special type of spinal deformity characterized by an increased curvature of the thoracic spine. This phenotype probably results of progressive motor dysfunction due to age-dependent axonal degeneration in the spinal cord. A similar phenotype has also been described in mice lacking the huntingtin interacting protein 1 (*HIP1*) (Metzler *et al.* 2003) or in mice with a mutant methyl-CpG binding protein 2 (*MECP2*) gene, which represent a model system for Rett syndrome, a neurodevelopmental disorder characterized by the loss of language and motor skills during early childhood (Shahbazian *et al.* 2002). Additionally, it was demonstrated that APP/PS1KI mice develop an age-dependent decline in working memory as tested by Y-maze, cross-maze and T-CAT, starting at the age of 6 months. The ability to successfully perform these tests was not affected by the motor deficits at the same age, as shown by higher frequencies of arm entries in APP/PS1KI mice in the Y-maze, and unchanged mean session duration in the T-CAT free-choice trials. The higher frequency of arm entries in the 6 month-old APP/PS1KI mice might be attributed to a higher general activity, which has been previously reported in a different APP-transgenic mouse line (Ambree *et al.* 2006).

Working memory assesses recent memory related to the optimal foraging strategy in the wild (Dember & Fowler 1958), depends on the integrity of prefrontal and hippocampal systems (Divac 1975) and has previously been shown to be impaired in another AD mouse model (Lovasic *et al.* 2005). The decline in working memory coincides with the previously reported onset of CA1 neuron loss at the age of 6 months in this mouse model (Casas *et al.* 2004).

APP/PS1KI mice at 6 months of age showed a significantly reduced alternation performance in the Y-maze and cross-maze compared to their age-matched PS1KI littermates. This result differs from spatial working memory measures in other AD mouse models, where no impairment was detected (Lalonde *et al.* 2004; Savonenko *et al.* 2003). As this task does not place a high demand on hippocampus-dependent learning and memory, it is perspicuous that only mice with severe hippocampal deficits show impairment in this task. The T-CAT has been shown previously to be a valuable tool to measure hippocampal dysfunction (Gerlai 1998). In this spontaneous alternation task, APP/PS1KI mice performed significantly worse than their PS1KI littermates at the age of 6 months, with alternation rates below chance level. Two month-old APP/PS1KI mice were not different in both working memory tests, pointing to an age-dependent process, as expected. All working memory tasks show a strong decline in the measured performance in APP/PS1KI mice between two and six months of age, while from six months on to the age of twelve months only minor changes in working memory performance were detected. This can be explained by the fact, that around 80% of total neuron loss observed in APP/PS1KI mice hippocampal CA1 region occurs up to six months of age, while only 20% take place between six and twelve months.

A variety of Alzheimer's disease mouse models with the development of motor impairment and spinal pathology have been previously described; however, most of them express human Tau protein and none of them harbors amyloid pathology (Lewis *et al.* 2000; Spittaels *et al.* 1999; Terwel *et al.* 2005). An abnormal paw-clasping reflex has been described in different APP/PS1 mice (Wirths *et al.* 2006; Wirths *et al.* 2006), and in mice transgenic for human four-repeat tau (Probst *et al.* 2000) or human apolipoprotein E4 transgenic mice (Tesseur *et al.* 2000), which all displayed marked signs of axonal degeneration. Detailed quantification of this clasping phenotype revealed that it is highly significant in APP/PS1KI mice already at 6 months of age, accompanied by a reduced average stride length becoming significant at the same time point.

Deficiencies in motor performance, including gait disturbances and postural deficits have been reported in AD patients, raising the question whether underlying axonal alterations contribute to this particular feature of the disease (O'Keefe *et al.* 1996; Pettersson *et al.* 2002; Scarmeas *et al.* 2004). It has further been shown that motor signs have a predictive value in AD, as e.g. postural-gait abnormalities carry an increased risk for institutionalization and mortality (Scarmeas *et al.* 2005). A tremendous decrease of motor abilities was observed

during aging in the APP/PS1KI mice. Highly significant deficits in the balance beam, string suspension and vertical grip hanging tasks were detected as early as 6 months of age. These mice further showed a reduced latency to fall in the rotarod task, compared to age-matched PS1KI mice. However, a clear improvement was noted during training for both groups, leading to the assumption that the execution of motor behavior rather than motor learning abilities is impaired in APP/PS1KI mice. A similar finding has been reported in 12 month-old APP_{swe}/PS1_{M146L} transgenic mice (Ewers *et al.* 2006). The rotarod task has been shown to be a sensitive indicator of cerebellar lesions in mouse mutants (Lalonde & Strazielle 2001). However, due to the used Thy1.2-promotor construct, APP expression in this brain region is very restricted. Therefore, axonal deficits, loss of connecting neurons with the cerebellum and/or impairment of other brain regions like the motor cortex and basal ganglia might result in the described motor phenotype. As the PS1KI mice were used as a control group, it is of particular interest that no impairment in motor coordination tasks has been recently reported in a different homozygous PS1KI (I213T) mouse model (Lalonde & Strazielle 2005).

Analysis of exploration, anxiety and locomotor activity in the open field paradigm revealed no age- or genotype-dependent deficits in the total traveled distance or the time spent in the inner (exploration) zone at the two analyzed time points. A similar result has been previously reported in 7 month-old APP_{swe} + PS1/ΔE9 mice (Lalonde *et al.* 2004) or in 13 month-old APP_{swe} mice (Lee *et al.* 2004), which did not differ from control mice in this task. A strong reduction in rearing events was detected in 9 month-old APP/PS1KI mice, which is in line with motor deficits revealed in the sensory-motor task battery. Rearing behavior in the open field has been reported to reflect exploratory behavior and motor activity (Archer 1973). However, considering the unchanged traveled distance in the open field and the increased number of arm entries in the Y-maze, the reduced rearing frequency is most likely due to impaired motor activity, rather than reduced exploratory drive.

Several APP transgenic models have been demonstrated to show impairments during acquisition in the hidden platform version of the Morris water maze, a task which has become one of the standard measures of working memory deficits in mice (Hsiao *et al.* 1996; Janus 2004; Lalonde *et al.* 2002). Analysis of swimming parameters revealed a significantly reduced swimming distance and speed in APP/PS1KI mice of 6 months of age and older, accompanied by alterations in swimming behavior in aged mice (12 months). Therefore, the often used Morris water maze task as a test for reference memory impairment was omitted in

the APP/PS1KI mouse model. The underlying motor deficits displayed by the forced swimming task preclude drawing any conclusions from these experiments. The assessment of reference memory using tasks like the Morris water maze therefore has to be always combined with an extensive analysis of motor performance in order to avoid misinterpretation due to an overlap of motor and cognitive deficiency.

Axonal deficits have been previously published in another APP/PS1 transgenic mouse model (Wirhys *et al.* 2006), as well as in APP single transgenic mice already at a young age well before other neuropathological lesions were observed (Stokin *et al.* 2005). Stokin *et al.* showed that axonal defects consisted of swellings that accumulated abnormal amounts of microtubule-associated and molecular motor proteins, organelles, and vesicles. Impairing axonal transport by reducing the dosage of a kinesin molecular motor protein enhanced the frequency of axonal defects and increased the level of intraneuronal A β peptides and plaque deposition. The authors concluded that reductions in microtubule-dependent transport may stimulate proteolytic processing of APP, triggering typical AD pathology. In the APP/PS1KI model the situation is different. Due to overexpression of APP and expression of mutant knocked-in PS1, there is a robust and early intraneuronal accumulation of a variety of N-modified A β peptides (Wirhys *et al.* 2006). It is important to note that 85% of the A β peptides end at position 42 (Casas *et al.* 2004). It is to speculate that the two PS1 knock-in mutations induce a loss of function in β -secretase cleavage of APP, therefore elevated C99 levels were observed in these mice, together with an increase in A β_{x-42} levels (Casas *et al.* 2004). Recently, Kumar-Singh *et al.* have demonstrated that several PS1 mutations significantly increased the ratio of A β_{42} /A β_{40} *in vitro* by significantly decreasing A β_{40} with accumulation of APP C-terminal fragments, a sign of decreased β -secretase activity (Kumar-Singh *et al.* 2006). This suggests that A β_{40} might be protective for neuronal integrity; however, it has been recently shown that increased A β_{40} levels lead to congophilic amyloid angiopathy (CAA) and microvessel rupture in a transgenic mouse model (Herzig *et al.* 2004). The two PS1 mutations (M233T/L235P) in the APP/PS1KI mouse may therefore also induce a loss of PS1 function resulting in reduced A β_{40} levels and an increased A β_{42} /A β_{40} ratio. The consequence clearly is an increase in intraneuronal A β_{42} levels, which might induce axonal degeneration in brain and spinal cord and a robust neuron loss in CA1 of the hippocampus. I have demonstrated that both pathological features coincide with the observed changes in body weight, body shape, working memory and motor performance. It has been previously shown that plaque load does not correlate with neuron loss in another AD transgenic model (Schmitz *et al.* 2004).

Moreover, plaque-independent axonal degeneration has been previously demonstrated (Wirths *et al.* 2006; Wirths *et al.* 2006) Therefore, intraneuronal A β_{x-42} accumulation as an early pathological event might promote the observed behavioral deficits.

5.2 PATHOLOGY-DEPENDENT DEVELOPMENT OF INFLAMMATION IN AN APP/PS1KI MOUSE MODEL OF ALZHEIMER`S DISEASE

APP/PS1KI mice used for this study are characteristic for developing a severe age-dependent phenotype of Alzheimer disease. This phenotype is prominently present at six months of age and features besides massive accumulation of intracellular A β and extracellular A β plaque build-up also a striking neuron loss in hippocampal CA1 region evident already at six months of age, motor deficits in accordance with axonopathy as well as a remarkable loss in working memory performance proven by results from working memory related tasks like Y-, T-maze (Casas *et al.* 2004; Wirths *et al.* 2007; Wirths *et al.* 2002; Wirths *et al.* 2006). Contrastingly, at 2 months of age APP/PS1KI mice showed no eye-catching phenotypical difference compared to age-matched PS1KI control mice. In terms of immunohistochemical consideration the most eminent difference between these two genotypes at 2 months of age is an extensive positive immunohistostaining for intracellular A β in hippocampal CA1 neurons, which obviously is not sufficient to induce any observable phenotype in APP/PS1KI mice at least with the motor and memory tests of our choice. A detailed histochemical and behaviour analysis of these mice can be looked up in Casas *et al.* 2004 and Wirths *et al.* 2002, 2004, 2006 and 2007 (Casas *et al.* 2004; Wirths *et al.* 2007; Wirths *et al.* 2002; Wirths *et al.* 2006).

Going well in line with the unobtrusive behavioural phenotype and the poor histochemical findings according to A β plaque pathology in young APP/PS1KI animals, glial fibrillary acidic protein (GFAP) came out to show the only significantly increased expression on the mRNA level at two months of age. In AD brains GFAP is prominently upregulated in the vicinity of amyloid plaques. In young APP/PS1KI mice with beginning extracellular plaque deposition upregulated GFAP mRNA-synthesis may indicate beginning activation of astrocytes as a result of intracellular A β formation in CA1 neurons.

No broader indication of early inflammatory processes was detectable, though a wide variety of genes involved in several complement inflammation pathways was observed. One

explanation could be that the formation of extracellular plaque material is the main trigger for inflammatory responses in the brains of this AD mouse model. Extracellular plaque pathology increases quickly and dramatically in this APP/PS1KI mouse model from the second month on. Extracellular plaque deposits are abundantly present at six months of age while PS1KI control mice are showing no plaque pathology at all at any age.

With this assumption in mind, it is no surprise at all to find a broad range of inflammatory genes massively upregulated in their mRNA expression in APP/PS1KI mice compared to PS1KI control mice at six months of age. The pattern of upregulation indicates mainly a highly intense activation of the glia system in APP/PS1KI mice at six months of age. Glia cells are the most common cell type in the human brain and represent a discrete population of phagocytes that appear first as colonies of embryonic brain and that migrate during further development throughout the CNS (Giulian 1999). Microglia are present in white and gray matter as well. The glia system of the brain is subdivided in several cellular subspecies, most important of them thought to be implicated in inflammation response are microglia and astroglia cells (astrocytes). Microglia are mostly composed of mesodermally derived macrophages. Microglia cells are ascribed to hold a putative role for neurons guarding their functions in the CNS. They are believed to act as immunocompetent defense cells taking lead in organization of the immune response of the CNS towards inflammation events. In healthy brain, microglia exist in general in a quiescent state, that is characterized by low expression of surface receptors, minimal secretory activity, and - in case of contact with astroglia or neurons - minimal migratory behaviour. Microglia cells switching from the quiescent to the reactive state are one of the hallmarks of AD immune pathology (Giulian 1999). Activated microglia are known for their capability to uptake extracellular A β , what appears to be an attempt to remove this excessively spreading protein from the brain (Chen *et al.* 2006). It is well known, that A β and neuritic plaques are capable to induce activation of microglia in AD affected CNS leading also to clustering of microglia around amyloid plaque deposition sites in the brain (Tuppo & Arias 2005). As a consequence of activation, microglia start to secrete a broad range of scavenger receptors, cytokines, reactive oxygen species and complement proteins – all inflammatory mediators involved in triggering numerous signalling pathways.

In six-month-old APP/PS1KI mice all signs of extensive glia activation were found in abundance.

Most prominently increased was GFAP, which has been already increased at two months of age. GFAP is expressed in astrocytes and APP/PS1KI mice show a well-defined pattern of astrogliosis and reactive astrocytes at two and six months of age as can be seen from immunohistochemical analysis using GFAP-directed antibody (Fig. 20, 21). The detected increase of GFAP on mRNA and protein level could be caused by higher expression rates of GFAP in activated astrocytes or by the increase of the total number of astrocytes in the brain due to proliferation as a follow-up process to A β -induced inflammation separately or in a coactive manner.

Msr2 and analysed members of toll like receptor family (TLR2, TLR4, TLR7, TLR9) did also reveal strong upregulation of mRNA levels in APP/PS1KI mice. While scavenger receptors have been implicated in the binding process from A β to astrocytes and in the clearance of fragmented DNA from the brain (Alarcon *et al.* 2005; Li *et al.* 2004b), toll-like receptors (TLRs) are a group of pattern-recognition receptors in the innate immune system of the brain, that have been shown to play a crucial role in activation of the microglia system. In response to insults by for example pathogens and damaged host cells, TLRs can induce the activation of phagocytes and tissue dendritic cells, that leads to the secretion of cytokines, chemokines and other co-stimulatory molecules needed for protective immune responses, efficient damaged tissue removal and for the stimulation of adaptive immunity (Tahara *et al.* 2006). Increased TLR signalling is well described to induce a broad range of genes implicated in phagocytosis and inflammation. Chen *et al.* reported promoted cellular uptake of A β in primary murine microglial cells from newborn C57BL/6 mice and murine microglial cell line N9 by activation of TLR2 (Chen *et al.* 2006). This is in well compliance with the intense upregulation especially of TLR2 in six-month-old APP/PS1KI mice compared to PS1KI littermate controls. Furthermore, Tahara *et al.* were able to show, that activation of microglia (BV-2 cell) with specific ligands for TLR2, TLR4 or TLR9 markedly boosts the uptake and ingestion of A β *in vitro* (Tahara *et al.* 2006).

Secondly, I observed expression patterns of a variety of cytokine genes. Cytokines are inflammatory mediators produced by activated microglia, that trigger and contribute to the so called “cytokine cycle”. They represent as well as their nearby but nevertheless distinct relatives from the family of chemokines intercellular and intracellular signalling factors. A number of cytokines and chemokines as well has been found to be upregulated in AD compared to non demented (ND) individuals. This holds especially true for the major

proinflammatory mediators IL-1 β , IL-6, and TNF α , which can induce cytotoxic or cytopathic effects in the CNS (Dickson *et al.* 1993).

Interleukin1- β has been shown to be increased on protein level in homogenates from frontal, parietal, temporal cortex, hypothalamus, thalamus and hippocampus in humans with AD compared to controls (Cacabelos *et al.* 1994). Microglia-derived IL-1 β is described as a potent immunomodulating cytokine that triggers various inflammatory mediators in astrocytes and neurons (Mrak *et al.* 1995). IL-1 β is directly localized to plaque-associated microglia and appears to be directly involved in AD pathophysiological alterations (Griffin *et al.* 1989). However, in APP/PS1KI mice no statistical significant increased expression of IL-1 β could be found at any timepoint. Though, it is to mention, that at ten months of age there is a statistical trend, indicating a tendency to increased IL-1 β mRNA-levels in comparison to age-matched PS1KI mice.

Surprisingly, also the expression of the proinflammatory cytokine IL-6 remained unchanged, although increased protein levels have been found in human AD brains (Hempel *et al.* 2005). IL-6 is a pleiotropic cytokine that mediates immune response and inflammatory reactions affecting CNS cell growth and differentiation (Akiyama *et al.* 2000). During development, IL-6 is expressed in the nervous system ubiquitously. Microglia, astroglia, neurons, and endothelial cells are described as capable to synthesize IL-6 (Frei *et al.* 1989; Hempel *et al.* 2005; Marz *et al.* 1998).

TNF- α as a further proinflammatory cytokine secreted by activated macrophages and microglia is believed to promote cell survival and death in the CNS. An increase of TNF- α was immunohistochemically shown in the vicinity to senile plaques, implying its participation in A β -induced inflammation (Akiyama *et al.* 2000; Tuppo & Arias 2005; Zhao *et al.* 2003). Recently, though the mechanism remains unsolved, it was shown that TNF α plays a pivotal role for the neurotoxicity of A β (Zhao *et al.* 2003). Contradictory, some reports also suggest a neuroprotective function of TNF- α by reducing cdk5 induced tau hyperphosphorylation (Orellana *et al.* 2007).

IL-10 is thought to be an anti-inflammatory cytokine capable of suppressing microglia activation by the A β -component of senile plaques and of protecting dopaminergic neurons against inflammation-mediated neurodegeneration (Arimoto *et al.* 2006; Szczepanik *et al.*

2001). However, despite massive glia activation mRNA-levels of IL-10 kept unchanged relative to age-matched controls at 2, 6 and 10 months of age. On the other hand Rota et al. recently reported about unchanged levels of IL-10 in sera and CSF of AD patients compared to non demented controls (Rota *et al.* 2006).

A further multifunctional cytokine said to be implied in the progression of AD pathology is transforming growth factor beta (TGF- β). TGF- β is produced by glial and neuronal cells as well. TGF- β has been described to be upregulated in response to brain injury, stroke and under neurodegenerative conditions. Furthermore, TGF- β is thought to possess angiogenic properties besides its capability to promote amyloidogenesis. Tarkowski et al. reported evidence about increased intrahecal levels of the angiogenic factors vascular endothelial growth factor (VEGF) and TGF- β (Tarkowski *et al.* 2002). Well supplemented from the literature, I found a clearly significant increase of TGF- β in APP/PS1KI mice at six and ten months as well. In CSF of human AD patients a significant correlation between levels of TNF- α and TGF- β has been described and it has been suggested, that TNF- α could be responsible to trigger the production of TGF- β at least to a certain extent (Tarkowski *et al.* 2002). However, with TNF- α showing just a statistically not significant trend for age-dependent upregulation in mRNA-expression, I cannot derive clear evidence for this connection from our data nor can I exclude it. Also a beneficial function of TGF- β has been reported. Wyss-Coray et al. described in a transgenic mouse model overexpressing hAPP and TGF- β , that increased expression TGF- β promotes microglial A β clearance and reduces plaque burden (Wyss-Coray *et al.* 2001), pointing to a protective role of TGF- β in AD pathology.

Interestingly, angiogenesis implicated factors VEGF mRNA expression was slightly significant upregulated in APP/PS1KI mice at six months but not any more at ten months of age. The perception of angiogenesis is the formation of new blood vessels from existing vasculature. Normally, angiogenesis is implicated in embryogenesis, tissue growth, development and regeneration, but it also underlies the advancement of cancer and inflammation processes (Pogue & Lukiw 2004; Semenza 2003; Zadeh & Guha 2003). Hypoxia has been shown to induce higher expression of VEGF, while IL-1 β is known to being able to substitute for key aspects of hypoxia signalling, including induction of VEGF gene expression (Ottino *et al.* 2004; Pogue & Lukiw 2004).

The cytokine receptor MCSF-R (macrophage colony stimulating factor) is expressed in macrophages, glia and neurons as well and has been found to be elevated expressed in plaque associated and in reactive microglia. It has been previously shown that MCSF-R strongly fosters proinflammatory effects of A β on cultured microglia cells and is highly capable of activating microglia and other macrophage-like cells (Murphy *et al.* 2000). Increased MCSF-R expression has been reported in brain microglia of a mouse model for mechanical injury and ischemia stroke (Raivich *et al.* 1998). Moreover, MCSF-R is believed to function as a signalling molecule that is implicated in directing activated microglia to sites of insult by promoting cell migration and proliferation (Giulian 1999). Our observation of highly upregulated expression of MCSF-R in APP/PS1KI mice at six and ten months of age featuring massively activated glia cells fits well to the assumed function of this protein.

The cell surface glycoprotein major histocompatibility complex type II (MHC-II) has been reported to be upregulated in activated microglia of human AD by numerous reports, especially in brain regions of pathological relevance for this disease like e.g. the hippocampus (Parachikova *et al.* 2006; Perlmutter *et al.* 1992). Surprisingly, no age-dependent increase of MHC-II was found in APP/PS1KI mice. Moreover, although not statistically significant, an age-dependent decline of MHC-II expression seems to take place in APP/PS1KI mice. This is in contrast to the literature, where for example even in normal ageing a continuous upregulation of MHC-II is being reported (Akiyama *et al.* 2000; Perry *et al.* 1993; Streit & Sparks 1997).

F4/80 and CD11/B are also well defined markers for detection of activated microglia. Both were found to be highly significant upregulated according to their level of mRNA expression in APP/PS1KI mice at six and ten months of age. This can be interpreted as additional underlinement of the inflammation pathology of the glia system in these mice. Again, it has to be noted, that the increase in gene expression is more incisive comparing six to two month old APP/PS1KI mice than ten and six months old animals.

FAS is a gene often brought into discussion about apoptotic neuron cell death in AD and represents a part of the death receptor subfamily. FAS has been reported to be associated with senile plaques and astrocytes of AD patients (Nishimura *et al.* 1995) and in tangle bearing and non-tangle bearing neurons in the frontal cortex of AD patients. Several downstream enzymes of FAS belonging to the caspase family are also implicated in various apoptotic pathways

(Yew *et al.* 2004). In APP/PS1KI mice, FAS was found to show highly significant upregulation at six months and ten months as well compared to age-matched controls. However, if the upregulation of FAS can be interpreted as an indication for apoptosis induced neuron death in APP/PS1KI mice is to be provided with a strong questionmark. TUNEL-staining in six months old APP/PS1KI mice did not reveal any positive stained neurons (data not shown). It has to be mentioned, that the responsibility of apoptotic processes for neuron death in AD and neurodegenerative diseases in general is still a matter of intense debate and widely questionmarked by some researchers (Jellinger 2006).

Recently, in AD patients and two different APP/PS1 AD mouse models a prominent upregulation of S100A6 protein was reported. S100A6 is an acidic $\text{Ca}^{2+}/\text{Zn}^{2+}$ binding protein with a 11 kDa molecular weight and is part of the S100 family.

S100A6 immunoreactivity was shown to be concentrated in astrocytes surrounding classical senile plaques with a dense core of A β as well as to a minor extent also in diffuse plaques. Astrocytes showing a staining for S100A6 were also positive for GFAP and S100B protein (Boom *et al.* 2004). The authors of this study speculate about an implication of S100A6 in the regulation of Ca^{2+} and Zn^{2+} homeostasis in AD, based on the findings that intracellular Ca^{2+} levels have been shown to arise induced by aggregated A β and, secondly, that elevated concentrations of Zn^{2+} have been reported for neocortical areas and A β deposits (Boom *et al.* 2004).

In APP/PS1KI mice osteopontin (SPP1) was significantly higher expressed at six and ten months in comparison to age-matched PS1KI control mice.

Osteopontin is a secreted phosphoprotein and multifunctional Ca^{2+} binding cytokine involved in diverse biological functions, including inflammation, oxidative stress, cell migration and antiapoptotic processes (Meller *et al.* 2005; Wung *et al.* 2007). In inflammation SPP1 is believed to play a role both in acute and chronic inflammation and to be involved in the recruitment of macrophages and T-cells (Mazzali *et al.* 2002). Furthermore osteopontin is of importance in cell adhesion, stress-related angiogenesis and macrophage-directed IL-10 suppression (Akama *et al.* 1998). Besides their potential to enforce direct damage, reactive oxygen species (ROS) have also been shown to change cell signalling pathways, which may lead to further deleterious effects. Also, A β has been shown to increase several markers typical for oxidative stress, e.g. superoxide anion production rises in microglia cells treated

with A β . Oxidative stress in general is believed to foster neuronal destruction in AD brains by lipid peroxidation, tyrosine nitrosylation or DNA oxidative damage (Akama *et al.* 1998).

To get an impression about the AD affected brains response to oxidative stress, I observed the expression pattern of the family of metallothioneins displaying some important defense proteins against free radicals. The human brain is compared to other organs much more at risk to get damaged by free radicals, because its cell membranes are built up to a especially high degree by polyunsaturated fatty acids that are especially prone to oxidation by ROS. Furthermore the brain itself produces significant amounts of nitric oxide and owns only poor to moderate enzyme activities of oxidative stress defense enzymes like catalase, superoxide dismutase and glutathione peroxidase (Carrasco *et al.* 2003).

There is compelling evidence from the literature, that the members of metallothionein family accomplish a neuroprotective mission in the inflammation affected brain by protecting cells from oxidative damage (Carrasco *et al.* 2006; Carrasco *et al.* 2003; Giralt *et al.* 2002; Giralt *et al.* 2002; Penkowa *et al.* 2006). Metallothioneins are small, cystein-rich intracellular proteins, that are almost ubiquitously expressed. Metallothioneins are known to possess a high affinity for binding Zn²⁺ and Cu²⁺. In rodents, the family of metallothioneins subdivides into four distinct proteins classified as metallothionein 1 – 4 (MT-1, MT-2, MT-3, MT-4). MT4 is the only one not expressed in the brain and therefore has not been in the scope of this study. MT-1 and MT-2 are expressed coordinatively in CNS and in most tissues as well (Carrasco *et al.* 2003), whereas MT-3 is the only family member that is expressed exclusively in the brain. Expression of MT-3 takes place predominantly in neurons but is also reported for astrocytes under special circumstances. In APP/PS1KI mice, a strong increase of gen expression for MT-1, MT-2 and MT-3 was observed at six months of age compared to PS1KI control mice while no significant change was found at two months of age. These findings perfectly underline the often made presumption that AD affected brains try to counteract the deleterious effects of oxidative stress by expression of protective proteins like metallothioneins. Interestingly, again at ten months of age no further increase in the expression of metallothionein genes could be detected in a direct comparison to the expression level observed at six months of age in APP/PSKI mice.

Another main source of oxidative stress in AD is anticipated to be founded in disturbances of iron metabolism in the brain. Although iron is essential for cell metabolism, it is also known

to display a source of cytotoxicity in case of disturbance of this metabolism (Castellani *et al.* 2007; Wung *et al.* 2007). Recently, osteopontin has been reported to act as a potent neuroprotectant against ischemic injury due to stroke (Meller *et al.* 2005). Wung *et al.* reported recently SPP1 to be 41% increased in AD hippocampal neurons compared to age-matched ND controls, while no other neuronal cell types were stained. SPP1 expression was found to be dependent upon A β load (Wung *et al.* 2007). The authors suggested that SPP1 upregulation may be a result of cell-cycle related changes and/or may work as a compensatory response to neuronal degeneration in AD affected brain (Wung *et al.* 2007).

While microglia in general are known to play neurotrophic roles in the healthy brain, in AD research the main focus is directed to the potential neurotoxic actions of the glia system. Activated microglia and astrocytes are capable to secrete a broad range of pro-inflammatory cytokines like interleukin-1 β and neurotoxic substances like free radicals and thereby contribute to AD pathology (Hu *et al.* 1998). For example activated glia cells are suspected to be implicated in the formation of reactive oxygen species (ROS) in the brain and therefore contribute to the increase of oxidative stress often reported in brains of AD. Furthermore, reactive astrocytes are known to produce nitric oxide mediated by cytokine-induction of inducible nitric oxide synthase (iNOS) (Moore & O'Banion 2002).

Egana *et al.* reported that iron induced oxidative stress can modify tau phosphorylation patterns in hippocampal cell cultures from E18.5 rat embryos (Egana *et al.* 2003). High concentrations have been reported in human brain cells, that can be released from dying cells to give rise to the production of highly aggressive hydroxyl radicals in a Fenton reaction like pathway (Castellani *et al.* 2007; Mattson 2004).

Transferrin (Trf) and Ferritin light chain (Ftl) mRNA expression were found to be significantly upregulated at six and ten months of age in APP/PS1KI mice compared to age-matched PS1KI controls. With transferrin and ferritin light chain the expression of genes whose corresponding proteins are known for their iron binding properties and their implication in cell iron metabolism were analyzed. Transferrin is the predominant protein for iron transport and essential for surviving. Weekly injections of Trf were reported to be crucial to keep Trf-deficient mice alive (Kaplan *et al.* 1988). Diferric transferrin is taken up by the cell via endocytosis dependent on and mediated by expression of the transferrin receptor located on the surface of the cells (Koeller *et al.* 1989). Expression of Trf receptor is known to be directly controlled by iron concentrations (Casey *et al.* 1989).

Ferritin light chain is another main player in the cellular iron management and is mainly considered to function as an intracellular iron storage protein (Connor & Menzies 1995). Ferritin light chain has been associated with slow uptake of iron and promotion of iron mineralization at the ferritin core (Arosio *et al.* 1991; Connor & Menzies 1995).

Upregulation of the expression of iron metabolism enmeshed proteins may be interpreted as an attempt of the cell to encounter excess iron and its pernicious follow-up effects in oxidative stress cascade in AD pathology affected mouse brain.

In conclusion, our study yields new insights in the APP/PS1KI mouse model of AD and provides a detailed analysis of the expression pattern of inflammation associated genes in these mice. Furthermore I compared the development of inflammatory processes to the progress of AD-like pathology in these mice. The bottom-line is, that inflammation appears to be a follow-up event to the development of AD pathology with the formation of extracellular plaque deposits standing in the focus of potential inflammation triggering events. AD referred pathological process in APP/PS1KI mice is next to its summit already at six months of age. Therefore it can be understood, that the most prominent changes in upregulation of inflammation connected genes are observed from two to six months, while – in most cases - only very modest changes were detected comparing six and ten months old APP/PS1KI mice.

As a result of this work, the APP/PS1KI mouse model may be considered as a suitable model to observe the widely discussed potential beneficial effects of anti-inflammatory therapies on the progress of AD. The APP/PS1KI model may be especially appropriate for such studies not only because of the rich potential read-out on the molecular level as shown in this study, but also because its read-out on the behavioural and stereological level, where these mice display severe working memory and motoric deficits as well as extensive neuron loss from six months of age on.

5.3 CHOLESTEROL AS A BIOMARKER IN ALZHEIMER`S DISEASE

I studied plasma cholesterol levels in transgenic mouse models of Alzheimer`s disease and control mice and found a significant decrease of plasma cholesterol in the APP transgenic animals which were on a homozygous PS1 knock-in background. Total Plasma cholesterol

levels remained mostly unchanged in young and aged wildtype, PS1KI and APP^{SL} control mice.

The finding of decreased plasma cholesterol in aged and pathology affected APP/PS1KI mice is well in line with numerous epidemiological studies, that report about decreased plasma cholesterol levels in AD patients (Kuusisto *et al.* 1997; Panza *et al.* 2006; Solfrizzi *et al.* 2002). Moreover, data from the Italian Longitudinal Study on Aging (ILSA) (2983 participants) suggested, that there is no relation between higher plasma cholesterol and an increased risk for progression of mild cognitive impairment (MCI) to dementia. A multivariate analysis of this study yielded, that only age was a risk factor for incident MCI, while a protective effect was suggested for higher level education and increased serum cholesterol (Solfrizzi *et al.* 2004).

Recently, Mielke *et al.* reported in a population-based 70-year-old birth cohort followed for 18 years that increasing levels of plasma total cholesterol at ages of 70, 75, and 79 are related to a reduced risk of dementia between ages 79 and 88 (Mielke *et al.* 2005). However, the association of high levels of plasma cholesterol during late-life with a decreased risk of AD is in contrast to other reports that suggest high total plasma cholesterol in mid-life to be a risk factor for later dementia (Kuusisto *et al.* 1997). These opposing results may derive from the timing of total cholesterol measurement related to age and clinical onset of dementia. One hypothesis may be, that in mid-life individuals prone to develop dementia in their later life, levels of total plasma cholesterol start to decline several years before onset of the disease. Well in line with this hypothesis, a retroperspective study on autopsy cases of over 40 years old patients revealed a significant correlation between increased plasma cholesterol levels in mid-life period and the presence of amyloid deposition in these patients brain (Pappolla *et al.* 2003).

Our finding of decreased plasma cholesterol in aged APP/PS1KI mice may support the hypothesis of decreased plasma cholesterol in late-life as an accompanying factor during development of dementia. Because young and normal control mice showed mostly unchanged levels of plasma cholesterol, in APP/PS1KI mice decline of plasma cholesterol seems to co-occur with progression of AD-pathology.

5.4 24(S)-HYDROXYCHOLESTEROL AS A BIOMARKER IN ALZHEIMER`S DISEASE

I found no significant change in the ratio of 24(S)-hydroxycholesterol from two to six months neither for wildtype, APP751SL, PS1KI nor APP751SLxPS1KI mice. For the first three mice models these results were anticipated, because all of these three genotypes show no significant pathological change like abundant plaque formation or neuron loss at 6 months-of-age.

If the hypothesis of 24(S)-hydroxycholesterol as a biomarker correlated to AD pathology in APP/PS1KI mice should held true, in the APP751SLxPS1KI mice an increased ratio of 24(S)-hydroxycholesterol to total cholesterol would have been expected. These mice show a massive neuron loss and abundant plaque pathology accompanied by extensive neuroinflammation already at six months of age. An increased efflux of 24(S)-hydroxycholesterol from the brain to the plasma has been hypothesized as an early biomarker of AD (Lutjohann *et al.* 2001; Papassotiropoulos *et al.* 2002). Surprisingly, no increase of the ratio of total to 24(S)-hydroxycholesterol was detected in this mouse model comparing six and two-month-old animals, though AD pathology is far developed at the latter age. This result seems to us very noteworthy because this mouse model recapitulates the neuropathology of AD very well. First signs of A β deposition in APP751SL/PS1KI mouse brain is seen at 2.5 months of age compared to six months in APPSL mice as previously described (Casas *et al.* 2004). APP751SL/PS1KI mice develop a marked reduction of the hippocampal pyramidal cell layer thickness that is particularly prominent in the CA1/2 regin at 10 months of age in both males and females. Female APP751SL/PS1KI mice show a hippocampal CA1/2 neuron loss of 33% at six months and 41% at 12 months of age, as male animals showing no thinned out pyramidal cell layer at six months of age by macroscopic analysis. The observed CA1 neuronal loss in APP751SL/PS1KI mice extends homogenously throughout the pyramidal cell layer and is not related to the local proximity of extracellular A β deposits. It is therefore distinct from the neuronal loss observed in most other transgenic models, which has been limited to the close vicinity of A β deposits. In summary, APP751SL/PS1KI mice represent the first transgenic model of AD showing early onset and severe neuronal loss.

The use of mouse models to study the coherences between cholesterol metabolism and AD is well established (Refolo *et al.* 2001). In the present model I did not find any evidence for 24(S)-hydroxycholesterol plasma concentration as an early onset biomarker for AD as proposed in other studies (Kolsch *et al.* 2003; Papassotiropoulos *et al.* 2002; Schonknecht *et al.* 2002).

It has been described in man that about 90% of 24(S)-hydroxycholesterol is of cerebral origin because the 24(S)-hydroxylase enzyme CYP46 is almost exclusively located in the human brain (Lutjohann *et al.* 2002). Feeding mice with deuterated cholesterol showed that only 50% of total 24(S)-hydroxycholesterol is of cerebral origin (Lund *et al.* 1999; Meaney *et al.* 2000). Brain 24(S)-hydroxycholesterol levels were 131 ng/mg protein in 15 days old wildtype mice but were undetectable in this tissue in age matched Cyp46^{-/-} animals (Lund *et al.* 1999). However, Cyp46^{-/-} knockout mice showed serum levels of 24(S)-hydroxycholesterol of 11 ng/mL compared to age-matched wildtype mice with serum levels of 24(S)-hydroxycholesterol ranging from 60 to 90 ng/mL (Lund *et al.* 1999). Moreover, using semiquantitative immunoblotting of the cholesterol 24(S)-hydroxylase, it has been shown that there was approximately 100 times more 24(S)-hydroxylase protein per gram in brain as could be found in liver. The latter is believed to contribute most if not all of the extracerebral amount of 24(S)-hydroxycholesterol (Lund *et al.* 1999). Overall, Cyp46 seems to be the major enzyme converting cholesterol into 24(S)-hydroxycholesterol in mouse and man. Recently, plasma 24(S)-hydroxycholesterol has been discussed not to be a biomarker for AD. Though, rather high levels of this oxysterol may be a modifiable risk factor for AD as are high levels of cholesterol (Irizarry 2004).

5.5 PYROGLUTAMATE AMYLOID BETA AS A POTENTIAL TRIGGER FOR SPORADIC ALZHEIMER`S DISEASE

5.5.1 DOMINANT AGGREGATION OF BETA-AMYLOID STARTING WITH PYROGLUTAMATE AT POSITION 3 IN THE APP/PS1KI MOUSE MODEL

At the age of 6 months APP/PS1KI mice develop working memory deficits (Wirths *et al.* 2007), and abundant axonal degeneration (Wirths *et al.* 2006). Interestingly, 85% of total A β in this model consists of A β_{42} , which exhibits a large heterogeneity at the N-terminus (Casas *et al.* 2004; Wirths *et al.* 2006). The amount of A $\beta_{N3(pE)}$ is ~90 pg/mg w.w. (at 6 months of age) and is therefore the highest level reported so far in an APP mouse model. A $\beta_{N3(pE)}$ not only aggregates in plaques, but also in CA1 neurons between 2 and 6 months of age, supporting a role in intraneuronal toxicity.

Intracellular A β deposition has been previously shown in human AD (Gouras *et al.* 2000) and in Down's syndrome patients (Gyure *et al.* 2001; Mori *et al.* 2002). The localization of these peptides has been demonstrated to be predominantly in abnormal endosomes (Cataldo *et al.* 2004), multivesicular bodies and within pre- and postsynaptic compartments (Langui *et al.* 2004; Takahashi *et al.* 2002). Takahashi *et al.* demonstrated that A β_{42} aggregates into oligomers within endosomal vesicles and along microtubules of neuronal processes, both in Tg2576 neurons with time in culture, as well as in Tg2576 and human AD brain (Takahashi *et al.* 2004).

Long-standing evidence shows that progressive cerebral deposition of A β plays a seminal role in the pathogenesis of AD (Selkoe 1991). There is great interest, therefore, in understanding the proteolytic processing of APP and its proteases responsible for cleaving at the amino- and carboxy-terminus of the A β region. Ragged peptides with a major species beginning with phenylalanine at position 4 of A β have been reported already in 1985 by Masters *et al.* (Masters *et al.* 1985). This finding has been disputed, because no amino-terminal sequence could be obtained from cores purified in a sodium dodecyl sulfate-containing buffer, which mounted in the suggestion that the N-terminus is blocked (Gorevic *et al.* 1986; Selkoe *et al.* 1986). In 1992, Mori *et al.* first described the presence of A $\beta_{N3(pE)}$ using mass spectrometry of purified A β protein from AD brains, which explains the difficulties in sequencing the amino-terminus (Mori *et al.* 1992). They reported that only 10-

15% of the total A β isolated by this method begins at position 3 with a A $\beta_{N3(pE)}$. Later it became clear that A $\beta_{N3(pE)}$ represents a dominant fraction of A β peptides in AD and Down's syndrome brain (Guntert *et al.* 2006; Harigaya *et al.* 2000; Hosoda *et al.* 1998; Iwatsubo *et al.* 1996; Kuo *et al.* 1997; Kuo *et al.* 2001; Miravalle *et al.* 2005; Piccini *et al.* 2005; Piccini *et al.* 2007; Russo *et al.* 1997; Saido *et al.* 1995; Saido *et al.* 1996; Tekirian *et al.* 1998). Amino-terminal deletions in general enhance aggregation of β -amyloid peptides *in vitro* (Pike *et al.* 1995). The same is true for A $\beta_{N3(pE)}$, which has a higher aggregation propensity (He & Barrow 1999), stabilizes A β (Kuo *et al.* 1998b), and shows an increased toxicity compared to full-length A β and underlined therefore the potential of A β peptides in general and in particular of A $\beta_{N3(pE)}$ for neurotoxicity (Youssef *et al.* 2007). Other studies reported that the toxicity of pyroglutaminated amyloid beta-peptides A $\beta_{N3(pE)-40/42}$ is similar to that of A β_{1-40} and A β_{1-42} (Tekirian *et al.* 1999), and that the A $\beta_{N3(pE)}$ is not the major variant in AD brain (Lemere *et al.* 1996). In contrast, Schilling *et al.* have demonstrated that N3(pE)-modified peptides display an up to 250-fold acceleration in the initial formation of A β aggregates (Schilling *et al.* 2006), and presented *in vitro* evidence that the cyclization of glutamate at position 3 of A β is driven enzymatically by glutaminyl cyclase (QC). QC inhibition leads to significantly reduced A $\beta_{N3(pE)}$ formation, showing the importance of QC-activity during cellular maturation of pE-containing peptides (Cynis *et al.* 2006).

QC inhibition leads to significantly reduced A $\beta_{3(pE)}$ formation, showing the importance of QC-activity during cellular maturation of pyroglutamate-containing peptides (Cynis *et al.* 2006). APP transgenic mouse models have been reported to show no (Kuo *et al.* 2001) or low A $\beta_{3(pE)}$ levels (Guntert *et al.* 2006), in contrast to the APP/PS1KI mouse, which harbours considerable amounts of A $\beta_{3(pE)}$ detected by 2D-gel electrophoresis of whole brain lysates (Casas *et al.* 2004).

Recently, Maeda *et al.* (Maeda 2007) have shown that the localization and abundance of [11C]PIB autoradiographic signals were closely associated with those of amino-terminally truncated and modified A $\beta_{3(pE)}$ deposition in AD and APP transgenic mouse brains, implying that the detectability of amyloid by [11C]PIB-PET is dependent on the accumulation of specific A β subtypes. In addition, deficiency of the physiological A β degrading enzyme, i.e. neprilysin (NEP), results in generation of A $\beta_{3(pE)}$, which is metabolically stable and

pathologically causative, via conversion of $A\beta_{1-42}$ to $A\beta_{3E-42}$ followed by N-terminal glutamate cyclization (Iwata 2007).

In conclusion, these data add evidence to the pathological role of $A\beta_{N3(pE)}$ in AD. An excess of accumulation of $A\beta_{N3(pE)}$, with a high aggregation propensity and increased toxicity, therefore may lead to an enhanced intra- and extracellular $A\beta$ aggregation and plaque formation.

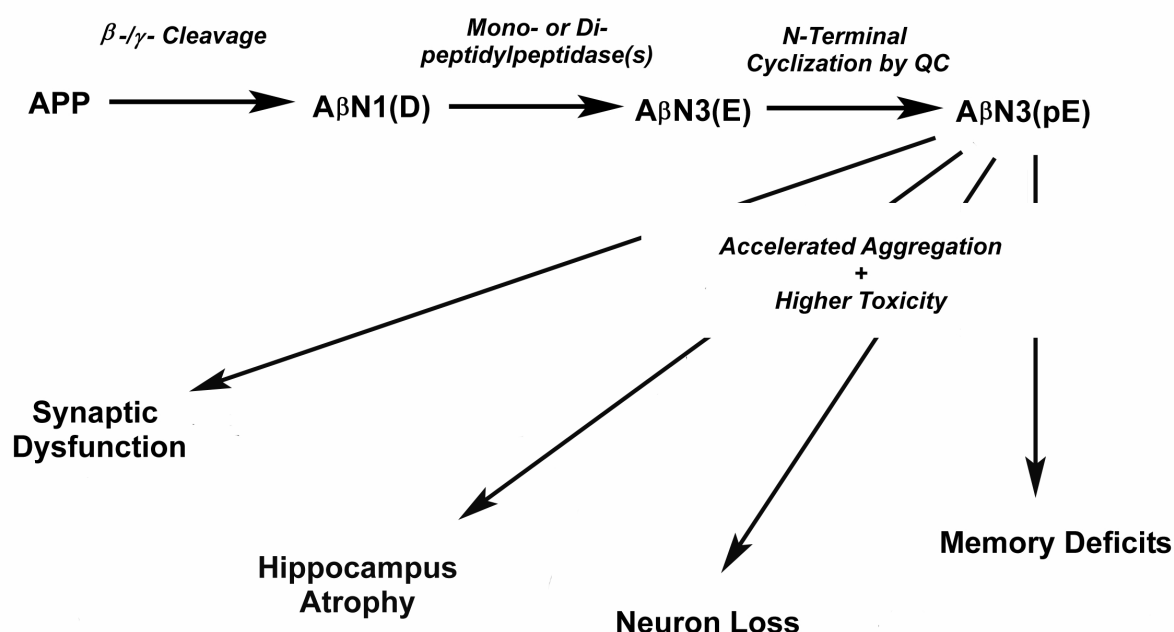


Fig. 33: Scheme of $A\beta_{N3(pE)}$ action on neurodegeneration in Alzheimer's disease. APP is cleaved by β - and γ -secretase function liberating $A\beta_{N1(D)}$. $A\beta_{N3(E)}$ is generated by putative mono-, or dipeptidylpeptidases, which is further modified by N-terminal enzymatic cyclization of glutamate by glutaminy cyclase generating $A\beta_{N3(pE)}$. $A\beta_{N3(pE)}$ is resistant to most aminopeptidases, has a higher stability, aggregation rate and toxic profile as compared to other $A\beta$ peptides. It may therefore serve as a seed for other $A\beta$ species for intra- and extraneuronal $A\beta$ accumulation. $A\beta_{N3(pE)}$ accumulation leads to synaptic dysfunction, neuron death, and hippocampus atrophy (adapted from (Saido *et al.*, 1995)).

To observe the pathologic impact of $A\beta_{N3(pE)}$ peptides separately, the mouse models TBA1, TBA2 and mQC-transgenic mice were generated. The results are discussed in the following chapters.

5.5.2 OVEREXPRESSION OF mQC IN mQC-TRANSGENIC MICE

Substantial overexpression of mQC compared to wildtype animals was verified in both homozygous and heterozygous mice transgenic for mQC. Overexpression of mRNA levels was confirmed for the kidney as a peripheral organ. Most importantly for the usability of this mouse model for analyzing the impact of mQC on the neuropathological changes in Alzheimer disease mouse models, I found a multiple expression increase of mQC mRNA in the brain. By activity measurements in EDTA-plasma it was shown, that higher expression of mQC mRNA led to higher concentrations of biological active mQC-enzyme on the peptide level. As consequence of this results, I decided to cross heterozygous mQC-mice with heterozygous TBA1 mice to analyze the influence of mQC overexpression on the formation of $A\beta_{3(pE)}$.

5.5.3 *IN VIVO* FORMATION AND NEUROTOXICITY OF PYRO-GLUTAMATE $A\beta$ IN TBA1 AND TBA2 MICE

To specifically investigate the neurotoxicity of $A\beta_{3(pE)}$ generation *in vivo*, transgenic mice that express $A\beta_{3E}$ with the normal glutamate at the N-terminus (TBA1) and mice that express $A\beta_{3Q}$ starting at position 3 with glutamine (TBA2) were generated. Due to the replacement of N-terminal glutamate by glutamine, the $A\beta$ peptides are more prone to conversion into pyroglutamate by QC activity in the TBA2 model (Schilling *et al.* 2004). The severity of the neurological phenotype observed in the TBA2 model, accompanied with the massive neuronal loss and premature mortality reflects the enormous toxicity of $A\beta_{3(pE)-42}$. However, the possibility that unprocessed $A\beta_{3Q-42}$ has been stabilized by $A\beta_{3(pE)-42}$ accumulation, and also contributes to the observed severe pathology cannot be ruled out. Applying a mouse $A\beta_{1-40}$ specific ELISA, I did not find elevated mouse $A\beta$ -species in SDS soluble brain extracts (not shown), suggesting that mouse $A\beta_{1-40}$ is not precipitated together with human $A\beta$ variants. In conclusion the major peptide in TBA2 brain extracts is $A\beta_{x-42}$, which is likely not posttranslationally transformed into $A\beta_{3(pE)}$. In addition, it can not be ruled out that besides $A\beta_{3(pE)}$ other N-truncated $A\beta_{x-42}$ variants also aggregate and contribute to the observed neurotoxicity in the TBA2 model. On the other hand, Iwata *et al.* have clearly shown that $A\beta_{3(pE)-42}$ has the longest half live compared to that of all other $A\beta_{x-42}$ peptides starting with unmodified aspartate, alanine, glutamate, phenylalanine or with modified aspartate (Iwata

2007). In addition, they have demonstrated that deficiency of the A β -degrading enzyme neprilysin (NEP) results in generation of metabolically stable and pathologically causative A $\beta_{3(pE)-42}$. Therefore, it may be concluded that A $\beta_{3(pE)}$ peptides serve as a seed for A β accumulation in the TBA2 model. The neurotoxicity of the N-truncated and posttranslationally transformed A $\beta_{3(pE)-42}$ species observed in our TBA2 mouse model is corroborated by the pharmacological inhibition of QC activity by the QC inhibitor P150, which significantly reduces the level of A $\beta_{3(pE)}$ *in vitro* (Cynis *et al.* 2006) and in Tg2576 mice *in vivo* (Schilling 2007). These results demonstrate that pharmacological treatment of A $\beta_{3(pE)}$ formation and deposition may serve as new therapeutic approach to treat AD-like neurodegeneration.

6 REFERENCES

- Akama, K.T., Albanese, C., Pestell, R.G. & Van Eldik, L.J. (1998) Amyloid beta-peptide stimulates nitric oxide production in astrocytes through an NFkappaB-dependent mechanism. *Proc Natl Acad Sci U S A* 95 5795-5800.
- Akiyama, H., Barger, S., Barnum, S., Bradt, B., Bauer, J., Cole, G.M., Cooper, N.R., Eikelenboom, P., Emmerling, M., Fiebich, B.L., Finch, C.E., Frautschy, S., Griffin, W.S., Hampel, H., Hull, M., Landreth, G., Lue, L., Mrak, R., Mackenzie, I.R., *et al* (2000) Inflammation and Alzheimer's disease. *Neurobiol Aging* 21 383-421.
- Alarcon, R., Fuenzalida, C., Santibanez, M. & von Bernhardi, R. (2005) Expression of scavenger receptors in glial cells. Comparing the adhesion of astrocytes and microglia from neonatal rats to surface-bound beta-amyloid. *J Biol Chem* 280 30406-30415. .
- Alexander, N.B., Mollo, J.M., Giordani, B., Ashton-Miller, J.A., Schultz, A.B., Grunawalt, J.A. & Foster, N.L. (1995) Maintenance of balance, gait patterns, and obstacle clearance in Alzheimer's disease. *Neurology* 45 908-914.
- Ambree, O., Touma, C., Gortz, N., Keyvani, K., Paulus, W., Palme, R. & Sachser, N. (2006) Activity changes and marked stereotypic behavior precede Abeta pathology in TgCRND8 Alzheimer mice. *Neurobiol Aging* 27 955-964.
- Archer, J. (1973) Tests for emotionality in rats and mice: a review. *Anim Behav* 21 205-235.
- Arendash, G.W., Gordon, M.N., Diamond, D.M., Austin, L.A., Hatcher, J.M., Jantzen, P., DiCarlo, G., Wilcock, D. & Morgan, D. (2001) Behavioral assessment of Alzheimer's transgenic mice following long-term Abeta vaccination: task specificity and correlations between Abeta deposition and spatial memory. *DNA Cell Biol* 20 737-744.
- Arimoto, T., Choi, D.Y., Lu, X., Liu, M., Nguyen, X.V., Zheng, N., Stewart, C.A., Kim, H.C. & Bing, G. (2006) Interleukin-10 protects against inflammation-mediated degeneration of dopaminergic neurons in substantia nigra. *Neurobiol Aging* 10 10.
- Arnaud, L., Robakis, N.K. & Figueiredo-Pereira, M.E. (2006) It may take inflammation, phosphorylation and ubiquitination to 'tangle' in Alzheimer's disease. *Neurodegener Dis* 3 313-319.
- Arosio, P., Levi, S., Santambrogio, P., Cozzi, A., Luzzago, A., Cesareni, G. & Albertini, A. (1991) Structural and functional studies of human ferritin H and L chains. *Curr Stud Hematol Blood Transfus* 127-131.

- Askanas, V., Alvarez, R.B. & Engel, W.K. (1993) beta-Amyloid precursor epitopes in muscle fibers of inclusion body myositis. *Ann Neurol* 34 551-560.
- Baddeley, A.D., Bressi, S., Della Sala, S., Logie, R. & Spinnler, H. (1991) The decline of working memory in Alzheimer's disease. A longitudinal study. *Brain* 114 2521-2542.
- Bayer, T.A., Wirths, O., Majtenyi, K., Hartmann, T., Multhaup, G., Beyreuther, K. & Czech, C. (2001) Key Factors in Alzheimer's Disease: β -amyloid Precursor Protein Processing, Metabolism and Intraneuronal Transport. *Brain Pathology* 11 1-11.
- Bjorkhem, I., Andersson, U., Ellis, E., Alvelius, G., Ellegard, L., Diczfalussy, U., Sjoval, J. & Einarsson, C. (2001) From brain to bile. Evidence that conjugation and omega-hydroxylation are important for elimination of 24S-hydroxycholesterol (cerebrosterol) in humans. *J Biol Chem* 276 37004-37010.
- Bjorkhem, I. & Meaney, S. (2004) Brain cholesterol: long secret life behind a barrier. *Arterioscler Thromb Vasc Biol* 24 806-815.
- Blanchard, V., Moussaoui, S., Czech, C., Touchet, N., Bonici, B., Planche, M., Canton, T., Jedidi, I., Gohin, M., Wirths, O., Bayer, T.A., Langui, D., Duyckaerts, C., Tremp, G. & Pradier, L. (2003) Time sequence of maturation of dystrophic neurites associated with A β deposits in APP/PS1 transgenic mice. *Exp Neurol* 184 247-263.
- Blennow, K. (2005) CSF biomarkers for Alzheimer's disease: use in early diagnosis and evaluation of drug treatment. *Expert Rev Mol Diagn* 5 661-672.
- Blennow, K. & Hampel, H. (2003) CSF markers for incipient Alzheimer's disease. *Lancet Neurol* 2 605-613.
- Bobinski, M., de Leon, M.J., Wegiel, J., Desanti, S., Convit, A., Saint Louis, L.A., Rusinek, H. & Wisniewski, H.M. (2000) The histological validation of post mortem magnetic resonance imaging-determined hippocampal volume in Alzheimer's disease. *Neuroscience* 95 721-725.
- Bodovitz, S. & Klein, W.L. (1996) Cholesterol modulates alpha-secretase cleavage of amyloid precursor protein. *J Biol Chem* 271 4436-4440.
- Boom, A., Pochet, R., Authalet, M., Pradier, L., Borghgraef, P., Van Leuven, F., Heizmann, C.W. & Brion, J.P. (2004) Astrocytic calcium/zinc binding protein S100A6 over expression in Alzheimer's disease and in PS1/APP transgenic mice models. *Biochim Biophys Acta* 1742 161-168.
- Boutajangout, A., Leroy, K., Touchet, N., Authalet, M., Blanchard, V., Tremp, G., Pradier, L. & Brion, J.P. (2002) Increased tau phosphorylation but absence of formation of

- neurofibrillary tangles in mice double transgenic for human tau and Alzheimer mutant (M146L) presenilin-1. *Neurosci Lett* 318 29-33.
- Bretillon, L., Lutjohann, D., Stahle, L., Widhe, T., Bindl, L., Eggertsen, G., Diczfalusy, U. & Bjorkhem, I. (2000) Plasma levels of 24S-hydroxycholesterol reflect the balance between cerebral production and hepatic metabolism and are inversely related to body surface. *J Lipid Res* 41 840-845.
- Burright, E.N., Clark, H.B., Servadio, A., Matilla, T., Feddersen, R.M., Yunis, W.S., Duvick, L.A., Zoghbi, H.Y. & Orr, H.T. (1995) SCA1 transgenic mice: a model for neurodegeneration caused by an expanded CAG trinucleotide repeat. *Cell* 82 937-948.
- Busciglio, J., Pelsman, A., Wong, C., Pigino, G., Yuan, M., Mori, H. & Yankner, B.A. (2002) Altered metabolism of the amyloid beta precursor protein is associated with mitochondrial dysfunction in Down's syndrome. *Neuron* 33 677-688.
- Cacabelos, R., Alvarez, X.A., Fernandez-Novoa, L., Franco, A., Mangues, R., Pellicer, A. & Nishimura, T. (1994) Brain interleukin-1 beta in Alzheimer's disease and vascular dementia. *Methods Find Exp Clin Pharmacol* 16 141-151.
- Calhoun, M.E., Wiederhold, K.H., Abramowski, D., Phinney, A.L., Probst, A., Sturchler-Pierrat, C., Staufenbiel, M., Sommer, B. & Jucker, M. (1998) Neuron loss in APP transgenic mice. *Nature* 395 755-756.
- Carrasco, J., Adlard, P., Cotman, C., Quintana, A., Penkowa, M., Xu, F., Van Nostrand, W.E. & Hidalgo, J. (2006) Metallothionein-I and -III expression in animal models of Alzheimer disease. *Neuroscience* 143 911-922.
- Carrasco, J., Penkowa, M., Giralt, M., Camats, J., Molinero, A., Campbell, I.L., Palmiter, R.D. & Hidalgo, J. (2003) Role of metallothionein-III following central nervous system damage. *Neurobiol Dis* 13 22-36.
- Carter, J. & Lippa, C.F. (2001) Beta-amyloid, neuronal death and Alzheimer's disease. *Curr Mol Med* 1 733-737.
- Casas, C., Sergeant, N., Itier, J.M., Blanchard, V., Wirths, O., van der Kolk, N., Vingtdeux, V., van de Steeg, E., Ret, G., Canton, T., Drobecq, H., Clark, A., Bonici, B., Delacourte, A., Benavides, J., Schmitz, C., Tremp, G., Bayer, T.A., Benoit, P., *et al* (2004a) Massive CA1/2 neuronal loss with intraneuronal and N-terminal truncated Abeta42 accumulation in a novel Alzheimer transgenic model. *Am J Pathol* 165 1289-1300.
- Casey, J.L., Koeller, D.M., Ramin, V.C., Klausner, R.D. & Harford, J.B. (1989) Iron regulation of transferrin receptor mRNA levels requires iron-responsive elements and

- a rapid turnover determinant in the 3' untranslated region of the mRNA. *Embo J* 8 3693-3699.
- Castellani, R.J., Moreira, P.I., Liu, G., Dobson, J., Perry, G., Smith, M.A. & Zhu, X. (2007) Iron: The Redox-active Center of Oxidative Stress in Alzheimer Disease. *Neurochem Res* 17 17.
- Cataldo, A.M., Petanceska, S., Terio, N.B., Peterhoff, C.M., Durham, R., Mercken, M., Mehta, P.D., Buxbaum, J., Haroutunian, V. & Nixon, R.A. (2004) Abeta localization in abnormal endosomes: association with earliest Abeta elevations in AD and Down syndrome. *Neurobiol Aging* 25 1263-1272.
- Chen, K., Iribarren, P., Hu, J., Chen, J., Gong, W., Cho, E.H., Lockett, S., Dunlop, N.M. & Wang, J.M. (2006) Activation of Toll-like receptor 2 on microglia promotes cell uptake of Alzheimer disease-associated amyloid beta peptide. *J Biol Chem* 281 3651-3659.
- Chetelat, G., Desgranges, B., de la Sayette, V., Viader, F., Berkouk, K., Landeau, B., Lalevee, C., Le Doze, F., Dupuy, B., Hannequin, D., Baron, J.C. & Eustache, F. (2003) Dissociating atrophy and hypometabolism impact on episodic memory in mild cognitive impairment. *Brain* 126 1955-1967.
- Chishti, M.A., Yang, D.S., Janus, C., Phinney, A.L., Horne, P., Pearson, J., Strome, R., Zuker, N., Loukides, J., French, J., Turner, S., Lozza, G., Grilli, M., Kunicki, S., Morissette, C., Paquette, J., Gervais, F., Bergeron, C., Fraser, P.E., *et al* (2001) Early-onset amyloid deposition and cognitive deficits in transgenic mice expressing a double mutant form of amyloid precursor protein 695. *J Biol Chem* 276 21562-21570.
- Coleman, P.D. & Yao, P.J. (2003) Synaptic slaughter in Alzheimer's disease. *Neurobiol Aging* 24 1023-1027.
- Connor, J.R. & Menzies, S.L. (1995) Cellular management of iron in the brain. *J Neurol Sci* 134 33-44.
- Cummings, J.L., Vinters, H.V., Cole, G.M. & Khachaturian, Z.S. (1998) Alzheimer's disease: etiologies, pathophysiology, cognitive reserve, and treatment opportunities. *Neurology* 51 S2-17; discussion S65-17.
- Cynis, H., Schilling, S., Bodnar, M., Hoffmann, T., Heiser, U., Saido, T.C. & Demuth, H.U. (2006) Inhibition of glutaminy cyclase alters pyroglutamate formation in mammalian cells. *Biochim Biophys Acta* 1764 1618-1625.

- Dai, J., Buijs, R.M., Kamphorst, W. & Swaab, D.F. (2002) Impaired axonal transport of cortical neurons in Alzheimer's disease is associated with neuropathological changes. *Brain Res* 948 138-144.
- D'Andrea, M.R., Nagele, R.G., Wang, H.Y., Peterson, P.A. & Lee, D.H. (2001) Evidence that neurones accumulating amyloid can undergo lysis to form amyloid plaques in Alzheimer's disease. *Histopathology* 38 120-134.
- Dember, W.N. & Fowler, H. (1958) Spontaneous alternation behavior. *Psychol Bull* 55 412-428.
- Dere, E., De Souza-Silva, M.A., Frisch, C., Teubner, B., Sohl, G., Willecke, K. & Huston, J.P. (2003) Connexin30-deficient mice show increased emotionality and decreased rearing activity in the open-field along with neurochemical changes. *Eur J Neurosci* 18 629-638.
- Dickson, D.W., Lee, S.C., Mattiace, L.A., Yen, S.H. & Brosnan, C. (1993) Microglia and cytokines in neurological disease, with special reference to AIDS and Alzheimer's disease. *Glia* 7 75-83.
- Dietschy, J.M. & Turley, S.D. (2001) Cholesterol metabolism in the brain. *Curr Opin Lipidol* 12 105-112.
- Divac, I. (1975) Magnocellular nuclei of the basal forebrain project to neocortex, brain stem, and olfactory bulb. Review of some functional correlates. *Brain Res* 93 385-398.
- Dodart, J.C., Meziane, H., Mathis, C., Bales, K.R., Paul, S.M. & Ungerer, A. (1999) Behavioral disturbances in transgenic mice overexpressing the V717F beta-amyloid precursor protein. *Behav Neurosci* 113 982-990.
- Dudal, S., Krzywkowski, P., Paquette, J., Morissette, C., Lacombe, D., Tremblay, P. & Gervais, F. (2004) Inflammation occurs early during the Abeta deposition process in TgCRND8 mice. *Neurobiol Aging* 25 861-871.
- Egana, J.T., Zambrano, C., Nunez, M.T., Gonzalez-Billault, C. & Maccioni, R.B. (2003) Iron-induced oxidative stress modify tau phosphorylation patterns in hippocampal cell cultures. *Biometals* 16 215-223.
- Erbel-Sieler, C., Dudley, C., Zhou, Y., Wu, X., Estill, S.J., Han, T., Diaz-Arrastia, R., Brunskill, E.W., Potter, S.S. & McKnight, S.L. (2004) Behavioral and regulatory abnormalities in mice deficient in the NPAS1 and NPAS3 transcription factors. *Proc Natl Acad Sci U S A* 101 13648-13653.
- Eriksen, J.L. & Janus, C.G. (2007) Plaques, tangles, and memory loss in mouse models of neurodegeneration. *Behav Genet* 37 79-100.

- Ewers, M., Morgan, D.G., Gordon, M.N. & Woodruff-Pak, D.S. (2006) Associative and motor learning in 12-month-old transgenic APP+PS1 mice. *Neurobiol Aging* 27 1118-1128.
- Frei, K., Malipiero, U.V., Leist, T.P., Zinkernagel, R.M., Schwab, M.E. & Fontana, A. (1989) On the cellular source and function of interleukin 6 produced in the central nervous system in viral diseases. *Eur J Immunol* 19 689-694.
- Gandy, S. & Petanceska, S. (2000) Regulation of Alzheimer beta-amyloid precursor trafficking and metabolism. *Biochim Biophys Acta* 1502 44-52.
- George, A.J., Holsinger, R.M., McLean, C.A., Laughton, K.M., Beyreuther, K., Evin, G., Masters, C.L. & Li, Q.X. (2004) APP intracellular domain is increased and soluble A β is reduced with diet-induced hypercholesterolemia in a transgenic mouse model of Alzheimer disease. *Neurobiol Dis* 16 124-132.
- Gerlai, R. (1998) A new continuous alternation task in T-maze detects hippocampal dysfunction in mice. A strain comparison and lesion study. *Behav Brain Res* 95 91-101.
- Giralt, M., Penkowa, M., Hernandez, J., Molinero, A., Carrasco, J., Lago, N., Camats, J., Campbell, I.L. & Hidalgo, J. (2002a) Metallothionein-1+2 deficiency increases brain pathology in transgenic mice with astrocyte-targeted expression of interleukin 6. *Neurobiol Dis* 9 319-338.
- Giralt, M., Penkowa, M., Lago, N., Molinero, A. & Hidalgo, J. (2002b) Metallothionein-1+2 protect the CNS after a focal brain injury. *Exp Neurol* 173 114-128.
- Giulian, D. (1999) Microglia and the immune pathology of Alzheimer disease. *Am J Hum Genet* 65 13-18.
- Glabe, C. (2001) Intracellular mechanisms of amyloid accumulation and pathogenesis in Alzheimer's disease. *J Mol Neurosci* 17 137-145.
- Goedert, M. & Jakes, R. (1990) Expression of separate isoforms of human tau protein: correlation with the tau pattern in brain and effects on tubulin polymerization. *Embo J* 9 4225-4230.
- Golde, T.E., Estus, S., Usiak, M., Younkin, L.H. & Younkin, S.G. (1990) Expression of beta amyloid protein precursor mRNAs: recognition of a novel alternatively spliced form and quantitation in Alzheimer's disease using PCR. *Neuron* 4 253-267.
- Gomez-Isla, T., Price, J.L., McKeel, D.W., Jr., Morris, J.C., Growdon, J.H. & Hyman, B.T. (1996) Profound loss of layer II entorhinal cortex neurons occurs in very mild Alzheimer's disease. *J Neurosci* 16 4491-4500.

- Gong, J.S., Sawamura, N., Zou, K., Sakai, J., Yanagisawa, K. & Michikawa, M. (2002) Amyloid beta-protein affects cholesterol metabolism in cultured neurons: implications for pivotal role of cholesterol in the amyloid cascade. *J Neurosci Res* 70 438-446.
- Gordon, M.N., King, D.L., Diamond, D.M., Jantzen, P.T., Boyett, K.V., Hope, C.E., Hatcher, J.M., DiCarlo, G., Gottschall, W.P., Morgan, D. & Arendash, G.W. (2001) Correlation between cognitive deficits and Abeta deposits in transgenic APP+PS1 mice. *Neurobiol Aging* 22 377-385.
- Gorevic, P.D., Goni, F., Pons-Estel, B., Alvarez, F., Peress, N.S. & Frangione, B. (1986) Isolation and partial characterization of neurofibrillary tangles and amyloid plaque core in Alzheimer's disease: immunohistological studies. *J Neuropathol Exp Neurol* 45 647-664.
- Gouras, G.K., Almeida, C.G. & Takahashi, R.H. (2005) Intraneuronal Abeta accumulation and origin of plaques in Alzheimer's disease. *Neurobiol Aging* 26 1235-1244.
- Gouras, G.K., Tsai, J., Naslund, J., Vincent, B., Edgar, M., Checler, F., Greenfield, J.P., Haroutunian, V., Buxbaum, J.D., Xu, H., Greengard, P. & Relkin, N.R. (2000) Intraneuronal Abeta42 accumulation in human brain. *Am J Pathol* 156 15-20.
- Griffin, W.S., Stanley, L.C., Ling, C., White, L., MacLeod, V., Perrot, L.J., White, C.L., 3rd & Araoz, C. (1989) Brain interleukin 1 and S-100 immunoreactivity are elevated in Down syndrome and Alzheimer disease. *Proc Natl Acad Sci U S A* 86 7611-7615.
- Guntert, A., Dobeli, H. & Bohrmann, B. (2006) High sensitivity analysis of amyloid-beta peptide composition in amyloid deposits from human and PS2APP mouse brain. *Neuroscience* 143 461-475. Epub 2006 Sep 2027.
- Gyure, K.A., Durham, R., Stewart, W.F., Smialek, J.E. & Troncoso, J.C. (2001) Intraneuronal abeta-amyloid precedes development of amyloid plaques in Down syndrome. *Arch Pathol Lab Med* 125 489-492.
- Hampel, H., Haslinger, A., Scheloske, M., Padberg, F., Fischer, P., Unger, J., Teipel, S.J., Neumann, M., Rosenberg, C., Oshida, R., Hulette, C., Pongratz, D., Ewers, M., Kretschmar, H.A. & Moller, H.J. (2005) Pattern of interleukin-6 receptor complex immunoreactivity between cortical regions of rapid autopsy normal and Alzheimer's disease brain. *Eur Arch Psychiatry Clin Neurosci* 255 269-278.
- Hampel, H., Mitchell, A., Blennow, K., Frank, R.A., Brettschneider, S., Weller, L. & Moller, H.J. (2004) Core biological marker candidates of Alzheimer's disease - perspectives for diagnosis, prediction of outcome and reflection of biological activity. *J Neural Transm* 111 247-272.

- Hardy, J. & Allsop, D. (1991) Amyloid deposition as the central event in the aetiology of Alzheimer's disease. *Trends Pharmacol Sci* 12 383-388.
- Hardy, J. & Selkoe, D.J. (2002) The amyloid hypothesis of Alzheimer's disease: progress and problems on the road to therapeutics. *Science* 297 353-356.
- Harigaya, Y., Saido, T.C., Eckman, C.B., Prada, C.M., Shoji, M. & Younkin, S.G. (2000) Amyloid beta protein starting pyroglutamate at position 3 is a major component of the amyloid deposits in the Alzheimer's disease brain. *Biochem Biophys Res Commun* 276 422-427.
- He, W. & Barrow, C.J. (1999) The A beta 3-pyroglutamyl and 11-pyroglutamyl peptides found in senile plaque have greater beta-sheet forming and aggregation propensities in vitro than full-length A beta. *Biochemistry* 38 10871-10877.
- Herzig, M.C., Winkler, D.T., Burgermeister, P., Pfeifer, M., Kohler, E., Schmidt, S.D., Danner, S., Abramowski, D., Sturchler-Pierrat, C., Burki, K., van Duinen, S.G., Maat-Schieman, M.L., Staufenbiel, M., Mathews, P.M. & Jucker, M. (2004) Abeta is targeted to the vasculature in a mouse model of hereditary cerebral hemorrhage with amyloidosis. *Nat Neurosci* 7 954-960.
- Hiraoka, Y., Ohno, M., Yoshida, K., Okawa, K., Tomimoto, H., Kita, T. & Nishi, E. (2007) Enhancement of alpha-secretase cleavage of amyloid precursor protein by a metalloendopeptidase nardilysin. *J Neurochem* 7 7.
- Holcomb, L., Gordon, M.N., McGowan, E., Yu, X., Benkovic, S., Jantzen, P., Wright, K., Saad, I., Mueller, R., Morgan, D., Sanders, S., Zehr, C., O'Campo, K., Hardy, J., Prada, C.M., Eckman, C., Younkin, S., Hsiao, K. & Duff, K. (1998) Accelerated Alzheimer-type phenotype in transgenic mice carrying both mutant amyloid precursor protein and presenilin 1 transgenes. *Nat Med* 4 97-100.
- Hosoda, R., Saido, T.C., Otvos, L., Jr., Arai, T., Mann, D.M., Lee, V.M., Trojanowski, J.Q. & Iwatsubo, T. (1998) Quantification of modified amyloid beta peptides in Alzheimer disease and Down syndrome brains. *J Neuropathol Exp Neurol* 57 1089-1095.
- Howland, D.S., Trusko, S.P., Savage, M.J., Reaume, A.G., Lang, D.M., Hirsch, J.D., Maeda, N., Siman, R., Greenberg, B.D., Scott, R.W. & Flood, D.G. (1998b) Modulation of secreted beta-amyloid precursor protein and amyloid beta-peptide in brain by cholesterol. *J Biol Chem* 273 16576-16582.
- Hsia, A.Y., Masliah, E., McConlogue, L., Yu, G.Q., Tatsuno, G., Hu, K., Kholodenko, D., Malenka, R.C., Nicoll, R.A. & Mucke, L. (1999a) Plaque-independent disruption of

- neural circuits in Alzheimer's disease mouse models. *Proc Natl Acad Sci U S A* 96 3228-3233.
- Hsiao, K.K., Chapman, P., Nilsen, S., Eckman, C., Harigaya, Y., Younkin, S., Yang, F. & Cole, G. (1996) Correlative memory deficits, Abeta elevation and amyloid plaques in transgenic mice. *Science* 274 99-102.
- Hu, J., Akama, K.T., Krafft, G.A., Chromy, B.A. & Van Eldik, L.J. (1998) Amyloid-beta peptide activates cultured astrocytes: morphological alterations, cytokine induction and nitric oxide release. *Brain Res* 785 195-206.
- Hull, M., Berger, M. & Heneka, M. (2006) Disease-modifying therapies in Alzheimer's disease: how far have we come? *Drugs* 66 2075-2093.
- Hye, A., Lynham, S., Thambisetty, M., Causevic, M., Campbell, J., Byers, H.L., Hooper, C., Rijdsdijk, F., Tabrizi, S.J., Banner, S., Shaw, C.E., Foy, C., Poppe, M., Archer, N., Hamilton, G., Powell, J., Brown, R.G., Sham, P., Ward, M., *et al* (2006) Proteome-based plasma biomarkers for Alzheimer's disease. *Brain* **129** 3042-3050.
- Irizarry, M.C. (2004) Biomarkers of Alzheimer disease in plasma. *NeuroRx* 1 226-234.
- Iwata, N.e.a. (2007) N-terminal modification of amyloid-beta peptide, Abeta x-42 , in Alzheimer's disease and mouse models. *Nature*, *co-submitted*.
- Iwatsubo, T., Saido, T.C., Mann, D.M., Lee, V.M. & Trojanowski, J.Q. (1996) Full-length amyloid-beta (1-42(43)) and amino-terminally modified and truncated amyloid-beta 42(43) deposit in diffuse plaques. *Am J Pathol* 149 1823-1830.
- Jack, C.R., Jr., Dickson, D.W., Parisi, J.E., Xu, Y.C., Cha, R.H., O'Brien, P.C., Edland, S.D., Smith, G.E., Boeve, B.F., Tangalos, E.G., Kokmen, E. & Petersen, R.C. (2002) Antemortem MRI findings correlate with hippocampal neuropathology in typical aging and dementia. *Neurology* 58 750-757.
- Janus, C. (2004) Search strategies used by APP transgenic mice during navigation in the Morris water maze. *Learn Mem* 11 337-346.
- Jellinger, K.A. (2006) Challenges in neuronal apoptosis. *Curr Alzheimer Res* 3 377-391.
- Kaplan, J., Craven, C., Alexander, J., Kushner, J., Lamb, J. & Bernstein, S. (1988) Regulation of the distribution of tissue iron. Lessons learned from the hypotransferrinemic mouse. *Ann N Y Acad Sci* 526 124-135.
- Koeller, D.M., Casey, J.L., Hentze, M.W., Gerhardt, E.M., Chan, L.N., Klausner, R.D. & Harford, J.B. (1989) A cytosolic protein binds to structural elements within the iron regulatory region of the transferrin receptor mRNA. *Proc Natl Acad Sci U S A* 86 3574-3578.

- Kolsch, H., Heun, R., Kerksiek, A., Bergmann, K.V., Maier, W. & Lütjohann, D. (2004) Altered levels of plasma 24S- and 27-hydroxycholesterol in demented patients. *Neurosci Lett* 368 303-308.
- Kolsch, H., Ludwig, M., Lütjohann, D. & Rao, M.L. (2001) Neurotoxicity of 24-hydroxycholesterol, an important cholesterol elimination product of the brain, may be prevented by vitamin E and estradiol-17 β . *J Neural Transm* 108 475-488.
- Kolsch, H., Lütjohann, D., von Bergmann, K. & Heun, R. (2003) The role of 24S-hydroxycholesterol in Alzheimer's disease. *J Nutr Health Aging* 7 37-41.
- Koo, E.H., Sisodia, S.S., Archer, D.R., Martin, L.J., Weidemann, A., Beyreuther, K., Fischer, P., Masters, C.L. & Price, D.L. (1990) Precursor of amyloid protein in Alzheimer disease undergoes fast anterograde axonal transport. *Proc Natl Acad Sci U S A* 87 1561-1565.
- Kumar-Singh, S., Theuns, J., Van Broeck, B., Pirici, D., Vennekens, K., Corsmit, E., Cruts, M., Dermaut, B., Wang, R. & Van Broeckhoven, C. (2006) Mean age-of-onset of familial Alzheimer disease caused by presenilin mutations correlates with both increased A β 42 and decreased A β 40. *Hum Mutat* 27 686-695.
- Kuo, Y.M., Emmerling, M.R., Bisgaier, C.L., Essenburg, A.D., Lampert, H.C., Drumm, D. & Roher, A.E. (1998a) Elevated low-density lipoprotein in Alzheimer's disease correlates with brain A β 1-42 levels. *Biochem Biophys Res Commun* 252 711-715.
- Kuo, Y.M., Emmerling, M.R., Woods, A.S., Cotter, R.J. & Roher, A.E. (1997) Isolation, chemical characterization, and quantitation of A β 3-pyroglutamyl peptide from neuritic plaques and vascular amyloid deposits. *Biochem Biophys Res Commun* 237 188-191.
- Kuo, Y.M., Kokjohn, T.A., Beach, T.G., Sue, L.I., Brune, D., Lopez, J.C., Kalback, W.M., Abramowski, D., Sturchler-Pierrat, C., Staufenbiel, M. & Roher, A.E. (2001) Comparative analysis of amyloid- β chemical structure and amyloid plaque morphology of transgenic mouse and Alzheimer's disease brains. *J Biol Chem* 276 12991-12998.
- Kuo, Y.M., Webster, S., Emmerling, M.R., De Lima, N. & Roher, A.E. (1998b) Irreversible dimerization/tetramerization and post-translational modifications inhibit proteolytic degradation of A β peptides of Alzheimer's disease. *Biochim Biophys Acta* 1406 291-298.
- Kuusisto, J., Koivisto, K., Mykkanen, L., Helkala, E.L., Vanhanen, M., Hanninen, T., Kervinen, K., Kesaniemi, Y.A., Riekkinen, P.J. & Laakso, M. (1997) Association

- between features of the insulin resistance syndrome and Alzheimer's disease independently of apolipoprotein E4 phenotype: cross sectional population based study. *Bmj* 315 1045-1049.
- Lahiri, D.K., Maloney, B., Basha, M.R., Ge, Y.W. & Zawia, N.H. (2007) How and when environmental agents and dietary factors affect the course of Alzheimer's disease: the "LEARn" model (latent early-life associated regulation) may explain the triggering of AD. *Curr Alzheimer Res* 4 219-228.
- Lalonde, R., Dumont, M., Staufenbiel, M., Sturchler-Pierrat, C. & Strazielle, C. (2002) Spatial learning, exploration, anxiety, and motor coordination in female APP23 transgenic mice with the Swedish mutation. *Brain Res* 956 36-44.
- Lalonde, R., Kim, H.D. & Fukuchi, K. (2004) Exploratory activity, anxiety, and motor coordination in bigenic APPswe + PS1/DeltaE9 mice. *Neurosci Lett* 369 156-161.
- Lalonde, R. & Strazielle, C. (2001) Motor performance and regional brain metabolism of spontaneous murine mutations with cerebellar atrophy. *Behav Brain Res* 125 103-108.
- Lalonde, R. & Strazielle, C. (2005) PS1 knockin mice with the Japanese I213T mutation: effects on exploratory activity, motor coordination, and spatial learning. *Behav Brain Res* 162 182-190.
- Langui, D., Girardot, N., El Hachimi, K.H., Allinquant, B., Blanchard, V., Pradier, L. & Duyckaerts, C. (2004) Subcellular topography of neuronal Abeta peptide in APPxPS1 transgenic mice. *Am J Pathol* 165 1465-1477.
- Launer, L.J., White, L.R., Petrovitch, H., Ross, G.W. & Curb, J.D. (2001) Cholesterol and neuropathologic markers of AD: a population-based autopsy study. *Neurology* 57 1447-1452.
- Lee, K.W., Lee, S.H., Kim, H., Song, J.S., Yang, S.D., Paik, S.G. & Han, P.L. (2004) Progressive cognitive impairment and anxiety induction in the absence of plaque deposition in C57BL/6 inbred mice expressing transgenic amyloid precursor protein. *J Neurosci Res* 76 572-580.
- Lemere, C.A., Blusztajn, J.K., Yamaguchi, H., Wisniewski, T., Saido, T.C. & Selkoe, D.J. (1996) Sequence of deposition of heterogeneous amyloid beta-peptides and APO E in Down syndrome: implications for initial events in amyloid plaque formation. *Neurobiol Dis* 3 16-32.
- Lewis, J., McGowan, E., Rockwood, J., Melrose, H., Nacharaju, P., Van Slegtenhorst, M., Gwinn-Hardy, K., Paul Murphy, M., Baker, M., Yu, X., Duff, K., Hardy, J., Corral, A., Lin, W.L., Yen, S.H., Dickson, D.W., Davies, P. & Hutton, M. (2000)

- Neurofibrillary tangles, amyotrophy and progressive motor disturbance in mice expressing mutant (P301L) tau protein. *Nat Genet* 25 402-405.
- Li, Y., Liu, L., Liu, D., Woodward, S., Barger, S.W., Mrak, R.E. & Griffin, W.S. (2004) Microglial activation by uptake of fDNA via a scavenger receptor. *J Neuroimmunol* 147 50-55.
- Liu, Y., Peterson, D.A. & Schubert, D. (1998) Amyloid beta peptide alters intracellular vesicle trafficking and cholesterol homeostasis. *Proc Natl Acad Sci U S A* 95 13266-13271.
- Locatelli, S., Lutjohann, D., Schmidt, H.H., Otto, C., Beisiegel, U. & von Bergmann, K. (2002) Reduction of plasma 24S-hydroxycholesterol (cerebrosterol) levels using high-dosage simvastatin in patients with hypercholesterolemia: evidence that simvastatin affects cholesterol metabolism in the human brain. *Arch Neurol* 59 213-216.
- Lovasic, L., Bauschke, H. & Janus, C. (2005) Working memory impairment in a transgenic amyloid precursor protein TgCRND8 mouse model of Alzheimer's disease. *Genes Brain Behav* 4 197-208.
- Lukiw, W.J. & Bazan, N.G. (2000) Neuroinflammatory signaling upregulation in Alzheimer's disease. *Neurochem Res* 25 1173-1184.
- Lund, E.G., Guileyardo, J.M. & Russell, D.W. (1999) cDNA cloning of cholesterol 24-hydroxylase, a mediator of cholesterol homeostasis in the brain. *Proc Natl Acad Sci U S A* 96 7238-7243.
- Lutjohann, D., Bjorkhem, I., Locatelli, S., Dame, C., Schmolling, J., von Bergmann, K. & Fahnenstich, H. (2001) Cholesterol dynamics in the foetal and neonatal brain as reflected by circulatory levels of 24S-hydroxycholesterol. *Acta Paediatr* 90 652-657.
- Lutjohann, D., Brzezinka, A., Barth, E., Abramowski, D., Staufenbiel, M., von Bergmann, K., Beyreuther, K., Multhaup, G. & Bayer, T.A. (2002) Profile of cholesterol-related sterols in aged amyloid precursor protein transgenic mouse brain. *J Lipid Res* 43 1078-1085.
- Maeda, J. (2007) Longitudinal, quantitative assesment of amyloid, neuroinflammation and anti.amyloid treatment in a living mouse model of Alzheimer's disease enabled by PET. *Journal of Neuroscience*.
- Mandelkow, E.M., Stamer, K., Vogel, R., Thies, E. & Mandelkow, E. (2003) Clogging of axons by tau, inhibition of axonal traffic and starvation of synapses. *Neurobiol Aging* 24 1079-1085.
- Marx, J. (2007) Alzheimer's disease. A new take on tau. *Science* 316 1416-1417.

- Marz, P., Cheng, J.G., Gadiant, R.A., Patterson, P.H., Stoyan, T., Otten, U. & Rose-John, S. (1998) Sympathetic neurons can produce and respond to interleukin 6. *Proc Natl Acad Sci U S A* 95 3251-3256.
- Masters, C.L., Multhaup, G., Simms, G., Pottgiesser, J., Martins, R.N. & Beyreuther, K. (1985) Neuronal origin of a cerebral amyloid: neurofibrillary tangles of Alzheimer's disease contain the same protein as the amyloid of plaque cores and blood vessels. *Embo J* 4 2757-2763.
- Mattson, M.P. (2004) Metal-catalyzed disruption of membrane protein and lipid signaling in the pathogenesis of neurodegenerative disorders. *Ann N Y Acad Sci* 1012 37-50.
- Mazzali, M., Kipari, T., Ophascharoensuk, V., Wesson, J.A., Johnson, R. & Hughes, J. (2002) Osteopontin--a molecule for all seasons. *Qjm* 95 3-13.
- Meaney, S., Lutjohann, D., Diczfalussy, U. & Bjorkhem, I. (2000) Formation of oxysterols from different pools of cholesterol as studied by stable isotope technique: cerebral origin of most circulating 24S-hydroxycholesterol in rats, but not in mice. *Biochim Biophys Acta* 1486 293-298.
- Meller, R., Stevens, S.L., Minami, M., Cameron, J.A., King, S., Rosenzweig, H., Doyle, K., Lessov, N.S., Simon, R.P. & Stenzel-Poore, M.P. (2005) Neuroprotection by osteopontin in stroke. *J Cereb Blood Flow Metab* 25 217-225.
- Mendell, J.R., Sahenk, Z., Gales, T. & Paul, L. (1991) Amyloid filaments in inclusion body myositis. Novel findings provide insight into nature of filaments. *Arch Neurol* 48 1229-1234.
- Metzler, M., Li, B., Gan, L., Georgiou, J., Gutekunst, C.A., Wang, Y., Torre, E., Devon, R.S., Oh, R., Legendre-Guillemain, V., Rich, M., Alvarez, C., Gertsenstein, M., McPherson, P.S., Nagy, A., Wang, Y.T., Roder, J.C., Raymond, L.A. & Hayden, M.R. (2003) Disruption of the endocytic protein HIP1 results in neurological deficits and decreased AMPA receptor trafficking. *Embo J* 22 3254-3266.
- Mielke, M.M., Zandi, P.P., Sjogren, M., Gustafson, D., Ostling, S., Steen, B. & Skoog, I. (2005) High total cholesterol levels in late life associated with a reduced risk of dementia. *Neurology* 64 1689-1695.
- Miravalle, L., Calero, M., Takao, M., Roher, A.E., Ghetti, B. & Vidal, R. (2005) Amino-terminally truncated Abeta peptide species are the main component of cotton wool plaques. *Biochemistry* 44 10810-10821.
- Moechars, D., Dewachter, I., Lorent, K., Reverse, D., Baekelandt, V., Naidu, A., Tesseur, I., Spittaels, K., Haute, C.V., Checler, F., Godaux, E., Cordell, B. & Van Leuven, F.

- (1999b) Early phenotypic changes in transgenic mice that overexpress different mutants of amyloid precursor protein in brain. *J Biol Chem* 274 6483-6492.
- Moore, A.H. & O'Banion, M.K. (2002) Neuroinflammation and anti-inflammatory therapy for Alzheimer's disease. *Adv Drug Deliv Rev* 54 1627-1656.
- Moran, P.M., Higgins, L.S., Cordell, B. & Moser, P.C. (1995) Age-related learning deficits in transgenic mice expressing the 751-amino acid isoform of human beta-amyloid precursor protein. *Proc Natl Acad Sci U S A* 92 5341-5345.
- Mori, C., Spooner, E.T., Wisniewsk, K.E., Wisniewski, T.M., Yamaguch, H., Saido, T.C., Tolan, D.R., Selkoe, D.J. & Lemere, C.A. (2002) Intraneuronal Abeta42 accumulation in Down syndrome brain. *Amyloid* 9 88-102.
- Mori, H., Takio, K., Ogawara, M. & Selkoe, D.J. (1992) Mass spectrometry of purified amyloid beta protein in Alzheimer's disease. *J Biol Chem* 267 17082-17086.
- Mrak, R.E., Sheng, J.G. & Griffin, W.S. (1995) Glial cytokines in Alzheimer's disease: review and pathogenic implications. *Hum Pathol* 26 816-823.
- Murphy, G.M., Jr., Zhao, F., Yang, L. & Cordell, B. (2000) Expression of macrophage colony-stimulating factor receptor is increased in the AbetaPP(V717F) transgenic mouse model of Alzheimer's disease. *Am J Pathol* 157 895-904.
- Nguyen, T., Hamby, A. & Massa, S.M. (2005) Clioquinol down-regulates mutant huntingtin expression in vitro and mitigates pathology in a Huntington's disease mouse model. *Proc Natl Acad Sci U S A* 102 11840-11845.
- Nishimura, T., Akiyama, H., Yonehara, S., Kondo, H., Ikeda, K., Kato, M., Iseki, E. & Kosaka, K. (1995) Fas antigen expression in brains of patients with Alzheimer-type dementia. *Brain Res* 695 137-145.
- Notkola, I.L., Sulkava, R., Pekkanen, J., Erkinjuntti, T., Ehnholm, C., Kivinen, P., Tuomilehto, J. & Nissinen, A. (1998) Serum total cholesterol, apolipoprotein E epsilon 4 allele, and Alzheimer's disease. *Neuroepidemiology* 17 14-20.
- O'Keeffe, S.T., Kazeem, H., Philpott, R.M., Playfer, J.R., Gosney, M. & Lye, M. (1996) Gait disturbance in Alzheimer's disease: a clinical study. *Age Ageing* 25 313-316.
- Orellana, D.I., Quintanilla, R.A. & Maccioni, R.B. (2007) Neuroprotective effect of TNFalpha against the beta-amyloid neurotoxicity mediated by CDK5 kinase. *Biochim Biophys Acta* 1773 254-263.
- Ottino, P., Finley, J., Rojo, E., Ottlecz, A., Lambrou, G.N., Bazan, H.E. & Bazan, N.G. (2004) Hypoxia activates matrix metalloproteinase expression and the VEGF system

- in monkey choroid-retinal endothelial cells: Involvement of cytosolic phospholipase A2 activity. *Mol Vis* 10 341-350.
- Ozmen, L., Woolley, M., Albientz, A., Miss, M.T., Nelboeck, P., Malherbe, P., Czech, C., Gruninger-Leitch, F., Brockhaus, M., Ballard, T. & Jacobsen, H. (2005) BACE/APPV717F double-transgenic mice develop cerebral amyloidosis and inflammation. *Neurodegener Dis* 2 284-298.
- Papassotiropoulos, A., Lutjohann, D., Bagli, M., Locatelli, S., Jessen, F., Buschfort, R., Ptak, U., Bjorkhem, I., von Bergmann, K. & Heun, R. (2002) 24S-hydroxycholesterol in cerebrospinal fluid is elevated in early stages of dementia. *J Psychiatr Res* 36 27-32.
- Parachikova, A., Agadjanyan, M.G., Cribbs, D.H., Blurton-Jones, M., Perreau, V., Rogers, J., Beach, T.G. & Cotman, C.W. (2006) Inflammatory changes parallel the early stages of Alzheimer disease. *Neurobiol Aging* 17 17.
- Paylor, R., Nguyen, M., Crawley, J.N., Patrick, J., Beaudet, A. & Orr-Urtreger, A. (1998) Alpha7 nicotinic receptor subunits are not necessary for hippocampal-dependent learning or sensorimotor gating: a behavioral characterization of Acra7-deficient mice. *Learn Mem* 5 302-316.
- Penkowa, M., Caceres, M., Borup, R., Nielsen, F.C., Poulsen, C.B., Quintana, A., Molinero, A., Carrasco, J., Florit, S., Giralt, M. & Hidalgo, J. (2006) Novel roles for metallothionein-I + II (MT-I + II) in defense responses, neurogenesis, and tissue restoration after traumatic brain injury: insights from global gene expression profiling in wild-type and MT-I + II knockout mice. *J Neurosci Res* 84 1452-1474.
- Pennanen, C., Kivipelto, M., Tuomainen, S., Hartikainen, P., Hanninen, T., Laakso, M.P., Hallikainen, M., Vanhanen, M., Nissinen, A., Helkala, E.L., Vainio, P., Vanninen, R., Partanen, K. & Soininen, H. (2004) Hippocampus and entorhinal cortex in mild cognitive impairment and early AD. *Neurobiol Aging* 25 303-310.
- Perlmutter, L.S., Scott, S.A., Barron, E. & Chui, H.C. (1992) MHC class II-positive microglia in human brain: association with Alzheimer lesions. *J Neurosci Res* 33 549-558.
- Perry, V.H., Matyszak, M.K. & Fearn, S. (1993) Altered antigen expression of microglia in the aged rodent CNS. *Glia* 7 60-67.
- Petersen, R.C., Jack, C.R., Jr., Xu, Y.C., Waring, S.C., O'Brien, P.C., Smith, G.E., Ivnik, R.J., Tangalos, E.G., Boeve, B.F. & Kokmen, E. (2000) Memory and MRI-based hippocampal volumes in aging and AD. *Neurology* 54 581-587.
- Pettersson, A.F., Engardt, M. & Wahlund, L.O. (2002) Activity level and balance in subjects with mild Alzheimer's disease. *Dement Geriatr Cogn Disord* 13 213-216.

- Pfaffl, M.W., Horgan, G.W. & Dempfle, L. (2002) Relative expression software tool (REST) for group-wise comparison and statistical analysis of relative expression results in real-time PCR. *Nucleic Acids Res* 30 e36.
- Piccini, A., Russo, C., Gliozzi, A., Relini, A., Vitali, A., Borghi, R., Giliberto, L., Armirotti, A., D'Arrigo, C., Bachi, A., Cattaneo, A., Canale, C., Torrassa, S., Saido, T.C., Markesbery, W., Gambetti, P. & Tabaton, M. (2005) beta-amyloid is different in normal aging and in Alzheimer disease. *J Biol Chem* 280 34186-34192.
- Piccini, A., Zanusso, G., Borghi, R., Noviello, C., Monaco, S., Russo, R., Damonte, G., Armirotti, A., Gelati, M., Giordano, R., Zambenedetti, P., Russo, C., Ghetti, B. & Tabaton, M. (2007) Association of a presenilin 1 S170F mutation with a novel Alzheimer disease molecular phenotype. *Arch Neurol* 64 738-745.
- Pike, C.J., Overman, M.J. & Cotman, C.W. (1995) Amino-terminal deletions enhance aggregation of beta-amyloid peptides in vitro. *J Biol Chem* 270 23895-23898.
- Pogue, A.I. & Lukiw, W.J. (2004) Angiogenic signaling in Alzheimer's disease. *Neuroreport* 15 1507-1510.
- Probst, A., Gotz, J., Wiederhold, K.H., Tolnay, M., Mistl, C., Jaton, A.L., Hong, M., Ishihara, T., Lee, V.M., Trojanowski, J.Q., Jakes, R., Crowther, R.A., Spillantini, M.G., Burki, K. & Goedert, M. (2000) Axonopathy and amyotrophy in mice transgenic for human four-repeat tau protein. *Acta Neuropathol (Berl)* 99 469-481.
- Raivich, G., Haas, S., Werner, A., Klein, M.A., Kloss, C. & Kreutzberg, G.W. (1998) Regulation of MCSF receptors on microglia in the normal and injured mouse central nervous system: a quantitative immunofluorescence study using confocal laser microscopy. *J Comp Neurol* 395 342-358.
- Rapoport, M., Dawson, H.N., Binder, L.I., Vitek, M.P. & Ferreira, A. (2002) Tau is essential to beta -amyloid-induced neurotoxicity. *Proc Natl Acad Sci U S A* 99 6364-6369.
- Reddy, P.H., Mani, G., Park, B.S., Jacques, J., Murdoch, G., Whetsell, W., Jr., Kaye, J. & Manczak, M. (2005) Differential loss of synaptic proteins in Alzheimer's disease: implications for synaptic dysfunction. *J Alzheimers Dis* 7 103-117; discussion 173-180.
- Cynis, H., Schilling, S., Bodnar, M., Hoffmann, T., Heiser, U., Saido, T.C. & Demuth, H.U. (2006) Inhibition of glutaminy cyclase alters pyroglutamate formation in mammalian cells. *Biochim Biophys Acta* **1764** 1618-1625.

- Refolo, L.M., Pappolla, M.A., LaFrancois, J., Malester, B., Schmidt, S.D., Thomas-Bryant, T., Tint, G.S., Wang, R., Mercken, M., Petanceska, S.S. & Duff, K.E. (2001) A cholesterol-lowering drug reduces beta-amyloid pathology in a transgenic mouse model of Alzheimer's disease. *Neurobiol Dis* 8 890-899.
- Richards, J.G., Higgins, G.A., Ouagazzal, A.M., Ozmen, L., Kew, J.N., Bohrmann, B., Malherbe, P., Brockhaus, M., Loetscher, H., Czech, C., Huber, G., Bluethmann, H., Jacobsen, H. & Kemp, J.A. (2003) PS2APP transgenic mice, coexpressing hPS2mut and hAPPswe, show age-related cognitive deficits associated with discrete brain amyloid deposition and inflammation. *J Neurosci* 23 8989-9003.
- Romas, S.N., Tang, M.X., Berglund, L. & Mayeux, R. (1999) APOE genotype, plasma lipids, lipoproteins, and AD in community elderly. *Neurology* 53 517-521.
- Rota, E., Bellone, G., Rocca, P., Bergamasco, B., Emanuelli, G. & Ferrero, P. (2006) Increased intrathecal TGF-beta1, but not IL-12, IFN-gamma and IL-10 levels in Alzheimer's disease patients. *Neurol Sci* 27 33-39.
- Russo, C., Saido, T.C., DeBusk, L.M., Tabaton, M., Gambetti, P. & Teller, J.K. (1997) Heterogeneity of water-soluble amyloid beta-peptide in Alzheimer's disease and Down's syndrome brains. *FEBS Lett* 409 411-416.
- Russo, C., Violani, E., Salis, S., Venezia, V., Dolcini, V., Damonte, G., Benatti, U., D'Arrigo, C., Patrone, E., Carlo, P. & Schettini, G. (2002) Pyroglutamate-modified amyloid beta-peptides--AbetaN3(pE)--strongly affect cultured neuron and astrocyte survival. *J Neurochem* 82 1480-1489.
- Saido, T.C., Iwatsubo, T., Mann, D.M., Shimada, H., Ihara, Y. & Kawashima, S. (1995) Dominant and differential deposition of distinct beta-amyloid peptide species, A beta N3(pE), in senile plaques. *Neuron* 14 457-466.
- Saido, T.C., Yamao-Harigaya, W., Iwatsubo, T. & Kawashima, S. (1996) Amino- and carboxyl-terminal heterogeneity of beta-amyloid peptides deposited in human brain. *Neurosci Lett* 215 173-176.
- Sandbrink, R., Monning, U., Masters, C.L. & Beyreuther, K. (1997) Expression of the APP gene family in brain cells, brain development and aging. *Gerontology* 43 119-131.
- Savonenko, A.V., Xu, G.M., Price, D.L., Borchelt, D.R. & Markowska, A.L. (2003) Normal cognitive behavior in two distinct congenic lines of transgenic mice hyperexpressing mutant APP SWE. *Neurobiol Dis* 12 194-211.
- Scarmeas, N., Albert, M., Brandt, J., Blacker, D., Hadjigeorgiou, G., Papadimitriou, A., Dubois, B., Sarazin, M., Wegesin, D., Marder, K., Bell, K., Honig, L. & Stern, Y.

- (2005) Motor signs predict poor outcomes in Alzheimer disease. *Neurology* 64 1696-1703.
- Scarmeas, N., Hadjigeorgiou, G.M., Papadimitriou, A., Dubois, B., Sarazin, M., Brandt, J., Albert, M., Marder, K., Bell, K., Honig, L.S., Wegesin, D. & Stern, Y. (2004) Motor signs during the course of Alzheimer disease. *Neurology* 63 975-982.
- Schafer, S., Wirths, O., Multhaup, G. & Bayer, T.A. (2007) Gender dependent APP processing in a transgenic mouse model of Alzheimer's disease. *J Neural Transm* 114 387-394.
- Schilling, S., Hoffmann, T., Manhart, S., Hoffmann, M. & Demuth, H.U. (2004) Glutaminyl cyclases unfold glutamyl cyclase activity under mild acid conditions. *FEBS Lett* 563 191-196.
- Schilling, S., Lauber, T., Schaupp, M., Manhart, S., Scheel, E., Bohm, G. & Demuth, H.U. (2006) On the seeding and oligomerization of pGlu-amyloid peptides (in vitro). *Biochemistry* 45 12393-12399.
- Schilling, S.et.al. (2007) Inhibition of glutaminyl cyclase - a novel therapeutic concept for the causative treatment of Alzheimer's disease. *Nature*, co-submitted.
- Schmitz, C., Rutten, B.P., Pielen, A., Schafer, S., Wirths, O., Tremp, G., Czech, C., Blanchard, V., Multhaup, G., Rezaie, P., Korr, H., Steinbusch, H.W., Pradier, L. & Bayer, T.A. (2004) Hippocampal neuron loss exceeds amyloid plaque load in a transgenic mouse model of Alzheimer's disease. *Am J Pathol* 164 1495-1502.
- Schonknecht, P., Lutjohann, D., Pantel, J., Bardenheuer, H., Hartmann, T., von Bergmann, K., Beyreuther, K. & Schroder, J. (2002) Cerebrospinal fluid 24S-hydroxycholesterol is increased in patients with Alzheimer's disease compared to healthy controls. *Neurosci Lett* 324 83-85.
- Selkoe, D.J. (1991) The molecular pathology of Alzheimer's disease. *Neuron* 6 487-498.
- Selkoe, D.J. (2001) Alzheimer's disease: genes, proteins, and therapy. *Physiol Rev* **81** 741-766.
- Selkoe, D.J., Abraham, C.R., Podlisny, M.B. & Duffy, L.K. (1986) Isolation of low-molecular-weight proteins from amyloid plaque fibers in Alzheimer's disease. *J Neurochem* 46 1820-1834.
- Semenza, G.L. (2003) Targeting HIF-1 for cancer therapy. *Nat Rev Cancer* 3 721-732.
- Shahbazian, M., Young, J., Yuva-Paylor, L., Spencer, C., Antalffy, B., Noebels, J., Armstrong, D., Paylor, R. & Zoghbi, H. (2002) Mice with truncated MeCP2

- recapitulate many Rett syndrome features and display hyperacetylation of histone H3. *Neuron* 35 243-254.
- Shepherd, C.E., Grace, E.M., Mann, D.M. & Halliday, G.M. (2007) Relationship between neuronal loss and 'inflammatory plaques' in early onset Alzheimer's disease. *Neuropathol Appl Neurobiol* 33 328-333.
- Silbert, L.C., Quinn, J.F., Moore, M.M., Corbridge, E., Ball, M.J., Murdoch, G., Sexton, G. & Kaye, J.A. (2003) Changes in premorbid brain volume predict Alzheimer's disease pathology. *Neurology* 61 487-492.
- Sjogren, M., Mielke, M., Gustafson, D., Zandi, P. & Skoog, I. (2006) Cholesterol and Alzheimer's disease--is there a relation? *Mech Ageing Dev* **127** 138-147.
- Solfrizzi, V., Panza, F., D'Introno, A., Colacicco, A.M., Capurso, C., Basile, A.M. & Capurso, A. (2002) Lipoprotein(a), apolipoprotein E genotype, and risk of Alzheimer's disease. *J Neurol Neurosurg Psychiatry* 72 732-736.
- Spittaels, K., Van den Haute, C., Van Dorpe, J., Bruynseels, K., Vandezande, K., Laenen, I., Geerts, H., Mercken, M., Sciot, R., Van Lommel, A., Loos, R. & Van Leuven, F. (1999) Prominent axonopathy in the brain and spinal cord of transgenic mice overexpressing four-repeat human tau protein. *Am J Pathol* 155 2153-2165.
- St George-Hyslop, P.H. (2000) Molecular genetics of Alzheimer's disease. *Biol Psychiatry* 47 183-199.
- Stokin, G.B., Lillo, C., Falzone, T.L., Brusch, R.G., Rockenstein, E., Mount, S.L., Raman, R., Davies, P., Masliah, E., Williams, D.S. & Goldstein, L.S. (2005) Axonopathy and transport deficits early in the pathogenesis of Alzheimer's disease. *Science* 307 1282-1288.
- Streit, W.J., Mrak, R.E. & Griffin, W.S. (2004) Microglia and neuroinflammation: a pathological perspective. *J Neuroinflammation* 1 14.
- Streit, W.J. & Sparks, D.L. (1997) Activation of microglia in the brains of humans with heart disease and hypercholesterolemic rabbits. *J Mol Med* 75 130-138.
- Szczepanik, A.M., Funes, S., Petko, W. & Ringheim, G.E. (2001) IL-4, IL-10 and IL-13 modulate A beta(1--42)-induced cytokine and chemokine production in primary murine microglia and a human monocyte cell line. *J Neuroimmunol* 113 49-62.
- Sunderland, T., Gur, R.E. & Arnold, S.E. (2005) The use of biomarkers in the elderly: current and future challenges. *Biol Psychiatry* **58** 272-276.
- Tabira, T., Chui, D.H. & Kuroda, S. (2002) Significance of intracellular Abeta42 accumulation in Alzheimer's disease. *Front Biosci* 7 a44-49.

- Tahara, K., Kim, H.D., Jin, J.J., Maxwell, J.A., Li, L. & Fukuchi, K. (2006) Role of toll-like receptor signalling in Abeta uptake and clearance. *Brain* 129 3006-3019.
- Takahashi, R.H., Almeida, C.G., Kearney, P.F., Yu, F., Lin, M.T., Milner, T.A. & Gouras, G.K. (2004) Oligomerization of Alzheimer's beta-amyloid within processes and synapses of cultured neurons and brain. *J Neurosci* 24 3592-3599.
- Takahashi, R.H., Milner, T.A., Li, F., Nam, E.E., Edgar, M.A., Yamaguchi, H., Beal, M.F., Xu, H., Greengard, P. & Gouras, G.K. (2002) Intraneuronal Alzheimer abeta42 accumulates in multivesicular bodies and is associated with synaptic pathology. *Am J Pathol* 161 1869-1879.
- Takeda, K., Araki, W. & Tabira, T. (2004) Enhanced generation of intracellular Abeta42 amyloid peptide by mutation of presenilins PS1 and PS2. *Eur J Neurosci* 19 258-264.
- Tanzi, R.E. (1999) A genetic dichotomy model for the inheritance of Alzheimer's disease and common age-related disorders. *J Clin Invest* **104** 1175-1179.
- Tarkowski, E., Issa, R., Sjogren, M., Wallin, A., Blennow, K., Tarkowski, A. & Kumar, P. (2002) Increased intrathecal levels of the angiogenic factors VEGF and TGF-beta in Alzheimer's disease and vascular dementia. *Neurobiol Aging* 23 237-243.
- Tekirian, T.L., Saido, T.C., Markesbery, W.R., Russell, M.J., Wekstein, D.R., Patel, E. & Geddes, J.W. (1998) N-terminal heterogeneity of parenchymal and cerebrovascular Abeta deposits. *J Neuropathol Exp Neurol* 57 76-94.
- Tekirian, T.L., Yang, A.Y., Glabe, C. & Geddes, J.W. (1999) Toxicity of pyroglutaminated amyloid beta-peptides 3(pE)-40 and -42 is similar to that of A beta1-40 and -42. *J Neurochem* 73 1584-1589.
- Terwel, D., Lasrado, R., Snauwaert, J., Vandeweert, E., Van Haesendonck, C., Borghgraef, P. & Van Leuven, F. (2005) Changed conformation of mutant Tau-P301L underlies the moribund tauopathy, absent in progressive, nonlethal axonopathy of Tau-4R/2N transgenic mice. *J Biol Chem* 280 3963-3973.
- Tesseur, I., Van Dorpe, J., Bruynseels, K., Bronfman, F., Sciot, R., Van Lommel, A. & Van Leuven, F. (2000) Prominent axonopathy and disruption of axonal transport in transgenic mice expressing human apolipoprotein E4 in neurons of brain and spinal cord. *Am J Pathol* 157 1495-1510.
- Teunissen, C.E., De Vente, J., von Bergmann, K., Bosma, H., van Boxtel, M.P., De Bruijn, C., Jolles, J., Steinbusch, H.W. & Lutjohann, D. (2003) Serum cholesterol, precursors and metabolites and cognitive performance in an aging population. *Neurobiol Aging* 24 147-155.

- Tuppo, E.E. & Arias, H.R. (2005) The role of inflammation in Alzheimer's disease. *Int J Biochem Cell Biol* 37 289-305.
- Urbanc, B., Cruz, L., Le, R., Sanders, J., Ashe, K.H., Duff, K., Stanley, H.E., Irizarry, M.C. & Hyman, B.T. (2002) Neurotoxic effects of thioflavin S-positive amyloid deposits in transgenic mice and Alzheimer's disease. *Proc Natl Acad Sci U S A* 99 13990-13995.
- Van Broeck, B., Van Broeckhoven, C. & Kumar-Singh, S. (2007) Current insights into molecular mechanisms of Alzheimer disease and their implications for therapeutic approaches. *Neurodegener Dis* 4 349-365.
- Wagner, U., Utton, M., Gallo, J.M. & Miller, C.C. (1996) Cellular phosphorylation of tau by GSK-3 beta influences tau binding to microtubules and microtubule organisation. *J Cell Sci* 109 1537-1543.
- Wirths, O., Breyhan, H., Schafer, S., Roth, C. & Bayer, T.A. (2007) Deficits in working memory and motor performance in the APP/PS1ki mouse model for Alzheimer's disease. *Neurobiol Aging* Jan. 8.
- Wirths, O., Multhaup, G. & Bayer, T.A. (2004) A modified beta-amyloid hypothesis: intraneuronal accumulation of the beta-amyloid peptide--the first step of a fatal cascade. *J Neurochem* 91 513-520.
- Wirths, O., Multhaup, G., Czech, C., Feldmann, N., Blanchard, V., Tremp, G., Beyreuther, K., Pradier, L. & Bayer, T.A. (2002) Intraneuronal APP/A beta trafficking and plaque formation in beta-amyloid precursor protein and presenilin-1 transgenic mice. *Brain Pathol* 12 275-286.
- Wirths, O., Thelen, K., Breyhan, H., Luzon-Toro, B., Hoffmann, K.H., Falkai, P., Lutjohann, D. & Bayer, T.A. (2006) Decreased plasma cholesterol levels during aging in transgenic mouse models of Alzheimer's disease. *Exp Gerontol* 41 220-224.
- Wirths, O., Weis, J., Kayed, R., Saido, T.C. & Bayer, T.A. (2006) Age-dependent axonal degeneration in an Alzheimer mouse model. *Neurobiol Aging* Sept. 8.
- Wirths, O., Weis, J., Szczygielski, J., Multhaup, G. & Bayer, T.A. (2006) Axonopathy in an APP/PS1 transgenic mouse model of Alzheimer's disease. *Acta Neuropathol* 111 312-319.
- Wung, J.K., Perry, G., Kowalski, A., Harris, P.L., Bishop, G.M., Trivedi, M.A., Johnson, S.C., Smith, M.A., Denhardt, D.T. & Atwood, C.S. (2007) Increased expression of the remodeling- and tumorigenic-associated factor osteopontin in pyramidal neurons of the Alzheimer's disease brain. *Curr Alzheimer Res* 4 67-72.

- Wyss-Coray, T. (2006) Inflammation in Alzheimer disease: driving force, bystander or beneficial response? *Nat Med* 12 1005-1015.
- Wyss-Coray, T., Lin, C., Yan, F., Yu, G.Q., Rohde, M., McConlogue, L., Masliah, E. & Mucke, L. (2001) TGF-beta1 promotes microglial amyloid-beta clearance and reduces plaque burden in transgenic mice. *Nat Med* 7 612-618.
- Xia, W. (2000) Role of presenilin in gamma-secretase cleavage of amyloid precursor protein. *Exp Gerontol* 35 453-460.
- Yew, D.T., Ping Li, W. & Liu, W.K. (2004) Fas and activated caspase 8 in normal, Alzheimer and multiple infarct brains. *Neurosci Lett* 367 113-117.
- Youssef, I., Florent-Bechard, S., Malaplate-Armand, C., Koziel, V., Bihain, B., Olivier, J.L., Leininger-Muller, B., Kriem, B., Oster, T. & Pillot, T. (2007) N-truncated amyloid-beta oligomers induce learning impairment and neuronal apoptosis. *Neurobiol Aging* 23 23.
- Zadeh, G. & Guha, A. (2003) Angiogenesis in nervous system disorders. *Neurosurgery* 53 1362-1374; discussion 1374-1366.
- Zhang, R., Barker, L., Pinchev, D., Marshall, J., Rasamoeliso, M., Smith, C., Kupchak, P., Kireeva, I., Ingratta, L. & Jackowski, G. (2004) Mining biomarkers in human sera using proteomic tools. *Proteomics* 4 244-256
- Zhao, B., Stavchansky, S.A., Bowden, R.A. & Bowman, P.D. (2003) Effect of interleukin-1beta and tumor necrosis factor-alpha on gene expression in human endothelial cells. *Am J Physiol Cell Physiol* 284 C1577-1583.
- Zheng, W.H., Bastianetto, S., Mennicken, F., Ma, W. & Kar, S. (2002) Amyloid beta peptide induces tau phosphorylation and loss of cholinergic neurons in rat primary septal cultures. *Neuroscience* 115 201-211.

7 PUBLICATIONS

- **Breyhan H.**, Wirths O., Lütjohann D., Bayer T.A. (2005)
24(S)-Hydroxycholesterol plasma levels in a transgenic mouse model for Alzheimer's disease with neuron loss
Neurology, Psychiatry and Brain Research, 12:101-104
- Wirths O., Thelen K., **Breyhan H.**, Luzon-Toro B., Hoffmann K.H., Falkai P., Lütjohann D., Bayer T.A. (2006)
Decreased plasma cholesterol levels during aging in transgenic mouse models of Alzheimer's disease
Experimental Gerontology, 41(2): 220-224
- Bayer T.A., Schäfer S., **Breyhan H.**, Wirths O., Treiber C., Multhaup G. (2006)
A vicious cycle: Role of oxidative stress, intraneuronal A β and Cu in Alzheimer's disease
Clinical Neuropathology, 25(4): 163-171
- Wirths, O., **Breyhan H.**, Schäfer S., Roth C., Bayer T.A. (2007)
Deficits in working memory and motor performance in the APP/PS1ki mouse model of Alzheimer's disease
Neurobiology of Aging, in press
(Epub 8. Januar 2007, DOI: 10.1016/j.neurobiolaging.2006.12.004)
- **Breyhan H.***, Duan K.*, Wirths O.*, Saido T.C., Rettig J., Bayer T.A.
Dominant aggregation of beta-amyloid starting with pyroglutamate at position 3: synaptic deficits, neuron loss and hippocampus atrophy in the APP/PS1KI mouse
*Submitted (*equal contribution)*
- Bayer T.A.*, **Breyhan H.***, Wirths O.*, Cynis H., Schilling S., Demuth H.U.
A β _{3(pE)-42} triggers neurodegeneration and lethal neurological deficits in transgenic mice
*Submitted (*equal contribution)*

- Rohe M., Carlo A.S., **Breyhan H.**, Sporbert A., Militz D., Schmidt V., Wozny C., Harmeier A., Erdmann B., Bales K.R., Wolf S., Kempermann G., Paul S., Schmitz D., Bayer T.A., Willnow T.E., Andersen O.M.

SorLA controls APP-dependent stimulation of adult neurogenesis through ERK signaling

Submitted

- **Breyhan H.**, Wirths O., Marcello A., Bayer T.A.

Pathology-dependent development of neuroinflammation in an APP/PS1KI mouse model of Alzheimer's disease

In preparation

Conference Abstracts

- Bayer T.A., Wirths O., Schäfer S, **Breyhan H.**, Muckenthaler M, Delacourte A, Kayed R, Saido T, Multhaup G, Weis J., **New lessons from the APP/PS1 transgenic mouse model with neuron loss: metal biology, axonal degeneration and intraneuronal N-modified Abeta aggregation**, *Alzheimer's and Dementia* 2(3) Suppl. 1: S38-S39, July 2006
- T.A. Bayer, **H. Breyhan**, K. Duan, J. Rettig, O. Wirths, **Intraneuronal Abeta is a Major Risk Factor – Novel Evidence From the APP/PS1KI Mouse Model**, *Neurodegenerative Dis* 4(suppl 1) 1-364 (2007)
- **Breyhan H.**, Schäfer S., Wirths O., Muckenthaler M., Multhaup G., Bayer T.A., **Neuronal loss and changes in metal homeostasis in the APP751SLPS1ki mouse model of Alzheimer's disease**, *Alzheimer's and Dementia* 2(3) Suppl. 1:S.106, July 2006
- O.M. Andersen, V. Schmidt, M. Rohe, Sporbert, **H. Breyhan**, T.A. Bayer, T.E. Willnow, **SorLA and APP Trafficking**, *Neurodegenerative Dis* 4(suppl 1) 1-364 (2007)

- O. Wirths, **H. Breyhan**, J. Weis, , T.A. Bayer, **Age-Dependent Axonal Degeneration and Behavioural Impairment in the APP/PS1ki Mouse Model of AD**, *Neurodegenerative Dis 4(suppl 1) 1-364 (2007)*
- Bayer TA, Duan K, **Breyhan H**, Rettig J, Wirths O., **Synaptic deficits correlate with neuron loss and changes in behaviour in the APP/PS1ki mouse model**, *IBANGS 9th Annual meeting, Doorwerth (Netherlands), May 21-25, 2007-03-19*
- Bayer TA, Breyhan H, Duan K, Rettig J, **Wirths O. Paradigm shift in Alzheimer's Disease: Intraneuronal A β aggregation triggers neuron loss.** *European Neuropsychopharmacology (17) Suppl. 4:205 (2007)*

8 DANKSAGUNG

Sehr herzlich danke ich Herrn Professor Thomas Bayer für Betreuung und Begleitung dieser Arbeit sowie für die Übernahme des Referates.

Herrn Professor Adolfo Cavalié danke ich verbindlich für die Übernahme des Korreferates.

Herrn Doktor Oliver Wirths danke ich besonders für seine ausgezeichnete Kollegialität, seine vielseitigen Anregungen zu meiner Arbeit und die gute Zeit, die ich mit ihm gemeinsam verbringen durfte.

Herrn Professor Hans-Ulrich Demuth danke ich für die freundliche Aufnahme bei der Probiodrug AG sowie den spannenden Einblick in die Unternehmensentwicklung.

Herrn Doktor Stephan Schilling, Herrn Holger Cynis, Frau Katrin Schulz, Frau Birgit Koch, Herrn Eike Scheel sowie allen weiteren Kollegen, mit denen ich bei der Probiodrug AG zusammenarbeiten durfte, danke ich neben den hervorragenden Arbeitsbedingungen insbesondere auch für die ausgezeichnete Arbeitsatmosphäre, die mich zu meinen zahlreichen Aufenthalten immer wieder gerne nach Halle zurückgeführt hat.

Frau Katrin Rubly, Frau Doktor Stephanie Schäfer und Herrn Karl-Heinz Hoffmann danke ich für die gute Zusammenarbeit.

Diese Promotion wurde ermöglicht durch ein Stipendium der Stiftung der Deutschen Wirtschaft (sdw). Für das durch diese Förderung zum Ausdruck gebrachte Vertrauen bedanke ich mich sehr herzlich. Besonders möchte ich mich aber für die in der Förderzeit erfahrene ideelle Förderung durch die sdw bedanken, welche mich bei meiner persönlichen Weiterentwicklung wertvoll unterstützte. Das mir in der sdw gebotene Forum zum interdisziplinären Austausch habe ich stets sehr geschätzt. Namentlich danken darf ich insbesondere meinen Regionalbetreuern Herrn Dirk Reichel und Frau Doktor Gwendolin Mühlinghaus sowie Frau Natalia Smith und Herrn Friedrich Anders für eine inspirierende Sommerakademie.

9 Curriculum Vitae

Personal Data

Name: Henning Breyhan
Date of Birth : Salzgitter, June 11th 1976
Nationality: German

Scientific education

04/2000 – 03/2002 Basic studies of chemistry at the [RWTH Aachen](#)
04/2002 – 04/2004 Main study period in chemistry at the Rheinische Friedrich-Wilhelms-Universität in Bonn
05/2004 – 11/2004 Diploma thesis with Professor Konrad Sandhoff, Rheinische Friedrich-Wilhelms-Universität Bonn; Degree: Diplom-Chemiker
11/2004 – 10/2007 Ph.D. thesis with Professor Thomas Bayer in Homburg and Goettingen

Other education

07/1995 – 04/1996 Military service
04/1996 – 03/1999 Studies of Economics at the [Fachhochschule der Deutschen Bundesbank](#) in Hachenburg/Westerwald (University of Applied Sciences); Degree: Diplom-Betriebswirt (FH)
04/1999 – 03/2000 occupational activity in the Department of Economics in the [land central bank](#) of Hamburg

Scholarships

12/2005 – 11/2007 Klaus-Murmann-Ph.D.-scholarship of the Foundation of German Businesses ([sdw](#))

Göttingen, 10 Oct. 07

Henning Breyhan